

**NOVEL MICROCAPSULES VIA THE SELF-ASSEMBLY OF POLYMER
COLLOIDS AT THE OIL-WATER INTERFACE:
PREPARATION AND CHARACTERIZATION**

By

LISA M. CROLL, Hon.B.Sc.

A Thesis

Submitted to the School of Graduate Studies

in Partial Fulfilment of the Requirements

for the Degree

Doctor of Philosophy in Chemistry

McMaster University

©Copyright by Lisa M. Croll, January 2004

NOVEL MICROCAPSULES VIA SELF-ASSEMBLY OF POLYMER COLLOIDS

DOCTOR OF PHILOSOPHY (2004)
(Chemistry)

McMaster University
Hamilton, Ontario

TITLE: Novel Microcapsules via the Self-assembly of Polymer Colloids at the Oil-Water Interface: Preparation and Characterisation.

AUTHOR: Lisa M. Croll, Hon.BSc. (McMaster University)

SUPERVISOR: Harald D. H. Stöver

NUMBER OF PAGES: xviii, 148

For my family and friends.

ABSTRACT

Three different types of microcapsules are discussed in this thesis. The first, polyurea microcapsules serve as a basis for developing scanning transmission x-ray spectromicroscopy (STXM), an emerging technique for chemical analysis of nanoscale composites. Using STXM it was possible to visualise the location of two different polyurea species within a cross-section of polyurea microcapsule wall, approximately 200 nm thick.

The second type of microcapsules presented here are known as tectocapsules. These novel microcapsules were prepared by self-assembly of reactive poly(divinylbenzene-*alt*-maleic anhydride) microspheres and microgels at the oil-water interface and fixing them in place with poly(ethylenimines) (PEI). This resulted in the formation of highly permeable capsule walls consisting of interconnected microspheres that readily lost their core solvent upon drying. A mechanism for formation and rupture of tectocapsules is proposed.

The final type of microcapsules described here are called composite tectocapsules. These are capsules where colloids assembled at the oil-water interface are embedded in a polyurea matrix. These capsules were prepared with three types of colloids: poly(divinylbenzene-*alt*-maleic anhydride) microspheres and microgels, porous poly(divinylbenzene) microspheres, and porous poly(divinylbenzene) microspheres functionalised with maleic acid. Composite capsules containing porous poly(divinylbenzene) microspheres functionalised with maleic acid showed altered release rates versus standard polyurea microcapsules. This change in release is attributed

to solvent release through the microsphere's pores rather than the surrounding polyurea matrix. STXM was used to map the chemical compositions of these composite tectocapsules.

Acknowledgements

First I would like to thank my supervisor, Professor Harald Stöver for his help, encouragement and enthusiasm towards research and teaching. Thank you for giving me the guidance needed to produce good research and be accountable for my work but enough freedom to explore what was interesting.

I would also like to thank my supervisory committee, Dr. Paul Berti and Professor Robert Pelton for their suggestions and encouragement over the years. Their knowledge of chemistry and the rest of science is very much appreciated.

Thank you also to Professor Adam Hitchcock for his enthusiasm, time and patience in teaching me about STXM, which has become an invaluable tool in my work.

Sincere appreciation is also extended to Mrs. Marcia West for her time and expertise in sample preparation and imaging in the Health Science Electron Microscopy Unit, Mr. Klaus Schults in the Life Science Microscopy Facility, Dr. Don Hughes and Mr. Bryan Sayer in the Chemistry Department NMR Facility, Mr. Frank Gibbs for his help with TGA, and Mr. Mike Malott for is invaluable I.T. support.

To all of the members past and present of the Stöver Group: Your friendships have truly made my time here irreplaceable. I respect each one of you a great deal. Thank you for our many discussions on chemistry, science, culture and faith, I have learned a great deal from each of you. Thanks go to: Anna, Danielle, Daryl, Erica, Ester, Guodong, Jaffar, Janevieve, Jeff, Kui, Mukarram, Nick, Randy, WenHui, Xiangchun (Yin), and Yan.

Thanks also to the staff in the Chemistry Department office, Carol Dada, Josie Petrie, Barbara DeJean, and Tammy Feher. Especially Carol, who manages to keep us all in line but leave us with the feeling that someone is fighting for us.

To my friends, for everything: for friendship, scientific discussions, never dropping the rope, ski trips, and the cottage weekends. I am lucky to have known you all.

Finally, thank you to my family. To my Mom, who taught me to be good to the people around me and live my life for each day, as one never knows when you might not get another chance. To my Dad, for holding together a family that needed it, for teaching me to be independent, think for myself and that I can achieve whatever it is I decide to strive for, and also for teaching me that the world would not run without the many people doing thankless jobs, such as emptying our trash and cleaning our floors. To my brother, Andrew, and my sister, Amy, thank you both for your friendship, support and encouragement every step of the way. I am so glad to have you both as friends.

Table of Contents

	Page
Abstract	iv
Acknowledgements	vi
Table of Figures	xiii
List of Tables	xvi
List of Schemes	xvi
List of Abbreviations	xvi
Preface – Thesis Outline	1
Chapter 1 – Characterization of Nanocomposite Materials Using Scanning Transmission X-ray Spectromicroscopy: A Polyurea Microcapsule Example	
1.0 Introduction	6
1.1 Scanning Transmission X-ray Spectromicroscopy	9
1.1.1 STXM Characterization of Polymers	11
1.2 Microencapsulation	15
1.2.1 Interfacial Microencapsulation	16
1.2.2 Polyurea Microencapsulation	16
1.3 Objective and Scope of Research	24
1.4 Experimental	24
1.5 Results and Discussion	28

Table of Contents (cont'd)

	Page
1.5.1 Sample Preparation	31
1.5.2 Analysis of Capsule Wall Composition	33
1.5.2.1 Development of Model Compounds	34
1.5.2.2 Quantitative Analysis - Component Maps	38
1.5.2.3 Spectral Extraction Method	40
1.6 Conclusions	42
References	45
Chapter 2 – Formation of Tectocapsules: Assembly of Poly(divinylbenzene-<i>alt</i>-maleic anhydride) Microspheres at Microgels at the Oil-Water Interface	
2.0 Introduction	50
2.1 Particle Assembly at Interfaces	50
2.2 Surface Tension	52
2.3 Particle Selection	53
2.4 Objective and Scope of Research	58
2.5 Experimental	59
2.6 Results and Discussion	62
2.6.1 Experimental Set-up and Design	62
2.6.1.1 Shaker Design	63
2.6.1.2 Shaker Arm Length	64

Table of Contents (cont'd)

	Page
2.6.1.3 Surfactants versus Stabilizers	65
2.6.2 Tectocapsule Formation	67
2.6.2.1 Amine Molecular Weight Effects	68
2.6.2.2 Effects of Amine Addition Rate	70
2.6.2.3 Microsphere Chemistry	71
2.6.2.4 Core Solvent Effects	75
2.6.2.5 Particle Loading Effects	78
2.6.3 Gel-Tectocapsules	81
2.6.3.1 Amine Molecular Weight	85
2.6.3.2 Amine Addition Rate	87
2.6.4 Mechanism of Tectocapsule Formation and Bursting	88
2.7 Conclusions	91
References	92
 Chapter 3 – Composite Tectocapsules with Porous Microsphere Release Gates	
3.0 Introduction	96
3.1 Microcapsule Release	98
3.2 An Example of Core Solvent Effects	102
3.3 Objective and Scope of Research	105
3.4 Experimental	105

Table of Contents (cont'd)

	Page
3.5 Results and Discussion	112
3.5.1 Composite Capsules Containing Poly(divinylbenzene-55 - <i>alt</i> -maleic anhydride) Microspheres and Microgels.	112
3.5.2 Composite Tectocapsules with Porous Poly(divinylbenzene -55) Precipitation Microspheres.	119
3.5.2.1 Release From Composite Microspheres	122
3.5.3 Composite Tectocapsules with Non-porous Poly (divinylbenzene-55) Precipitation Microspheres.	125
3.5.4 STXM Analysis of Composite Tectocapsules	127
3.6 Conclusions	129
References	131
 Chapter 4 –Related Ongoing Research and Proposed Future Direction	
4.0 Introduction	134
4.1 Related Ongoing Research	134
4.1.1 Industrially Relevant Composite Tectocapsules	134
4.1.1.1 Introduction of Suspension Microspheres	134
4.1.1.2 Release of Mixed Fills	135
4.1.2 Confirmation of the Mechanism of Release from Composite Tectocapsules	136

Table of Contents (cont'd)

	Page
4.2. Future Work	137
4.2.1 Polyurea Membrane Analysis by STXM	137
4.2.1.1 Microspheres as Wall Markers	138
4.2.1.2 Model Membranes	138
4.2.2 Chemistry of Microspheres Used for Capsule Construction	138
4.2.2.1 Location of Functionalisation Reaction	139
4.2.3 Tectocapsules as Vehicles for the Encapsulation of Highly Viscous Liquids and Waxy Solids	140
4.2.4 Functional Release Gates	142
References	144
Epilogue – Thesis Summary	145

Table of Figures

Figure #	Title	Page
1.1	Optical Micrograph of Polyurea Microcapsules	6
1.2	Environmental scanning electron micrograph of Polyurea Capsules	7
1.3	Transmission Electron Micrographs of Polyurea Microcapsule Walls	8
1.4	X-ray Absorption Edges	10
1.5	NEXAFS Spectra of poly(divinylbenzene) and Spurr's Resin	11
1.6	Polyurethanes and Polyureas Differentiated with NEXAFS	13
1.7	Model of Polyurea Microcapsule Wall Formation	19
1.8	Proposed Composition of Polyurea Microcapsule Walls	23
1.9	STXM Image of a Polyurea Microcapsule Wall	32
1.10	NEXAFS Spectra of Models for Symmetric and Asymmetric Polyurea	35
1.11	NEXAFS Spectra of Selected Polyurea Models and Spurr's Resin	37
1.12	Component Maps	38
1.13	Composition Maps and Profiles	39
1.14	NEXAFS Spectra Extracted from Polyurea Microcapsule Walls	42
1.15	Revised Model of Polyurea Microcapsule Wall Composition	43
2.1	Cartoon of a Microcapsule with Walls Comprised of Microspheres	50
2.2	Summary of the Effects of Surface Tension on Particle Assembly	53
2.3	Cartoon of One Possible Morphology of Composite Microcapsule	55
2.4	Optical Micrographs of Wet and Dry Tectocapsules	63
2.5	Modified Wrist Shaker	64

Table of Figures (cont'd)

		Page
2.6	Experimental Set-up for Tectocapsule Formation	67
2.7	Effect of Amine Molecular Weight	69
2.8	Effect of Core Solvent	77
2.9	Effect of Microsphere Loading	79
2.10	ESEM of Tectocapsules	80
2.11	ESEM of Tectocapsule with Solid Core	81
2.12	Cartoon Depicting the Contact Area Between Neighbouring Particles	82
2.13	Poly(DVB55- <i>alt</i> -MAn) and (DVB6- <i>alt</i> -MAn) Gel-tectocapsules	84
2.14	ESEM of Poly(DVB6- <i>alt</i> -MAn) Gel-tectocapsules	86
2.15	Mechanism of Tectocapsule Formation and Rupture	88
2.16	Optical Micrograph of Tectocapsule Rupture	90
2.17	Optical Micrograph of Gel-tectocapsule Rupture	91
3.1	Cartoon of Release from a Composite Tectocapsule	97
3.2	Diffusion Release from Microcapsules	100
3.3	Theoretical Release Rate of a Microcapsule Versus Time	101
3.4	Solvent Effects on Polyurea Microcapsule Wall Morphology	103
3.5	Solvent Effects on Release Rate of Polyurea Microcapsules	104
3.6	Composite Tectocapsules with Poly(DVB55- <i>alt</i> -MAn) Microspheres	115
3.7	Wet Composite Tectocapsules with Poly(DVB- <i>alt</i> -MAn) Colloids	116
3.8	ESEM of Composite Tectocapsules with Poly(DVB- <i>alt</i> -MAn) Colloids	117

Table of Figures (cont'd)

		Page
3.9	TEM of Composite Tectocapsules with Poly(DVB- <i>alt</i> -MAn) Colloids	118
3.10	Composite Tectocapsules with Porous Poly(divinylbenzene) Microspheres	120
3.11	ESEM of Composite Tectocapsules with Porous Poly(DVB) Microspheres	121
3.12	TEM of Composite Tectocapsules with Porous Poly(DVB) Microspheres	122
3.13	Release Curves for Composite Tectocapsules with Porous Poly(DVB) Microspheres	123
3.14	Effect of Porous and Non-porous Poly(DVB) Microspheres on Release	126
3.15	STXM Component Maps of Composite Tectocapsules	127
3.16	NEXAFS Spectra and Composition Map of Composite Tectocapsules	128
3.17	Cartoon of Two Major Composite Tectocapsule Morphologies	129
4.1	Possible Monomers for Microsphere Functionalisation	139
4.2	Cartoon of Composite Tectocapsules with On-off Release Gates	142
4.3	Proposed Scheme for Protection and Deprotection of Alcohols	143

List of Tables

Table #	Title	Page
2.1	Effect of Surfactants and Stabilizers on Tectocapsule Formation	65
2.2	Solvent Properties	76

List of Schemes

Scheme #	Title	Page
1.1	Reaction of Aromatic Isocyanates with Water	20
1.2	Reaction of Aromatic Isocyanates with Aliphatic Amines	21
1.3	Biuret Formation by Reaction of an Isocyanate and Urea	22
2.1	Predicted Reaction of Anhydride Groups with Amine	68
2.2	Linkage Reactions of Amines with Acids and Anhydrides	73

List of Abbreviations

AIBN	2,2'-azobisisobutyronitrile
BuOAc	butyl acetate
C12 OAc	dodecyl acetate
DETA	diethylenetriamine

DVBX	mixture of divinylbenzene isomers, ethylvinylbenzene isomers and optionally 4-methylstyrene, where X equals the mole % of divinyl components (eg. DVB55)
ESEM	environmental scanning electron microscopy
HexOAc	hexyl acetate
IR	infrared
MA	maleic acid
MAn	maleic anhydride
MDI	4,4'-methylene diphenylene isocyanate
MEK	methyl ethyl ketone, 2-butanone
4-MeSty	4-methyl styrene
NEXAFS	near edge x-ray absorption fine structure
NMR	nuclear magnetic resonance
PEI	polyethylenimine
PPIF	poly [(phenyl isocyanate)- <i>co</i> -formaldehyde
PVA	polyvinylalcohol
PVP	polyvinylpyrrolidone
SMA	poly(styrene- <i>alt</i> -maleic anhydride)
SEM	scanning electron microscopy
STXM	scanning transmission x-ray spectromicroscopy
TDI	toluene diisocyanate
TEM	transmission electron microscopy

TEPA tetraethylenepentamine
TGA thermal gravimetric analysis

PREFACE – THESIS OUTLINE

This thesis has been prepared in a modified “sandwich” format. Each chapter is loosely based on a published journal article or manuscript but each has an expanded introduction. The overall objectives of this research and a brief description of the work in each chapter is presented below.

Chapter 1: Compositional Mapping of the Internal Structure of Polyurea Microcapsule Walls by Soft X-ray Spectromicroscopy.

Research Objective:

The goal of this research was to develop a scanning transmission x-ray spectromicroscopy (STXM) method that could be used for the chemical speciation of polyurea microcapsules, thus allowing the level of isocyanate hydrolysis during microcapsule formation to be assessed with a spatial resolution of ~50 nm.

Synopsis:

The first chapter describes the study of polyurea microcapsule wall composition on the nanometer scale using scanning transmission x-ray spectromicroscopy (STXM). An introduction into near edge x-ray absorption fine structure (NEXAFS) spectroscopy and polyurea chemistry are included.

This chapter addresses sample preparation and development of appropriate

reference spectra for the species being analyzed, both of which are critical to the outcome of the analysis.

Associated Manuscript:

“Compositional Mapping of the Internal Structure of Polyurea Microcapsule Walls by Soft X-ray Microspectroscopy” Lisa M. Croll, Ivo Kaprinarov, Adam P. Hitchcock, Harald D.H. Stöver, in preparation.

Chapter 2: Formation of Tectocapsules: Assembly of Poly(divinylbenzene-*alt*-maleic anhydride) Microspheres and Microgels at the Oil-Water Interface

Research Objective:

The goal of this research was to develop a method for assembling poly(divinylbenzene-*alt*-maleic anhydride) (DVB-MAN) microspheres at the oil-water interface and covalently fixing them in place to form highly porous capsular structures. The factors that affect the self-assembly and fixation of the microspheres at the oil-water interface were also investigated.

Synopsis:

The second chapter presents a detailed study into the factors that affect self-assembly of poly(DVB-MAN) microspheres at the oil-water interface. It also describes the use of amines for fixing the microspheres at the interface to form highly porous

microcapsules called “tectocapsules”. As well, a mechanism for tectocapsule formation and rupture is proposed. A discussion of particle assembly at the oil-water interface and a brief introduction to surface tension is given.

Associated Publications:

“The Formation of Tectocapsules by Assembly and Crosslinking of Poly(Divinylbenzene-*alt*-Maleic Anhydride) Spheres at the Oil-Water Interface” Lisa M. Croll and Harald D.H. Stöver, *Langmuir*, **19**(14), 5918, (2003).

“Mechanism of Self-Assembly and Rupture of Cross-linked Microspheres and Microgels at the Oil-Water Interface” Lisa M. Croll, Harald D.H. Stöver, *Langmuir*, **19**(24) 10077, (2003).

Chapter 3: Composite Tectocapsules with Porous Microsphere Release Gates.

Research Objective:

The goal of this research was to prepare composite microcapsules with porous microsphere release gates and to compare the release of xylenes from these capsules with traditional microcapsules.

Synopsis:

The third chapter describes the preparation of the first composite microcapsules where poly(divinylbenzene-*alt*-maleic anhydride) (DVB-MAn) microspheres and microgels were self-assembled at the oil-water interface and subsequently embedded in a polyurea matrix. After it was established that the presence of assembled microspheres did not disrupt polyurea wall formation, a second type of composites were prepared where poly(divinylbenzene) microspheres functionalised with maleic acid were incorporated into a polyurea matrix. Xylene release from these composite microcapsules was monitored gravimetrically. An introduction into microencapsulation and controlled delivery is also presented.

Associated Manuscripts:

“Composite Tectocapsules with Porous Microsphere Release Gates” Lisa M. Croll and Harald D.H. Stöver, *Macromolecules*, Accepted Dec. 2003.

“Composite Tectocapsules via the Self-Assembly of Functionalized Poly(divinylbenzene) Microspheres” Lisa M. Croll and Harald D.H. Stöver, *Pure and Applied Chemistry*, Accepted Jan. 2004.

“Composite Tectocapsules with Porous Microsphere Release Gates” Harald D.H. Stöver and Lisa M. Croll, US Patent Application #, Filed May 2003.

Chapter 4: Proposed Future Direction and Related Ongoing Research

Synopsis:

The goal of this chapter is to present ideas for future work associated with the research presented in Chapter 1 through 3 and summarize ongoing work that is related to and inspired by the work presented in this thesis.

Associated Manuscripts:

“Integrating Near Edge X-ray Absorption Fine Structure (NEXAFS) Microscopy and Crystallography: The effects of molecular order”, Lisa M. Croll, Jim Britten, Cynthia Morin, Adam P. Hitchcock, Harald D.H. Stöver, *J.Synchrotron Rad.*, **10**, 265, (2003).

“Composite Tectocapsules with Porous Suspension Particle Release Gates” Danielle M. Lewis, Lisa M.Croll, WenHui Li, Harald D.H. Stöver, in progress.

“New Embedding Resins for X-ray Spectromicroscopy and Transmission Electron Microscopy” Guodong Zheng, Tohru , Lisa M. Croll, Marcia West, Harald D.H. Stöver, Adam P. Hitchcock, in progress.

CHAPTER 1 – NANOSCALE CHARACTERISATION OF POLYUREA MICROCAPSULES USING SCANNING TRANSMISSION X-RAY SPECTROMICROSCOPY

1.0 Introduction

The properties and behaviour exhibited by polymeric materials such as filtration membranes, fibres and microcapsules, are dictated by both the polymer morphology and composition. Morphological characterisation of materials generally includes microscopy, such as optical microscopy or scanning and transmission electron microscopy. Optical microscopy typically has a resolution of around 400 nm and is therefore used to view larger materials such as the polyurea microcapsules shown in Figure 1.1. This image, taken in reflective light mode shows the microcapsules to be spherical and to range in diameter from approximately 20 μm to 150 μm . Little detail of the capsule surface can be resolved.

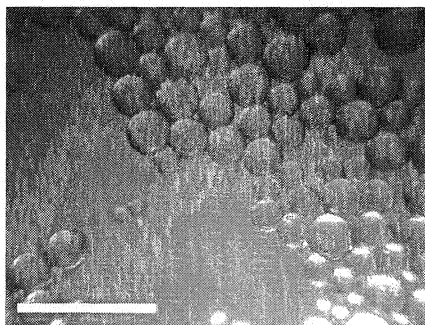


Figure 1. 1 Optical micrograph of polyurea microcapsules using reflective light. The scale bar is 500 μm .

The capsule surface can be visualised with greater resolution using a traditional scanning electron microscope (SEM), which has been used to resolve features of about 200 nm.¹ Figure 1.2 shows that the capsule surfaces are smooth and without macroscopic porosity.

Field emission SEM (FE-SEM) and force microscopies, such as atomic force microscopy (AFM) can give much better surface resolution, but like SEM and optical microscopy, provide little information about the internal structure. Transmission electron microscopy (TEM) can resolve

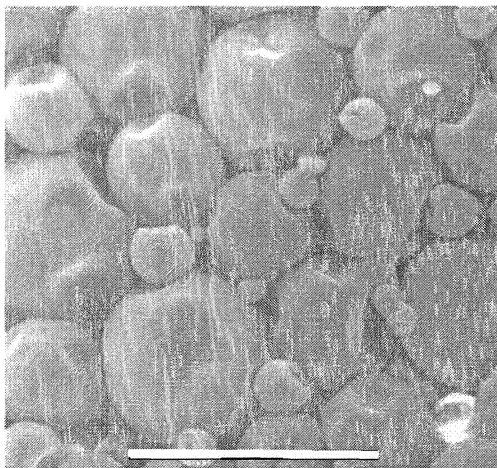


Figure 1. 2 Environmental scanning electron micrograph (ESEM) of polyurea microcapsules. Scale bar is 150 μm .

features smaller than 1 nm and can be used to gain detailed morphological information about the interior or cross-sections of a sample.¹ Larger samples, such as the polyurea microcapsule shown above, are embedded in an epoxy resin and microtomed into thin sections, generally 50 to 200 nm thick, which are supported on copper grids during imaging. These sections can then be imaged using a transmission electron microscope. Figure 1.3 shows TEM images of two different polyurea capsule wall cross-sections. Both of these capsule samples looked similar when examined by ESEM, but the TEM images clearly show the different wall structures. The capsules in Figure 1.3 A have a dense non-porous membrane and are non-leaky. Conversely, the capsules in Figure 1.3 B

consist of a thin dense layer of polyurea on the outside, backed by a thick porous inner layer. These capsules do release their fill slowly over several weeks. Thus it can be seen that changes in the polyurea morphology at the nano-scale are reflected in the release characteristics of the microcapsules.

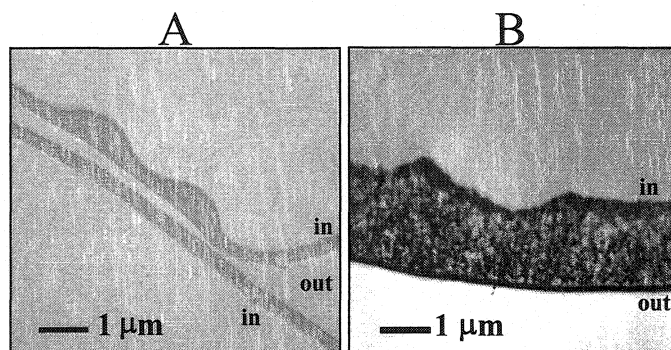


Figure 1. 3 Transmission electron micrographs of polyurea capsule wall cross-sections.

“in” indicates the inside, or organic side of the capsule wall and “out” indicates the outside, or aqueous side of the capsule wall.

Both the morphology and the chemical composition of such polymer walls greatly affect their properties, and need to be better understood to aid materials design. However, mapping their chemical composition presents a challenge for materials such as the polyurea walls shown above, which often have sub-micron thickness. Traditional chemical spectroscopies used for polymer studies such as infrared and nuclear magnetic resonance spectroscopy do not have sufficient spatial resolution to give access to such nano-scale structures, and the potential chemical composition gradients within them. Analytical transmission and scanning transmission electron microscopy have excellent

spatial resolution, as shown above, but typically do not have sufficient chemical sensitivity for quantitative chemical mapping beyond the elemental level.^{1,2}

This thesis chapter describes the use of synchrotron-based scanning transmission X-ray spectromicroscopy (STXM) to study nanocomposite polyurea capsules with high spatial and chemical resolution. A more detailed description of polyurea microcapsules and the process by which they are made appears below following an introduction to the STXM technique.

1.1 Scanning Transmission X-ray Spectromicroscopy (STXM)

X-rays passing through a material can be absorbed, scattered or transmitted. The number of photons that are absorbed at a given energy is related to the atomic composition, bonding, density and thickness of the material. These absorbed photons cause excitation or ejection of core electrons leading to either a short-lived excited state, or to ionization of the material. The energy at which core ionisation begins is known as the absorption edge. As the excitation by x-rays is associated with core electrons, each element has an absorption edge where the difference in x-ray absorption between the onset and peak of the edge is directly proportional to the amount of material present (Figure 1.4). Traditional x-ray spectroscopy utilised these absorption edges to quantitatively determine the elemental composition of a material.³

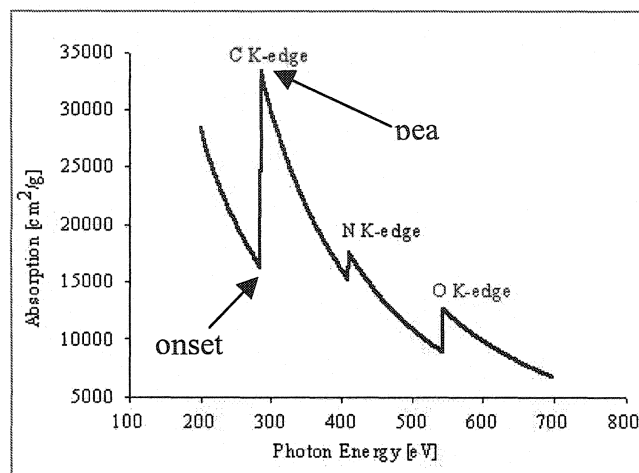


Figure 1. 4 X-ray absorption edges for carbon, nitrogen and oxygen.³

Modern analytical soft x-ray microscopy at synchrotron facilities use the fine structure near the x-ray absorption edge known as near edge X-ray absorption fine structure (NEXAFS) as the basis for chemical speciation. These bands can be up to 10 times as intense as the rise in intensity at the absorption edge and correspond to excited states created when core electrons were promoted to unoccupied molecular orbitals, π^* in the case of unsaturated molecules or σ^* in saturated species. For example, at the carbon edge, NEXAFS can be used to probe a material, or molecule, for the presence of C-C versus C=C and C \equiv C bonds as well as for other organic functional groups such as C=O and C \equiv N. In addition, when polarized synchrotron radiation is used, NEXAFS is sensitive to the orientation of specific bonds. For this reason much of the original interest in NEXAFS was directed towards investigating the structure and orientation of organic molecules bonded to surfaces.⁴

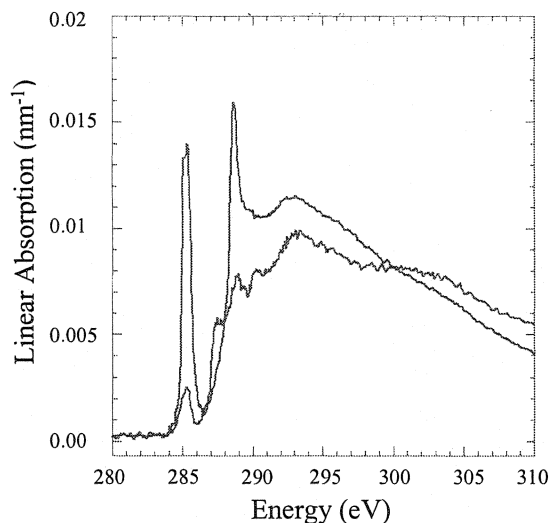


Figure 1. 5 NEXAFS spectra of poly(divinylbenzene) (green) and Spurr's epoxy resin (red), illustrating the C1s→ π^* transitions of an aromatic ring at ~285 eV and a carbonyl at ~289 eV.

Scanning transmission x-ray spectromicroscopy (STXM) has been applied successfully to spatially resolved studies of thin sections of polymers,^{5,6,7,8} biological systems⁹ and environmental problems.¹⁰ Since NEXAFS spectra of pure materials can be obtained with absolute intensity scales, which provide quantitative chemical analysis, scanning transmission X-ray microscopy can similarly be used for quantification at the sub-micron scale.¹¹

1.1.1 STXM Characterisation of Polymers

Numerous polymer characterisation problems have been addressed using STXM, particularly those where the chemical species involved are similar and thus cannot be differentiated in TEM experiments. While much of this work has been carried out in the last 5 years, some reviews of the area are already available.^{12,13} A short summary of

work, which demonstrates the chemical and spatial resolution of STXM spectromicroscopy, will be presented here.

Early STXM work by Koprinarov et al.¹⁴ illustrated the spatial and chemical resolution of the technique using core-shell polymer microspheres. In that work, changes in the ratio of ethylene glycol dimethacrylate (EDMA) to divinylbenzene (DVB) in the shell layer could be easily followed and the ratio of EDMA to DVB determined by STXM analysis was in good agreement with that predicted from comonomer composition. In like manner, it could be seen that EDMA penetration into the preformed DVB microsphere core was negligible. More recently, Hitchcock et al. have studied polyurethane foams containing styrene-acrylonitrile (SAN) filler particles of $\leq 1 \mu\text{m}$ diameter. Here the SAN particles could readily be distinguished from the polyurethane matrix. Furthermore, it was possible to show that the SAN particles were themselves inhomogeneous. These studies clearly demonstrate the potential for quantitative analysis on the nano and micron scale using STXM. However, in those studies the chemistry of the species being probed was very different. The good chemical sensitivity of NEXAFS is better illustrated by two studies of polyurethane foams reported by Urquart et al.^{15,16} Here it was shown that NEXAFS spectra could be used to differentiate polyurea and polyurethane species to within 20% of the predicted composition down to concentrations of ~ 10 mole percent, based on their ability to resolve the two different C=O peaks in the NEXAFS spectra. In addition it was shown that polyurethane foams prepared with different starting materials, toluene diisocyanate (TDI) and 4,4'-methylene diphenylene isocyanate (MDI), could be differentiated.

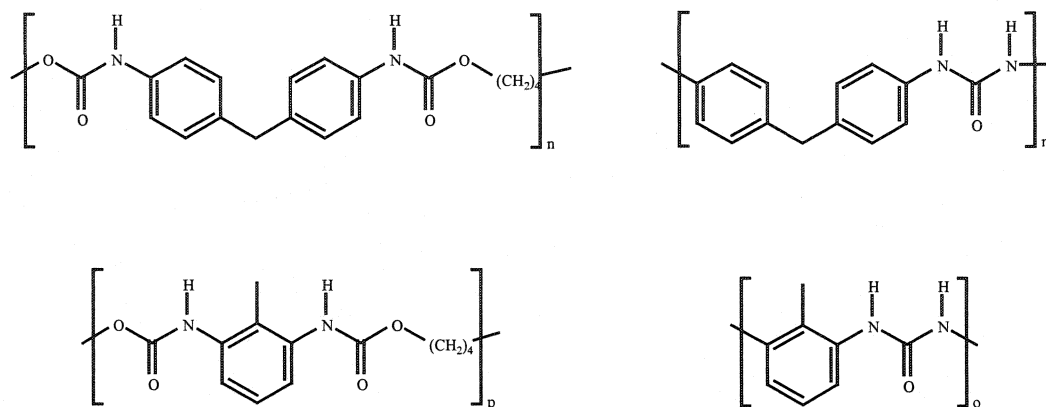


Figure 1. 6 Polyurethanes and polyureas differentiated by Urquart et al. using NEXAFS spectra. Using these models foams containing both polyurea and polyurethanes were quantitatively characterised using STXM.^{15,16}

As illustrated above, STXM is a powerful technique for performing chemical analysis of materials on the nano and micron scale. As STXM microscopes use plane polarised synchrotron radiation, they can additionally detect molecular ordering. This sensitivity of the NEXAFS spectra to molecular order was used by Ade et al.⁶ to characterise the orientation of polymer chains in poly(*p*-phenylene terephthalamide) (PPTA or Kevlar) fibers. The work showed that the phenyl groups of the polymer chains were distributed radially within the fibers. More recently, Fujimori et al.¹⁷ studied the orientation of fluorinated comb polymers adsorbed to glass surfaces and linked small changes in the fluoropolymer's chemical structure to changes in branch orientation in the final films.

The ability to utilise both the chemical sensitivity and the orientational sensitivity of a STXM microscope for analysis was illustrated by Smith et al.¹⁸ in a study that characterised oxybenzoate (VectraTM) liquid crystal domains within a polyethylene terephthalate (PET) matrix. This study not only revealed the size and location of the VectraTM phase but also showed regions of molecular order within the liquid crystal domains.

As the spatial resolution of STXM improves, being aware of its sensitivity to molecular orientation will become increasingly important. Not only will it be possible to determine of molecular orientation in samples that are too small or otherwise inappropriate for traditional x-ray crystallography, such as nanocrystals or surface monolayers as described above. At the same time, spectra of unknown materials can easily be misinterpreted if molecular order is not taken into consideration.

The samples used for the work described above were prepared as thinly cut dry sections. Although this method is ideal for many types of samples, drying can alter the structure of some materials significantly. At energies at or near the carbon edge oxygen and inorganic salts do not contribute to the NEXAFS spectra. This feature of NEXAFS allows for samples, such as hydro gels, to be analysed while swollen with water or saline, in an environment that more closely simulates their native conditions. For example, Mitchell et al.¹⁹ used STXM to show that swollen hydrogels can have non-uniform cross-linking depending on the rate of the cross-linking reaction.

Good NEXAFS spectra of the pure components are essential for quantitative analysis of composites. Accordingly, several groups have worked to generate libraries of

NEXAFS spectra^{15,20} and to understand the relationship between subtle changes in the chemical environment of a functional group and its corresponding spectral changes.^{21,22} Ideally, thin films of pure polymers are used to generate standard NEXAFS spectra if one cannot be found in the literature. However, this is not always possible as a result of the lack of vapour pressure and poor solubility of many polymers. In such cases it is necessary to approximate the spectrum of a component by some other means, such as using a chemically similar small molecule, generating a NEXAFS spectrum by molecular modelling techniques, microtoming an embedded sample of an insoluble polymer or by summing the spectra of the diatomic building blocks of a larger structure.^{4,8}

It can be seen from the work above that it is possible to differentiate many different types of polymers based on their different functional groups, including polyurethanes and polyureas that have very similar structures. This chapter aims to extend the area of polymer characterisation by studying nanocomposite microcapsules that contain two chemically similar polyurea species.

1.2 Microencapsulation

Microcapsules are particles, 1-200 μm in size, with a liquid or solid core covered in a polymeric shell. The shell of the microcapsule can be altered to serve different functions depending upon the desired application. The wall can protect the contents of the capsule from environmental degradation, reduce toxicity to handlers, and/or offer temporal and other control over the release of core material(s).²³

Microcapsules can be prepared by a number of methods, all of which can be broadly divided into two categories.²⁴ Type A processes are those in which the core material is suspended in a continuous liquid phase and the wall-forming polymer is formed in or precipitated from solution to coat the suspended phase. Most liquids are encapsulated via type A processes, which include complex coacervation, in situ polymerisation, solvent evaporation and interfacial polymerisation. In type B processes the core material is suspended in a gas phase and the wall forming polymer is sprayed or deposited on its surface. Many solids, such as seeds, are coated using type B processes, which include spray drying and extrusion methods.

1.2.1 Interfacial Microencapsulation

One common method for encapsulating agricultural chemicals is interfacial polycondensation of an oil-soluble monomer and a water-soluble monomer. Interfacial polymerisation is a type A process where the reaction between the two monomers takes place at the interface between the dispersed oil and continuous water phases, resulting in the encapsulation of the oil droplet by the forming polymer. Three examples of polymers used to form microcapsules by this method are polyamides, polyurethanes and polyureas. Despite the fact that such microcapsules are well documented in literature^{23,25,26,31-36} and patents,^{27,28,29,30} little detailed information on many aspects of wall formation is available.

1.2.2 Polyurea Microencapsulation

Polyurea microcapsules are widely used in the controlled delivery of agricultural chemicals, such as pesticides and fertilizers. They are generally formed by reaction between an oil soluble isocyanate and a water-soluble amine. Wall formation in this

system can be divided into three stages:³¹ 1) initial polycondensation, 2) polymer precipitation resulting in an initial wall, and 3) continued membrane growth.

1) In the initial step, polycondensation of the two monomers is taking place but precipitation of the polymer is not yet observed. The location at which the initial polycondensation occurs depends on the partitioning of the two monomers between the oil and water phases.^{26,31,33} In general, polyurea microcapsules are formed using amines that are at least partially soluble in both the aqueous and organic phases and isocyanates that are soluble only in the organic phase. In such systems, it is generally believed that growth of the membrane occurs in the oil phase of the capsule, close to but not at the oil-water interface. This theory, although not universally accepted, is supported by several lines of evidence. First, the negligible solubility of the isocyanate in the aqueous phase indicates that the reaction must occur in the oil phase. Secondly, the partition coefficient of the amine into the oil phase has been shown to affect the rate of reaction and the resulting conversion of the sample. Finally, the reaction between the amine and isocyanate can be quenched by lowering the pH of the aqueous phase. Addition of acid to the aqueous phase causes the amine to become protonated, reducing its affinity for the oil phase.²⁶ Reactions at this early stage of capsule formation tend to be kinetically controlled.³²

2) The resulting polycondensate precipitates near the interface, encapsulating the organic phase in polymer. The formation of this membrane is largely controlled by the solvency of the organic phase. The higher its solvency for the polymer, the thicker and more homogeneous the resulting polymer wall will be.³¹ This is likely the result of the

polymer being highly swollen, which facilitates in-diffusion of the amine leading to high conversion. The other major factor affecting the morphology of the forming microcapsules is the rate of precipitation of the polymer. Fast precipitation of the polymer, as from a poor solvent, results in a less uniform and more macroporous capsular wall. In a good solvent, the polymer grows in solution to a larger size and precipitates out much more slowly. The slow rate of precipitation allows time for the polymer chains to align and pack neatly together resulting in a morphology with fewer macropores.

3) The final stage of capsule formation is continued wall growth. During this stage, the polymer continues to form on the already existing capsule wall. In the case where one monomer is water insoluble the growth occurs in the oil phase. The rate of polymer formation at this stage is no longer kinetically controlled. The rate-limiting step of the reaction is now the diffusion of the water-soluble monomer through the polymer at the oil-water interface.^{31,32} Diffusion of monomer into the organic phase is controlled by the solubility of the monomer in the polymer and the organic phase, and decreases with increasing wall thickness and density.

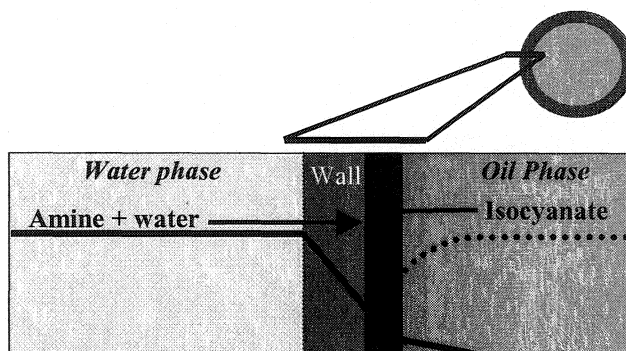
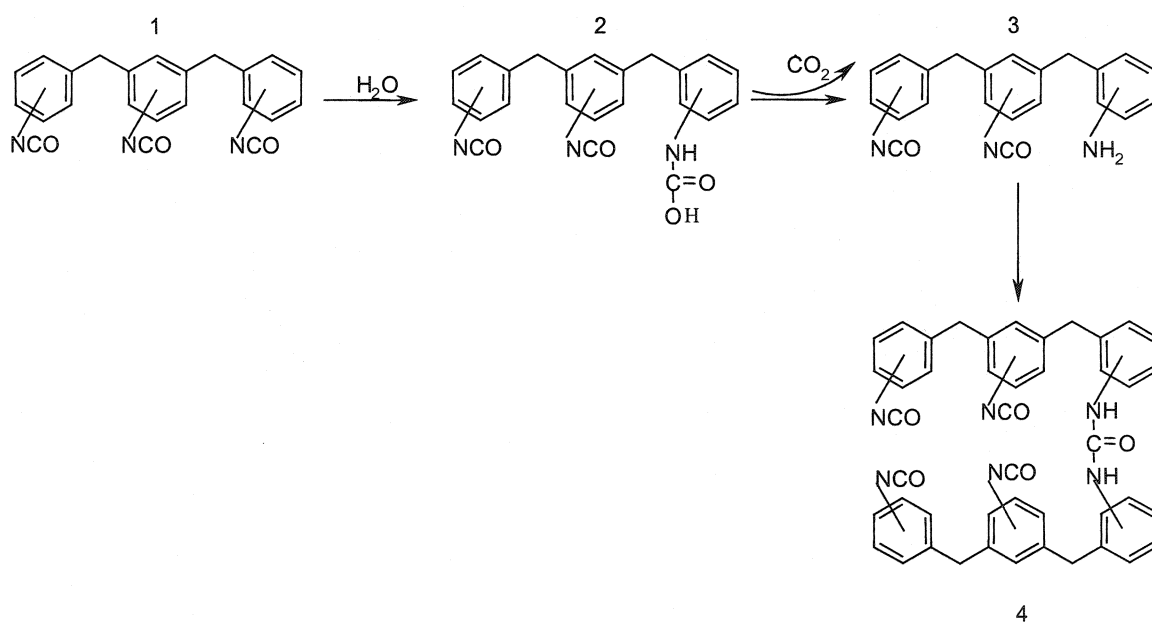


Figure 1. 7 Wall formation model illustrating wall growth occurring in a polyurea microcapsule. The concentration profiles of the amine and the isocyanate are represented by the solid and dashed lines, respectively and the shaded region indicates the main area of ongoing wall formation. As wall growth progresses the region of wall formation moves inward.

Overall, membrane growth and the performance of the resulting polyurea microcapsules is complex and is influenced by a number of interrelated parameters, including the concentration and partition coefficients of the monomers,^{31,33,34} monomer ratio,^{26,34} stirring speed,³⁵ reaction temperature,³⁴ solvency of both phases,^{31,34} as well as additives such as surfactants and stabilizers.^{34, 36}

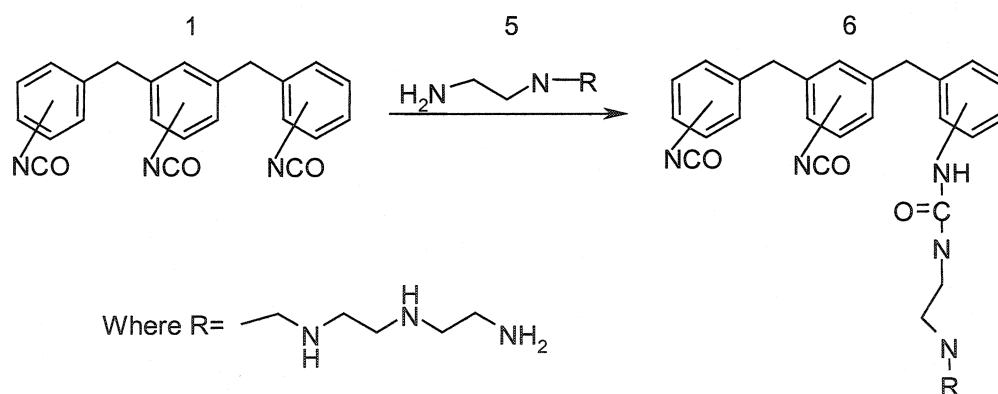
In addition to these factors, which can affect morphology and release characteristics, there are competing chemical reactions that can lead to changes in the composition of the forming membranes. First, during emulsification of the isocyanate/solvent mixture some hydrolysis of the isocyanate (1) will occur (Scheme 1.1).²⁵ Decarboxylation of the

carbamic acid intermediate (2) leads to formation of an aromatic amine (3), which quickly reacts with more isocyanate to form a SYMMETRIC polyurea (4), having two aromatically substituted nitrogens. This reaction can lead to the formation of a thin capsule wall around the oil droplet. The formation of this skin can be observed by optical microscopy. This process has been developed by Scher²⁵ to form capsules in the absence of amine.



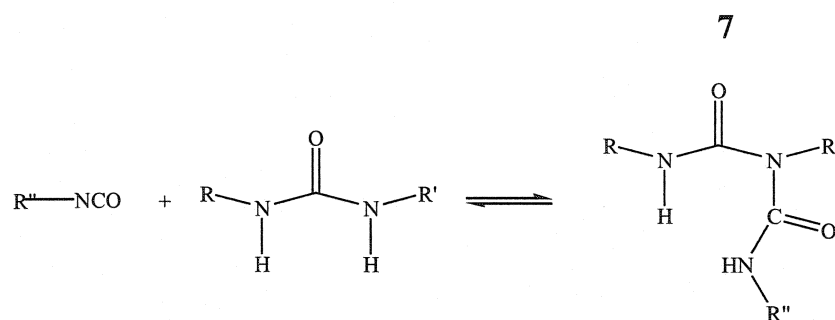
Scheme 1.1 A single reaction of aromatic isocyanates, poly [(phenyl isocyanate)-co-formaldehyde (PPIF, 1) with water, which results in the formation of a symmetric urea (4) oligomer.

Second, upon addition of amine to the aqueous phase, wall formation occurs much more rapidly. The amine used, tetraethylenepentamine (TEPA), is aliphatic (5) and reacts with the aromatic polyisocyanate to form an ASYMMETRIC urea linkage (6), having the aromatic group from the isocyanate on one nitrogen, and an aliphatic group from the amine (ethylene in this case) on the other nitrogen of the urea (Scheme 1.2). During this stage of wall formation, there is an ongoing competition between the amine and water reacting with the aromatic isocyanate (1). The relative amounts of each type of urea formed will depend on the relative diffusion rates of amine, water and isocyanate in solution as well as through the forming capsule wall, and on the relative reaction rates of water and amine with the isocyanate. A key step in wall formation involves diffusion of the amphiphilic aliphatic amine from the aqueous phase into the organic droplets.



Scheme 1. 2 A single reaction of an aromatic isocyanate (PPIF, 1) with an aliphatic amine, tetraethylenepentamine (TEPA, 5), resulting in the formation of an asymmetric urea (6) oligomer.

A second potential side reaction is biuret formation by reaction of a urea group with another isocyanate group (Scheme 1.3). This reaction is common to isocyanates,^{37,38,39} but generally requires temperatures of 100 to 150°C, and the urea group is less reactive than both amines and water.⁴⁰ Since our reactions are carried out at lower temperatures, 70 °C, in the presence of excess amine and water, biuret formation is not expected to occur to an appreciable extent.



Scheme 1. 3 Biuret (7) formation by reaction of a urea with an isocyanate.

The two steps of wall formation are summarised in Figure 1.7 below. It is expected that the side of the capsule wall in contact with the water will have a greater amount of symmetric urea and that the proportion of asymmetric urea will increase towards the inner surface of the capsule wall. This prediction is based on the observation that a thin capsule wall is formed during emulsification of the oil phase in the absence of any amine. However, it is known that aliphatic amines are, on average, 10 times more reactive towards isocyanate than water.⁴¹ Thus upon addition of amine, formation of asymmetric polyurea should dominate. This model also predicts that increasing the time the oil is

emulsified in the absence of amine should increase the amount of symmetric urea found in the capsular wall. Furthermore, the symmetric urea from the water reaction should be preferentially located on the outer portion of the capsule wall.

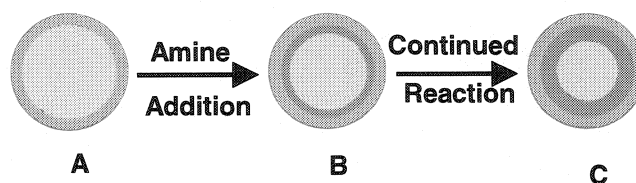


Figure 1. 8 Proposed distribution of the two types of urea across the capsular wall in a polyurea system. A) initial layer of symmetric urea resulting from emulsification of isocyanate in water, shown in green, B) region of asymmetric urea formation after addition of amine to aqueous phase, shown in blue C) continued growth of the asymmetric urea layer over time in the presence of amine.

Surprisingly, competitive reactions in interfacial polymeric systems in the presence of amine have not been studied previously to our knowledge, although the individual kinetics of reactions of small isocyanates towards water and amines have been studied.^{41,42} Reaction of isocyanate groups with water in homogeneous organic phases has been shown to be several orders of magnitude slower than the corresponding reaction with aliphatic amines. Of course, changes in the structure of isocyanate or amine could affect the relative reaction rates significantly. For example, aromatic amines are less reactive than aliphatic amines,⁴³ and within the group of aliphatic amines, the rate of reaction with isocyanates decreases with increasing substitution on or near the nitrogen.⁴² Conversely, aliphatic isocyanates are less reactive towards all nucleophiles compared to

aromatic isocyanates. Despite these varying reactivities of amines and isocyanates, in the presence of amine, water is considered not to compete significantly with the amine.⁴¹

1.3 Objective and Scope of Research

The objective of this research was to develop a scanning transmission x-ray microscope method for the analysis of polyurea microcapsules, and any other related polyurea materials developed in the future. Specifically, we focused on analysing the amount and spatial location of the two polyureas that result from the competing reactions of amine and water with isocyanate during capsule wall formation. Research emphasised understanding the difficulties and limitations associated with current sample preparation methods in the context of nano-scale chemical analysis of such materials and developing methods for overcoming some of these limitations. In addition, it was necessary to understand the effects of different urea models on the resultant NEXAFS spectra and the subsequent analysis of polyurea microcapsules.

1.4 Experimental

Materials.

Cyclohexane (99+%), ethylene diamine (99%), methylene chloride (HPLC), poly [(phenyl isocyanate)-*co*-formaldehyde] (PPIF, ca. 3.2 isocyanate groups/molecule, Mn ca. 400), poly(vinyl alcohol), (PVA 80% hydrolyzed, M.W. 9000-10 000), tetraethylenepentamine, (TEPA, tech.), *o*-tolyl isocyanate (99+%), and *p*-xylene (99+%) were purchased from Aldrich Chemical Company and used as received. Mondur MRS, (diphenyl methane diisocyanate and higher oligomers, ca. 2.6 isocyanate groups/molecule, Mn ca. 290) was donated by Bayer Corporation, and used as received.

Capsule Preparation.

A glass reactor (1 L) fitted with 4-prong stainless steel baffles (length 12 cm, width 1.1 cm) was charged with distilled water (300 g) and PVA (1.00 g). A six-bladed, 2" stainless steel stirrer was then inserted into the aqueous phase and the reactor was closed with a three-neck glass lid. The mixture was stirred at 300 rpm for 15 minutes to ensure complete dissolution of the PVA. The temperature of the reaction was controlled at 70°C using an internal thermocouple, with four 250 W infrared lamps mounted beneath the reactor serving as heat source. Next, isocyanate (2.0 g) dissolved in the core solvent, a 4:5 w/w mixture of *p*-xylene and cyclohexane (20.7 g) was added the reactor. The resulting two-phase system was allowed to emulsify for 30 minutes, unless otherwise stated. Following emulsification, the mixing speed was reduced to 200 rpm and TEPA (3.24 g dissolved in 18 g of distilled water) was added drop-wise to the oil-in-water emulsion over about 10 minutes. After the amine addition the reaction was allowed to continue for four hours. The mixture was then transferred to a separatory funnel (1 L), the aqueous layer was removed and the capsules were washed three times with distilled water. Samples of the washed capsules were stored in glass scintillation vials.

Synthesis of symmetric polyurea capsules

Capsules with walls composed of symmetric polyurea capsules were prepared according to the above microcapsule procedure with the exception that no amine was added to the system. This results in the formation of capsules with walls consisting of symmetric urea only.

Synthesis of N,N'-ethylene-bis-(N'(2-methyl phenyl))urea

Synthesis of this bis-urea model compound was carried out under nitrogen. All apparatus used was dried overnight at 120°C. *o*-Tolyl isocyanate (2.45 g) was dissolved in methylene chloride (50 mL). Ethylene diamine (1.12 g, mol) was dissolved in methylene chloride (10 mL) in a scintillation vial (20 mL), and 5 mL of this solution was added drop-wise by syringe to the stirring isocyanate solution. Immediately upon addition of the amine solution, the product precipitated from solution. After adding 5 mL of amine solution, a further 100 mL of methylene chloride was added to the reaction flask to facilitate mixing, and then the remainder of the amine solution was added dropwise. The resulting product was a fine white powder that was collected by filtration and washed with methylene chloride: yield 2.90g (96.7 %); m.p. 249-252 °C; ¹H-NMR (300 MHz, d₆-DMSO) δ 2.17 (s, 6H), 3.20 (d, 4H), 6.60 (m, 2H), 6.86 (m, 2H), 7.04-7.11 (m, 4H), 7.67 (s, 2H), 7.79 (d, 2H). ¹³C NMR (300 MHz, d₆-DMSO), δ 17.8, 120.6, 121.9, 125.9, 126.8, 130.0, 138.1, 155.5. The “missing” CH₂ peak was beneath the solvent signal and was located at δ 40.1 using a DEPT experiment. MS (electrospray, M_{calculated}=326.4), the three most intense peaks are listed: (2M+H⁺) 653.3; (M+H⁺) 327.2; (M- (C₆H₄CH₃NH)) 220.0. Both ¹H NMR and the melting point correspond to values previously reported in the literature.⁴⁴ The broadness of the melting point is attributed to partial decomposition of the sample at those temperatures

Environmental Scanning Electron Microscopy (ESEM)

A Phillips ElectroScan 2020 environmental scanning electron microscope was used for all ESEM work shown. Images were recorded digitally as well as with a Polaroid camera. Samples were prepared for analysis by ESEM using the following procedure:

A piece of glass microscope cover slip was applied to a clean ESEM stub with double-sided tape. Excess tape was then removed using a scalpel and the glass was cleaned with methanol. After cleaning, one drop of dilute capsules in water was placed on the glass and allowed to dry overnight. When dry, the stubs, with capsule sample, were sputter coated with a 4-5nm coating of gold. This gold coating is necessary to ensure the sample is sufficiently conductive to dissipate charges developed during analysis.

Transmission Electron Microscopy (TEM)

A Jeol 1200 EX transmission electron microscope was used for all TEM work shown. Samples were prepared for TEM analysis according to the following procedure:

A sample of capsules was filtered (reduced pressure Buchner, Whatman #1, 42.5 mm paper) to dryness and transferred to a mortar. The capsules were then crushed under liquid nitrogen, washed with toluene and re-filtered.

The capsule walls, left after the extraction above, were then dried overnight in a vacuum oven at room temperature. Following drying, the capsule shells were embedded in Spurr's¹ Resin and cured at elevated temperature. After curing, the resin bullets were

¹ Spurr's resin is a common embedding medium, comprised of: nonenyl succinic anhydride (NSA), the diglycidyl ether of poly (propylene glycol) (DER 736), vinylcyclohexene dioxide (ERL 4206), and 2-dimethylaminoethanol (DMAE).

microtomed to 100 nm thick slices. These samples can be used both for TEM and STXM analysis.

Scanning Transmission X-ray Microscopy (STXM)

Microcapsule wall samples were prepared for STXM analysis according to the method described for TEM, except that 200 nm thick sections were prepared. Samples of the bis-urea small molecule model were prepared by depositing crystals from an ethanol suspension onto a Si_3N_4 window.

Initial work on 30 minute emulsification capsule sample, diphenyl urea and N-phenyl N'-butylurea were carried out with the beam line 7.0 STXM^{45,46} at the Advanced Light Source (ALS). Subsequently, all images, image sequences, linescans, and spectra of 30 second and 2 hour capsule samples, bis-urea and polymeric models were recorded with the beam line 5.3.2 STXM at the ALS. This instrument provides images with better than 80 nm spatial resolution, and an energy resolution of about 100 meV. The reference spectra were recorded with the same instrument using similar acquisition parameters.

Radiation damage is a significant problem in x-ray microscopy.⁴⁷ Its major effect is to reduce the intensity of the carbonyl π^* peak (~ 288 eV) and increase the intensity of the C=C π^* signal at ~ 285 eV. A check for extent of damage was made after each image sequence by recording an image at 289 eV where a reduction in carbonyl intensity could be detected. Results were not used when excessive damage was observed.

1.5 Results and Discussion

During STXM analysis plane polarised x-rays from the synchrotron are passed through a monochromator and focused to a point of ~ 50 nm using a Fresnel zone plate.

An image of the sample is generated when the sample is then raster scanned across the focal point. The transmitted x-ray photons are counted behind the sample by an x-ray sensitive detector. Samples can be run in air when the carbon edge is being analysed, but to reduce adsorption of x-rays by air, the sample chamber is generally evacuated and filled with ~ 200 mBar helium.

Although an image of a sample at a single photon energy may give information about morphology of the material, STXM can provide much more than that. When images of the sample are collected at many sequential energies with a resolution of ~ 100 meV an image sequence or 'stack' is generated. This stack has a NEXAFS spectrum at each pixel of the image, which can be recovered by a variety of methods, to be discussed below.

For quantitative analysis the transmitted x-ray signal must be converted to optical density (OD, at energy E) using the relationship shown in Equation 1.1. I_0 is the incident x-ray flux

$$OD(E) = \ln(I_0/I) \qquad \text{Equation 1. 1}$$

and can be collected at the same time as sample analysis if a suitable hole in the sample is found. If this cannot be done, it is collected immediately before or after the collection of an image sequence. I is the transmitted flux through the sample and \ln is the natural logarithm. OD is linearly related to the properties of the sample by Equation 1.2, where $\mu(E)$ is the mass absorption coefficient at energy E, which can be derived from the NEXAFS spectra of the pure material, ρ is the density of the material and t is the sample thickness.

$$OD(E) = \mu(E)\rho t \quad \text{Equation 1.2}$$

Thus it can be seen that several factors affect the images and spectra acquired including sample composition and density, which are inherent to the material itself, and sample thickness which depends on the amount of material present and can be affected significantly by sample preparation methods.

Equation 1.2 assumes the presence of only one material, however the materials we were interested in contained two different polyurea species as well as the epoxy resin used for embedding. Therefore, it is necessary to define OD by Equation 1.3 where OD is defined a sum of the ODs of j non-interacting components where μ_j and ρ_j are the mass absorption coefficient and density of component j of the mixture and t_j represents the relative path length or thickness of component j .

$$OD = \mu(E)_1\rho_1t_1 + \mu(E)_2\rho_2t_2 + \dots + \mu(E)_j\rho_jt_j \quad \text{Equation 1.3}$$

Therefore if one measures OD at different photon energies (E) to build a “stack” and the mass absorption coefficient of each component in the mixture is known, Equation 1.3 can be solved at every pixel. Once the amount or thickness of a given component has been determined at each pixel, “component maps” can be generated that show the location and amount of each component.⁴⁸ The method chosen to do this is known as single value decomposition (SVD) analysis.

In order to investigate the spatial location of the two different polyureas within an asymmetric capsule membrane, the polymers must be spectroscopically different, and it must be possible to identify orientation of the membranes embedded in the epoxy. That

is, it must be possible to identify the inside and outside surfaces of the membrane. Therefore it was necessary to develop model spectra for symmetric and asymmetric polyurea, and specific sample preparation methods. This work will be discussed below.

1.5.1 Sample Preparation

For STXM analysis, samples must be x-ray transparent at the energies of analysis. Therefore samples should be 50-300 nm thick for standard carbon analysis but can be up to 2 μ m thick for oxygen and nitrogen analysis, and for low density samples, such as water swollen gels.¹⁹ As discussed above, capsules were crushed under liquid nitrogen, embedded in epoxy resin, and microtomed prior to analysis, such that a cross-section of capsule wall could be analysed. Although this process resulted in samples that could easily be imaged by both TEM and STXM it was difficult to unequivocally determine which side of the membrane had originally been on the outside of the capsule. In order to overcome this difficulty, capsules to be analysed were sputter coated with ~ 10 nm of gold prior to crushing under liquid nitrogen. This coating of gold could then serve as a marker of the outer wall of the capsule after embedding and microtoming.

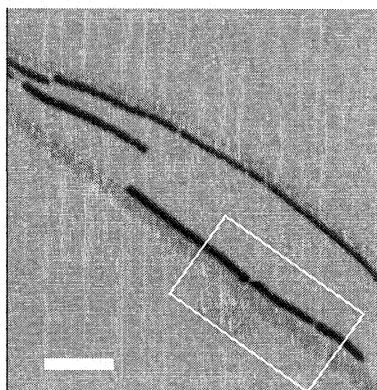


Figure 1. 9 STXM image at 285 eV of gold coated capsule wall fragments, where black regions are the gold coating, the dark grey lines are polyurea and the lighter grey background is Spurr's embedding resin. Scale bar is 2 μm .

The gold-coated microcapsules were embedded, microtomed and analysed by TEM and STXM. Some regions of the gold layer survived the embedding process and could easily be seen during STXM analysis (Figure 1.9). Regions of uncoated capsule wall and free gold were also visible. Such regions were common and suggest that the gold does not adhere well to the polyurea wall. Despite the limited affinity of the gold for the polyurea wall, regions where the gold remained in contact with the capsule wall could be found and used for analysis. The area indicated by the box in Figure 1.9 indicates a good region for analysis, given that the gold coating remains in contact with the capsule wall fragment.

1.5.2 Analysis of Capsule Wall Composition

From STXM analysis we wished to learn the following about these capsule samples:

1. Is it possible to identify both symmetric and asymmetric polyurea species in the capsule walls, given their similar chemical structure?
2. Is it possible to detect changes in the relative amounts of the two polyurea species based on different preparation procedures?
3. Can component maps be generated to show the location of the two polyurea species in the capsule wall?

After an image sequence or “stack” has been generated, it is necessary to extract the chemical information about the sample from that stack. There are several methods by which this can be done, some of which will be discussed below. The data analysis for the work discussed here was carried out using software designed and written by Hitchcock et al.⁴⁹ known as aXix2000, which is built on top of the data analysis package known as IDL (Research Systems Inc. an Eastman Kodak Company). This software package allows the user to perform many tasks including: aligning the images in a stack; calibrating energy scales; extracting spectra from any region of a stack; adding and subtracting spectra; directly comparing spectra from several different regions or samples; and generating quantitative information via the creation of component maps.

1.5.2.1 Development of Model Compounds

In order to fully characterise the capsule wall samples it was necessary to acquire STXM spectra for pure symmetric and asymmetric polyureas, and for Spurr's epoxy resin used for embedding. The spectra for Spurr's epoxy resin was simply extracted from regions in each sample not containing any wall fragments. Typically, model STXM spectra for polymers are obtained by casting a thin layer of polymer from solution onto a silicon nitride window. However, polyureas have limited solubility due to their strong hydrogen bonding and as a result it was not possible to cast the thin films needed for STXM analysis. To overcome this, a number of model compounds were explored to obtain reference spectra for the asymmetric and symmetric polyurea species.

C 1s NEXAFS spectra of three models for the symmetric species are shown: diphenyl urea, MDI-urea¹⁵ and the symmetric polyurea as obtained from a capsule prepared from PPIF without added amine (Figure 1.10). Figure 1.10 further shows the C 1s spectra of three models for the asymmetric urea: N'-phenyl-N-butyl-urea, a simulated spectrum of N'-phenyl-N-ethyl-urea generated by a weighted sum of the spectra of diphenyl urea and N'-phenyl-N-butyl-urea, and the spectrum from the inner wall of a capsule prepared from PPIF with a relatively short emulsification time (30 seconds) prior to amine (TEPA) addition, embedded in Spurr's resin.

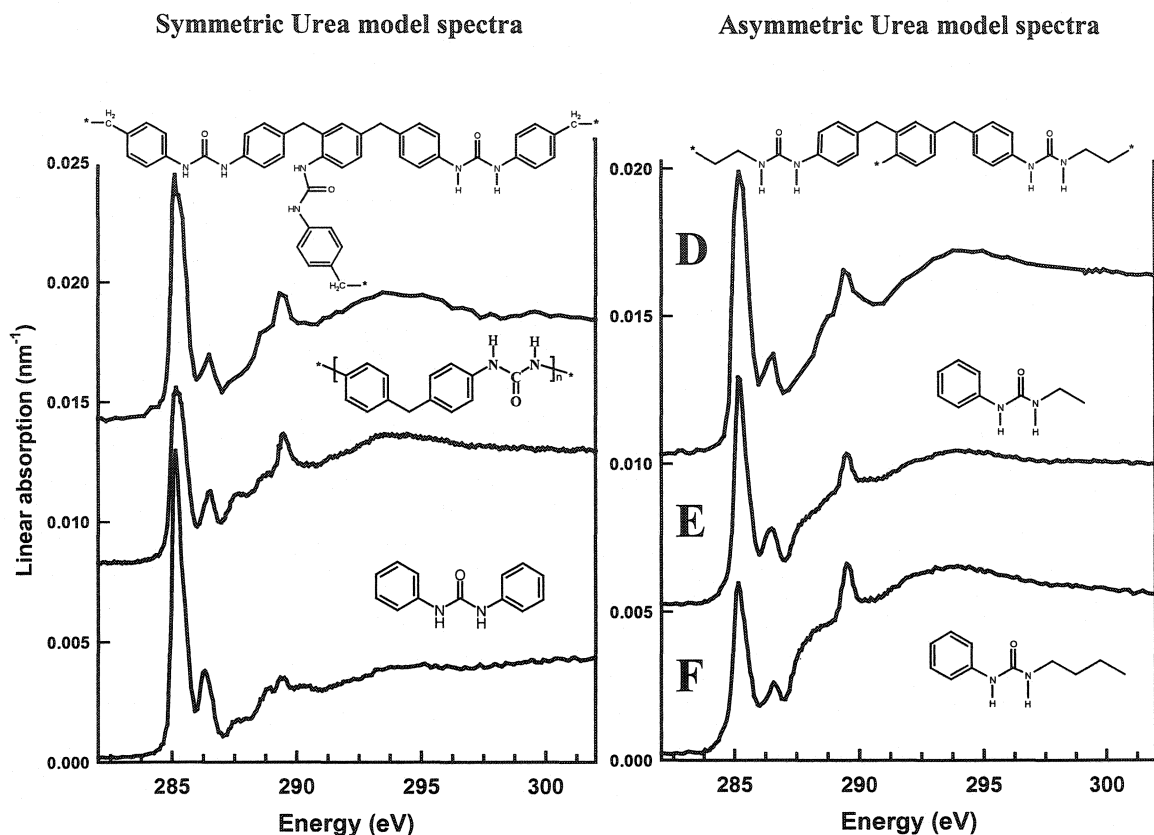


Figure 1.10 C 1s NEXAFS spectra of model species for the (left) symmetric and (right) asymmetric ureas. The vertical scales are set to linear absorption. Note: PPIF A and D show representative structures only.

The spectra of these reference materials were converted to linear absorption scales by matching the signal in the pre-edge and post-edge regions to the sum of the tabulated atomic mass absorption coefficients⁵⁰ appropriate for the chemical composition of each component.²⁹ The compositions of the repeat units were taken to be $C_{14}H_{12}N_2O$ for the symmetric species and $C_{16}H_{16}N_2O$ for the asymmetric species.

In general, there is good agreement between chemical composition and the positions of corresponding spectral features, and reasonable agreement in relative intensities in all

models investigated. However, the simple molecular models, diphenylurea and N'-phenyl-N-butyl-urea greatly overestimate the spectral differences between the symmetric and asymmetric polyurea structures because these model species do not have the correct ratio of phenyl to aliphatic content. The effect of using models with incorrect atomic and functional group ratios is discussed in Section 1.6.2.2 below.

In addition to the asymmetric models (Figure 1.10) we explored an ethylene bridged bis urea species ((N,N''-ethylene bis (N'(2-methyl phenyl)) urea). However, this species formed perfect single crystals and it was difficult to derive a spectrum of randomly oriented species from the polarization dependent results.⁵¹ For this reason, the bis urea was not pursued as a model compound for polyurea capsule.²

Since small molecules with the correct atomic and functional group ratios could not be formed, the best reference compounds for capsule analysis were determined to be: the symmetric polyurea (A); the polyurea formed with short emulsion time (30 s) capsule for the asymmetric urea (D). In addition, the spectrum for Spurr's epoxy was extracted from a capsule free region of each sample (Figure 1.11). This was because small variations in the epoxy formulation from sample to sample led to detectable differences in the epoxy spectra.

² Bis urea was used as a model compound to test the ability of STXM to determine molecular alignment and crystal orientation. This work lies outside the scope of this thesis and is not discussed here.

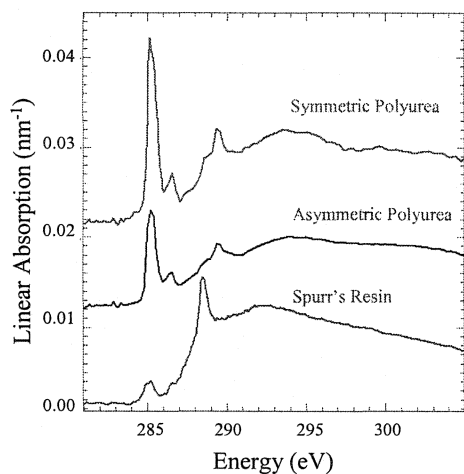


Figure 1. 11 NEXAFS spectra of the polyurea models and a typical spectrum for Spurr's embedding resin used for sample analysis.

The C 1s NEXAFS spectra of all components showed peaks corresponding to C 1s(C=O) \rightarrow $\pi^*_{C=O}$ transitions, which occur at 289.5 eV for both polyureas and at 288.5 eV for the epoxy. The \sim 1 eV energy shift between these $\pi^*_{C=O}$ resonances distinguished the epoxy from the polyureas of the capsule wall. The C 1s spectra of both the symmetric and asymmetric polyureas were dominated by the C 1s(C-H) \rightarrow π^*_{ring} transition at 285.1 eV. As the symmetric polyurea had twice the number of phenyl rings relative to asymmetric polyurea, its 285.1 eV peak was roughly twice as intense relative to the C 1s continuum intensity ($E > 300$ eV). While these C 1s spectra contained additional features which can be associated with C 1s excitations to σ^*_{CH} , σ^*_{CC} and σ^*_{CO} states,²⁴ it was the intensity of the π^*_{ring} transition relative to the $\pi^*_{C=O}$ and, particularly, relative to the continuum signal that provided the main analytical capability.

1.5.2.2 Quantitative Analysis - Component Maps

Data analysis of these samples worked well when using small molecule models (Figure 1.11C and F) where spectral differences were most pronounced. Shown in Figure 1.12 below are the component maps for symmetric and asymmetric polyurea and the

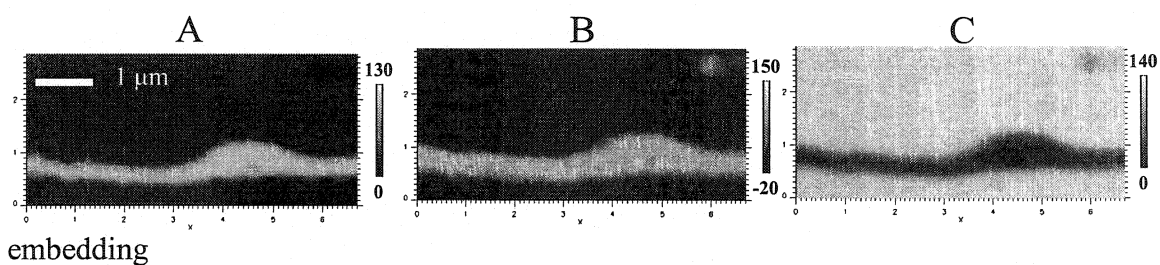


Figure 1. 12 Component maps for symmetric (A) and asymmetric (B) polyureas and embedding epoxy (C) of a polyurea wall fragment emulsified for 30 minutes, generated using small molecule models (Figure 1.11C and F).

epoxy. If these images are colour coded and superimposed, a composition map depicting the spatial location of the three components can be generated. It is then possible to construct wall profiles of the component maps that illustrate the amount of each component present. Shown in Figure 1.13 are two composition maps and wall profiles generated from the same wall fragment using two different sets of model compounds/spectra. Figure 1.13A corresponds to the component maps shown above in Figure 1.12 and was generated using diphenylurea and phenyl butylurea as the models for symmetric and asymmetric polyurea respectively (Figure 1.11 C and F, respectively). In Figure 13B symmetric polyurea (Figure 1.11A) was used in place of phenylurea,

resulting in a large change in the final ratio of the polyureas. It should also be noted that, despite the fact that the ratio of the two polyureas changed significantly, both sets of models resulted in composition maps and profiles depicting a compositional gradient across the membrane.

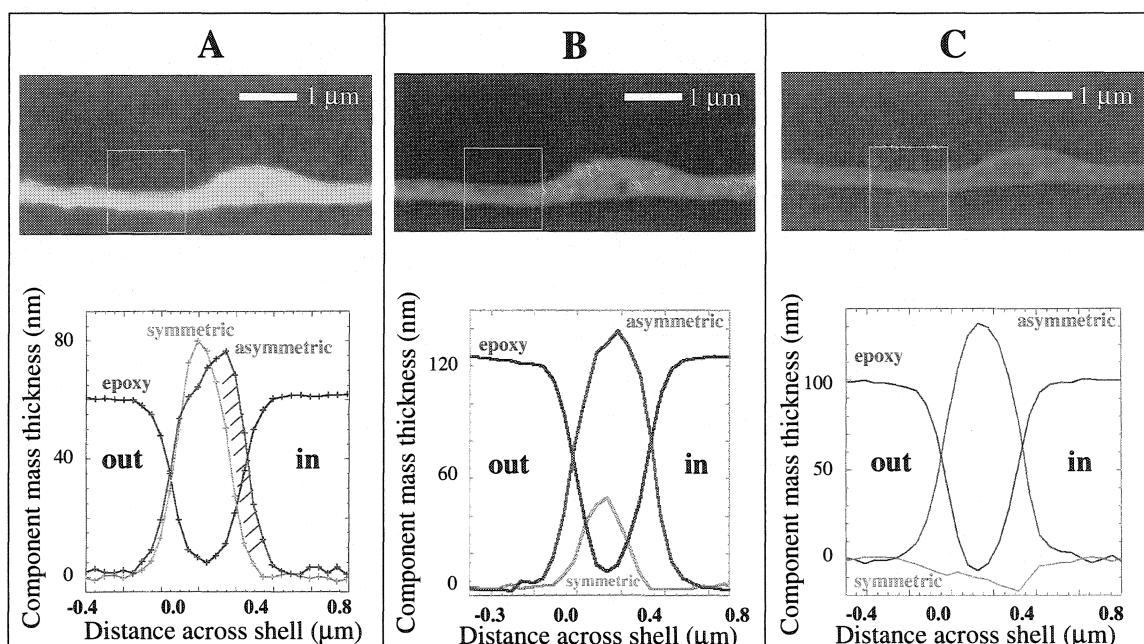


Figure 1.13 Composition maps (top) and profiles of the same capsule sample generated using different sets of model spectra for data analysis: simple molecular models for both symmetric and asymmetric polyureas (A), using a simple molecular model for asymmetric urea and polymeric model for symmetric polyurea (B) and using polymeric models for both symmetric and asymmetric polyurea (C). Profiles were generated from the regions indicated by the yellow boxes. Note: x and y scales are different.

As stated above, the best model spectra are generated from the polymers themselves. However, when the sample was fit with both polymeric models the results gave a negative amount of symmetric urea, though its asymmetry still matches that expected for a compositional gradient, suggesting that the concentration of phenyl groups decreases from the outside to the inside of the membrane. When the 2hr emulsification sample was fit with the same polymeric models a negative fit also resulted for the symmetric urea.

The poor fitting is believed to result from several facts: symmetric and asymmetric polyureas have very similar spectra, density variations and that the spectrum for asymmetric urea was extracted from a sample of unknown composition because a true model spectrum could not be obtained.

1.5.2.3 Spectral Extraction Method

A method to retrieve chemical information about a sample of interest is simply to extract the NEXAFS spectrum of the area of interest. This not only allows for the chemistry of a particular region to be determined but also enables the direct comparison of spectra from different regions in a single sample or regions from several different samples. The largest limitation of this method is that it does not allow for quantification of the components discovered in a particular sample. The samples examined above, which were emulsified for 30 minutes prior to amine addition did not clearly show the predicted gradient across the membrane. Therefore, we prepared capsules with a 2 hour emulsification time in an effort to enhance any asymmetry present in the capsule wall.

Using the spectral extraction method, wall fragments from two different batches of capsules prepared with emulsification times of 30 seconds and 2 hours were compared.

The capsule prepared with a short (30 second) emulsification time prior to amine addition was expected to consist predominantly of symmetric polyurea and to be homogeneous in composition across the capsule wall. Alternatively the capsule prepared with a 2 hour emulsification time prior to the addition of amine, was expected to show both symmetric and asymmetric polyureas and to be chemically asymmetric across the capsule wall, for the reasons discussed above.

In each case, spectra were extracted from the inner and outer capsule wall (Figure 1.13). The spectra extracted from the inner and outer capsule wall regions in the sample prepared with only a 30 second emulsification time are identical. This indicated that this capsule shows no chemical asymmetry. The two inner spectra extracted from the capsule that was emulsified for 2 hours were the same, indicating that these regions have the same composition. The spectrum taken from the inner region of the capsule wall had a smaller $C1s \rightarrow \pi^*_{ring}$ ($E \sim 285$ eV) to $C1s \rightarrow \pi^*_{C=O}$ ($E = 289.5$) ratio and $C1s \rightarrow \pi^*_{ring}$ ($E \sim 285$ eV) to $C1s \rightarrow \sigma^*_{aliphatic}$ ($E > 292$ eV) ratio relative to that of the spectrum from the outer region of the capsule wall. This does suggest that this inner region has more asymmetric polyurea, however, it must be noted that this spectrum is diluted with epoxy, as witnessed by the appearance of a peak at ~ 288.5 eV, and is therefore not a reliable indicator of composition.

Therefore, based on this information it is not possible to conclusively state that these membranes exhibit the predicted asymmetric composition. In the future, with higher beam resolution and/or thicker membranes it may be possible to address this problem further.

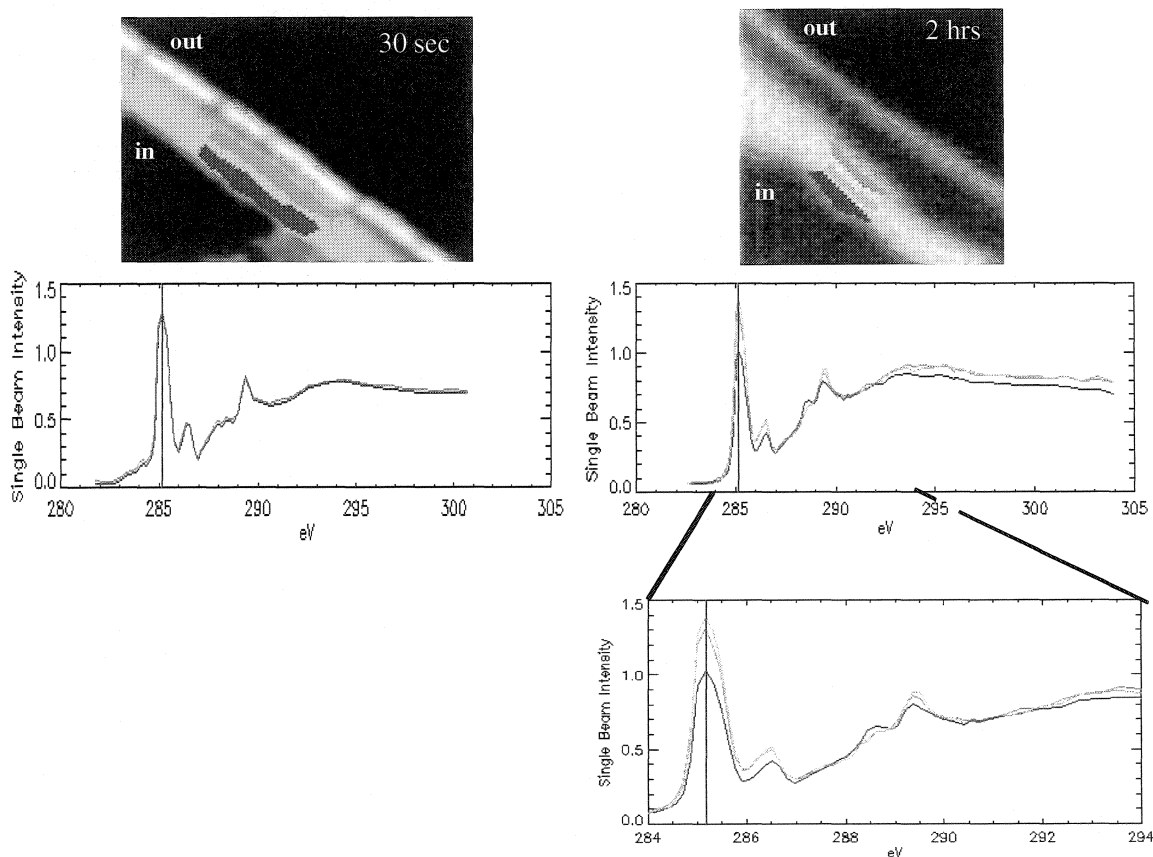


Figure 1. 14 STXM images at 285.16 eV and the NEXAFS spectra extracted from capsule wall fragments prepared with 30 second and 2 hour emulsification times. The coloured regions indicate the areas from which the spectra were extracted. Scale bar is 1 μ m. Note the red line corresponds the energy of the images shown.

1.6 Conclusions

This work was challenging for several reasons. First, the capsule walls under investigation have a cross-section of only ~200 nm. These thin membranes push the spatial resolution of the STXM which images with a beam of ~50nm. This limits our ability to analyse chemically distinct regions within them. Furthermore, controlling the

orientation of such thin membranes during the embedding process can not currently be done. Twisting and curling of the membranes may occur during embedding, which would further reduce the ability to resolve chemically unique areas. Secondly, the symmetric and asymmetric polyureas are chemically very similar and therefore have very similar NEXAFS spectra, which were difficult for the fitting software to differentiate. Despite these challenges we are confident in concluding the following:

1. During lengthy emulsification times (2 hours) a significant amount of isocyanate reacts with water to form symmetric urea prior to amine addition. This capsule wall can be seen using an optical microscope. Despite this, capsule walls appear to have a symmetric composition, or have asymmetry that is below what can be currently be detected with the 5.3.2 STXM at the ALS, and are comprised primarily of asymmetric polyurea.
2. Although composition maps generated using small molecule urea models are not believed to show correct values for the amounts of materials present they did suggest that the membranes have some compositional asymmetry.

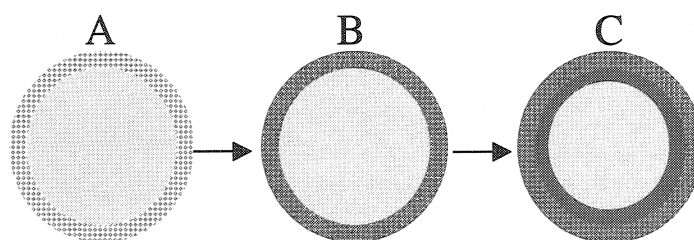


Figure 1. 15 Model of capsule wall formation depicting the chemical asymmetry believed to be present in polyurea capsule walls.

3. Capsules prepared with short emulsification times (≤ 30 seconds) were chemically symmetric, or had asymmetry that is below what can be currently be detected with the 5.3.2 STXM at the ALS. The chemistry of these capsules was symmetric, suggesting that when both water and amine are present, the amine reaction dominates. This is in agreement with rates of reaction of isocyanates with small molecule amines and water.

References

-
- ¹ Goodhew, P.J. and Humpheys, *Electron Microscopy and Analysis, 2nd Ed.* Taylor and Francis, London, 1988.
- ² Loretto, M.H. *Electron Beam Analysis of Materials, 2nd Ed.*, Chapman and Hall, London, 1994.
- ³ Koprinarov, I., Hitchcock, A.P., <http://unicorn.mcmaster.ca/PolySTXMintro-all.doc>, 2000.
- ⁴ J. Stöhr, *NEXAFS spectroscopy*, Springer-Verlag, Berlin, 1992
- ⁵ H. Ade, X. Zhang, S. Cameron, C. Costello, J. Kirz, and S. Williams, *Science*, **258**, 972, 1992.
- ⁶ H. Ade and B. Hsiao, *Science*, **262**, 1427, 1992.
- ⁷ H. Ade, *Exp. Methods in Physical Sciences*, JAR Samson and D.L. Ederer, eds (Academic Press, NY, 1998)
- ⁸ H. Ade and S.G. Urquhart, in “*Chemical Applications of Synchrotron Radiation*” T. K. Sham, ed. (World Scientific Publishing, 2002).
- ⁹ J. Kirz, C. Jacobsen and M. Howells, *Quarterly Reviews of Biophysics* **33**, 33, 1995.

-
- ¹⁰ A.P. Hitchcock, C. Morin, T. Tyliczszak, I.N. Koprinarov, H. Ikeura-Sekiguchi, J.R. Lawrence and G.G. Leppard, *Surf. Rev. Lett.* (2002) in press.
- ¹¹ A.P. Hitchcock, I. Koprinarov, L.M. Croll, H. Stöver and E.M. Kneedler, in preparation
- ¹² Ade, H.; Urquart, S. in *Chemical Applications of Synchrotron Radiation, Part 1*, Ed. T.K. Sham, World Scientific, New Jersey, 285, 2002.
- ¹³ H. Ade *Trends Polym. Sci*, **5**, 85, 1997.
- ¹⁴ I. Koprinarov, A.P. Hitchcock, W.H. Li, Y.M. Heng, H.D.H Stöver, *Macromolecules*, **34**, 4424, 2001.
- ¹⁵ S.G. Urquart, A.P. Smith, H.W. Ade, A.P. Hitchcock, E.G. Rightor, W. Lidy, *J. Phys. Chem. B*, **103**, 4603, 1999.
- ¹⁶ S.G. Urquart, A.P. Hitchcock, A.P. Smith, H.W. Ade, W. Lidy, E.G. Rightor, G.E. Mitchell, *J. Electron. Spectrosc. Relat. Phenom.* **100**, 119, 1999.
- ¹⁷ A. Fujimori, T. Araki, H. Nakahara, E. Ito, M. Hara, H. Ishii, Y. Ouchi, K. Seki, *Langmuir*, **18**, 1437, 2002.
- ¹⁸ A.P. Smith, C. Bai, H. Ade, R.J. Spontak, C.M. Balik, C.C. Koch, *Macromol. Rapid Commun.*, **19**, 557, 1998.

-
- ¹⁹ G.E. Mitchell, L.R. Wilson, M.T. Dineen, S.G. Urquhart, F. Hayes, E.G. Rightor, A.P. Hitchcock, H. Ade, *Macromolecules*, **35**, 1336, 2002.
- ²⁰ A.P. Hitchcock, S.G. Urquhart, E.G. Rightor, *J. Phys. Chem. B*, **96**, 8736, 1992.
- ²¹ S.G. Urquhart, H. Ade, *J. Phys. Chem. B*, **106**, 8531, 2002.
- ²² S.G. Urquhart, A.P. Hitchcock, R.D. Priester, E.G. Rightor, *J. Polym. Sci, Part B*, **33**, 1603, 1995.
- ²³ Paul, D.R. and Harris, F.W., *Controlled Release Polymeric Formulations*, Am. Chem. Soc., (1976).
- ²⁴ Kirk, R.E., Othmer, D.F., *Encyclopedia of Chemical Technology*, Mark, H.F., McKetta, J.J., Jr., Othmer, D.F., Standen, A., edit., Interscience, New York, (1974).
- ²⁵ Scher, H.B., *Controlled Release Pesticides*, Am. Chem. Soc., (1977).
- ²⁶ Yadav, S.K., Khilar, K.C., and Suresh, A.K., *AIChE J.*, **42**, 2616, (1996).
- ²⁷ Seitz, M.E., Brinker, R.J., and Travers, J.N., US Patent 5 925 595 (1997).
- ²⁸ Hasslin, H.W., US Patent 5 837 290 (1995).
- ²⁹ Vivant, G., US Patent 4 738 898 (1986).
- ³⁰ Scher, H.B., US Patent 4 140 516 (1977).
- ³¹ Arshady, R., *J. Microencapsulation*, **6**, 13, (1989).

- ³² Yadav, S.K., Suresh, A.K., and Khilar, K.C., *AIChE. J.*, **36**, 431, (1990).
- ³³ Morgan, P.W., *Condensation Polymers: Interfacial and Solution Methods*, Interscience Publishers, New York, (1965).
- ³⁴ Vanbesien, D.W., *Synthesis and Properties of Polyurea Micocapsules*, M.Sc. Thesis, McMaster University, (1999).
- ³⁵ Ni, P., Zhang, M., and Yan, N., *J. Membrane Sci.*, **103**, 51, (1995).
- ³⁶ Chao, D.Y., *J. App. Polym. Sci.*, **47**, 646, (1993).
- ³⁷ Szycher, M., *Szycher's Handbook of Polyurethanes*, CRC Press, Boca Raton, 1999.
- ³⁸ Balewski, A., Lesiak, T., and Ciemniak, G., *Angew. Makromol. Chem.*, **131**, 1, 1985.
- ³⁹ Balewski, A., Lesiak, T., and Ciemniak, G., *Angew. Makromol. Chem.*, **142**, 79, 1986.
- ⁴⁰ Johnson, P.C. in: *Advances in Polyurethane Technology* Buist, J.M. and Gudgeon, H. edit., John Wiley and Sons Inc., New York, (1968).
- ⁴¹ Giles, D.E., in: *The Chemistry of Cyanates and Their Thio Derivatives*, Patai, S. edit., John Wiley and Sons, Chichester, (1977).
- ⁴² Wright, P., and Cumming, A.P.C., *Solid Urethane Elastomers*, Gordon and Breach Science Publishers, New York, (1969).
- ⁴³ Buist, J.M., and Gudgeon, H., *Advance in Polyurethane Technology*, John Wiley and Sons Inc., New York, (1968)

-
- ⁴⁴ Guo, D.S., Huang R.Q., Gao, R.H., Wu, Z.G., *Chemical Journal of Chinese Universities*, **17**, 255, 1996.
- ⁴⁵ T. Warwick, H. Padmore, H. Ade, A.P. Hitchcock, E.G. Rightor and B. Tonner, *J. Electron Spectrosc.* **84**, 85 1997.
- ⁴⁶ T. Warwick, K. Franck, J.B. Kortwright, G. Meigs, M. Moronne, S. Myneni, E. Rotenberg, S. Seal, W.F. Steele, H. Ade, A. Garcia, S. Cerasari, J. Denlinger, S. Hayakawa, A.P. Hitchcock, T. Tyliczszak, E.G. Rightor, H.-J. Shin and B. Tonner, *Rev. Sci. Inst.* **69**, 2964 (1998).
- ⁴⁷ T. Coffey, S.G. Urquhart and H. Ade, *J. Electron Spectrosc. Rel. Phen.* **122**,65, 2002.
- ⁴⁸ I.N. Koprinarov, A.P. Hitchcock, C. McCrory, R.F. Childs, *J. Phys. Chem., Part B*, **106**, 5358, 2002.
- ⁴⁹ <http://unicorn.chemistry.mcmaster.ca/aXis2000.html>
- ⁵⁰ B.L Henke, E.M. Gullikson, and J.C. Davis, *At. Nucl. Data Tables*, **54**, 181, 1993.
- ⁵¹ L. M. Croll, C. Morin, A.P. Hitchcock, H.D.H Stöver, *J. Synchrotron*, **10**(3), 265, 2003.

**CHAPTER 2 - FORMATION OF TECTOCAPSULES: ASSEMBLY OF
POLY(DIVINYLBENZENE-*ALT*-MALEIC ANHYDRIDE) MICROSPHERES AND MICROGELS
AT THE OIL-WATER INTERFACE**

2.0 Introduction

This chapter will present a new class of microcapsules prepared from poly(divinylbenzene-*alt*-maleic anhydride) (DVB/MAn) microspheres and microgels. The DVB/MAn particles were assembled at the oil-water interface of an emulsion and covalently cross-linked in place to form macroporous capsule walls (Figure 2.1). A general review of particle assembly at interfaces and an introduction to polymer particles follows below. This chapter also lays the groundwork for the polyurea and microsphere composite capsules discussed in Chapter 3.

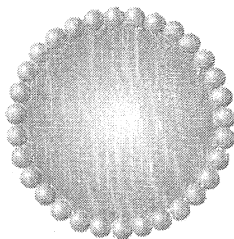


Figure 2. 1 Cross-section of a microcapsule prepared from polymer microsphere building blocks rather than traditional polymers.

2.1 Particle Assembly at Interfaces

Solid particles assembled at an oil-water interface were first observed independently by Ramsden¹ and Pickering² who were interested in preparing colloiddally stable pesticide formulations without using soaps. Pickering noted that reducing the particle size increased the stability of his emulsions. He further noted that this only applied to

materials that were insoluble in water but were “wetted more easily by water than by oil” since materials more easily wetted by oil were simply abstracted from the water by the oil causing colouration of the oil and not emulsification. Stabilisation of the oil droplets by the particles was attributed to the fact that particles protruding from the droplet’s surface prevented droplet-droplet contact and therefore coalescence. Later Bancroft³ developed a rule, which stated that the phase in which the particles were more soluble will become the external or continuous phase. In 1923, Hildebrand’s group⁴ confirmed this theory by observing mixtures of benzene in water stabilised with lampblack^{*,5} and stated that “...the powder must collect at the interface in order to be effective.” and “...this will occur only when the solid is wetted by both liquids, with a finite angle of contact of the interface with the solid.”

Since that time, the ability of fine particles to assemble at the oil-water interface has been exploited for many applications in addition to emulsion stabilisation^{6,7} such as extraction of fine particles from aqueous suspensions^{8,9} and formation of 2-dimensional colloidal crystals^{10,11}. Most recently, there has been increased interest in using such assembled colloids to form microcapsules for controlled delivery applications. For example, Caruso et al.^{12,13} used layer-by-layer (LbL) assembly of charged SiO₂ particles and polymers on the surface of charged polystyrene latex particles. Subsequent dissolution of the core template transformed these core-shell composite particles into hollow microspheres. Velev et al.^{14,15,16} reported the multi-step ionic assembly of

* Lampblack is a finely divided form of carbon that was produced by burning organic compounds in insufficient oxygen. It was typically used as a pigment and filler.⁵

charged polymer particles at the oil water interface, resulting in capsular structures without the need for a sacrificial core. In addition, microcapsules called colloidosomes¹⁷ have been reported where colloidal particles are assembled at an oil-water interface to form walls with defined porosity.

2.2 Surface Tension

The relationship between the surface tensions of three immiscible phases and their resultant equilibrium configuration in a stirred system was described in 1970 by Torza et al.¹⁸ Much of the more recent work in this area has been carried out in the context of composite polymer particles^{19,20,21} or microencapsulation^{22,23}.

Particle assembly at the oil-water interface and the formation of microcapsules with walls of assembled particles has been shown to follow the same relationships as traditional three phase systems.^{8,24} Therefore particle assembly, and/or wall formation, is governed by the surface tension between the three phases, which ultimately controls the Gibb's free energy of the system via equation 2.1.

$$\Delta G = (\gamma_{op} + \gamma_{pw}) - \gamma_{ow} \quad \text{Equation 2. 1}$$

Where ΔG is the change in Gibbs free energy and γ_{op} , γ_{pw} , γ_{ow} are the oil-particle, particle-water and oil-water interfacial tensions, respectively. At equilibrium the free energy of a system must be minimised. Therefore, depending on the surface tension between the three components of the system the following relationships may result:

$$\gamma_{op} > \gamma_{pw} + \gamma_{ow} , \text{ the particles are dispersed in the aqueous phase} \quad \text{Equation 2. 2}$$

$$\gamma_{pw} > \gamma_{po} + \gamma_{ow} , \text{ the particles are dispersed in the oil phase} \quad \text{Equation 2. 3}$$

$\gamma_{ow} > \gamma_{po} + \gamma_{pw}$, the particles are collected at the oil-water interface

Equation 2. 4

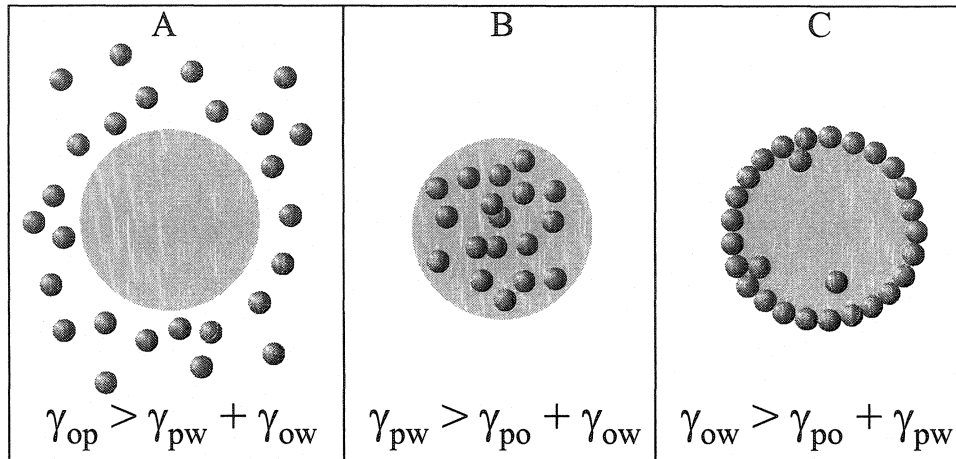


Figure 2. 2 Summary of the effects of surface tension on location of particles in an oil-water suspension. Conditions shown in C are required for successful microcapsule formation.

Therefore to prepare microcapsules from particles assembled at oil-water interfaces a system must have properties such that Equation 2.4 holds true.

2.3 Particle Selection

The goals of this research was to develop a family of highly porous microcapsules with potential applications in the controlled delivery of a variety of materials. In addition, it was desirable to develop an understanding of particle assembly at the oil-water interface, so that the particles could be incorporated into other microcapsule systems to construct composite microcapsule walls with novel release characteristics. Therefore, for this study, it was necessary to be able to control several key characteristics of the particles:

Monodispersed particle size. The size dispersity of a particle sample will affect the way that those particles can pack together at the interface. Generally, for hard spheres, monodispersed spheres can be close-packed[†] in a hexagonal array. As well, using monodisperse particles will facilitate studies into the effects of particle size.

Particle size that can be varied controllably. The particle size will determine the number of particles that can be assembled at the interface.

The size of the particles will also influence the rate at which they can migrate to the interface. This rate of migration will be important in composite systems where polymeric “glues” will be migrating to the interface at the same time as the particles. For example, if the polymeric glue migrates to the interface more quickly than the particles, the particles will be blocked from the interface, such that they are unlikely to influence release of core material (Figure 2.3).

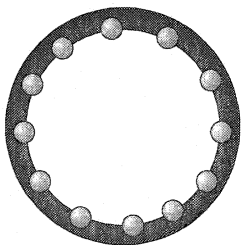


Figure 2. 3 One possible composite capsule, formed in a system where the polymer migrates to the oil-water interface faster than the microspheres.

[†] Packing is a term used to describe the arrangement of spheres at the interface. The packing of spheres may be ordered, similar to atoms in a crystal, or random with no repeating pattern. Efficient packing would result in a repeated packing pattern with a minimal amount of interstitial space.

This relationship between particle size and diffusion rate (D) can be seen in the Stokes-Einstein equation (Equation 2.5) where k_B = Boltzmann constant, T = temperature, η = viscosity of the medium and d = the diameter of the particle.²⁵ It shows that diffusivity scales inversely with particle diameter, i.e. a small “glue” polymer of diameter 1 nm would diffuse 1000 times faster than a polymer particle with a diameter of 1 μm .

$$D = \frac{k_B T}{3\pi\eta d} \quad \text{Equation 2.5}$$

Although rapid diffusion of the particles to the interface is desired, the particles must also not be too small. Particles of a few nanometers show significant thermal motion and can easily be displaced from the interface since they have sufficient energy to overcome the interfacial tension.²⁶ Assemblies of such particles may result in unstable capsules.

Variable morphologies. a) cross-link (XL) density: Varying the XL density affects the deformability and the swelling ratio of the particles. Particles with lower XL will be more malleable and may pack differently than hard spheres at the interface. Also, the lower the XL density the more a particle will swell in a good solvent. This swelling can affect the release of core material through the particles, since it will be easier for material to diffuse through a swollen polymer network. b) porosity: The ability to prepare particles, of the same chemistry, but with different porosity would allow for release channels to be designed into the spheres. In a given system, composites prepared with

particles of higher porosity would have a faster release rate than those made with less porous particles.

Variable chemistry. Access to particles with variable chemistry is very important. The chemistry of the particles will influence: migration of the particles to the oil-water interface, the ability to modify the particles, and the types of materials that may be released through the particle.

Possible Particle Candidates

Particles can be broken down into two broad categories, natural particles and synthetic particles. Natural particles, such as clays, are low in cost and therefore appealing industrially. However, they are generally difficult to modify, physically and chemically, which makes them less useful for the purposes of controlled release devices. For these reasons, synthetic polymer particles were used in this research. There are three primary types of polymer particles, suspension, emulsion, and precipitation.

Suspension Particles. Suspension particles are prepared by suspending a mixture of the water insoluble monomer and an oil soluble initiator in water containing a surfactant or steric stabilizer.^{27,28} In this system, particles grow in the monomer droplets. The resulting particles can be 5-1000 μm in diameter and are polydisperse. The polydispersity of these particles makes them less appealing for use in this work since the effects of particle size could not be accurately determined. As well, the surface coating of surfactant or stabilizer makes it difficult to design particles with varying surface chemistry.

Emulsion Particles. Emulsion particles are similar to suspension particles in that they begin as an oil-in-water emulsion in the presence of surfactant, but there is one key difference, the initiator is water-soluble.^{28,29} Using a water-soluble initiator results in particles that grow inside the surfactant micelles and not in the droplets of monomer. In this case the particle size is controlled by the number of micelles and the amount of monomer present. The resulting particles have a narrow polydispersity and their sizes are 100 – 1000 nm by traditional emulsion methods but can be as small as a few nanometers by microemulsion methods, and the polydispersity is narrow. The narrow polydispersity makes emulsion particles more appealing than suspension particles but the surface of emulsion particles is also covered in a layer of surfactant. This surfactant layer cannot be washed off and gives properties, such as ionic charges, to the particles that were not designed into the polymer itself. In addition, emulsion polymer particles have less flexibility in terms of porosity. Despite this, emulsion particles remain interesting because of the broad range of particle sizes that are accessible.

Seeded Swelling Particles. These particles combine the advantages of emulsion particles (narrow size distribution) with those of suspension particles (good control over porosity and functionality).^{30,31} However, they also suffer from the same problem as emulsion and suspension particles, in that they have a surface coating of stabilizer.

Precipitation Particles. Precipitation particles are different from emulsion and suspension particles in a number of ways. These particles are prepared from a homogeneous mixture of the monomer and initiator in a co-solvent system. As polymer forms it precipitates from solution, resulting in a heterogeneous mixture of particles and

solvent. These particles can be prepared in the range of 300-6000 nm and are often monodisperse. Another interesting feature of these particles is the fact that they are surfactant free. This absence of surfactant allows for the preparation of particles with a designed surface chemistry.

Precipitation particles have been thoroughly studied in our group. It is possible to make spherical particles of different sizes, cross-linking densities, morphologies and chemistries. They can be porous or non-porous, gels or solid spheres. Particles that have been previously prepared in our lab include: DVB, 50/50 DVB/MAn, DVB/Chloromethyl styrene, DVB/Methyl methacrylate, DVB/glycidyl methacrylate, DVB/hydroxyethyl methacrylate, and particles where DVB has been replaced by other cross-linking monomer such as EGDMA. Particles prepared with DVB have residual double bonds and other particles with built-in “chemical handles”, such as maleic anhydride or chloromethyl styrene, can be easily modified after formation to introduce desired polarity and reactivities.

Despite the fact that emulsion methods are industrially relevant and provide access to a wide range of particles sizes, the surface coating of surfactant cannot be easily washed off. Due to the surfactant free surface and the knowledge base existing in our lab on precipitation methods, these particles were selected for use in the proposed work.

2.4 Objective and Scope of Research

The goal of this research was to develop a method for assembling poly(divinylbenzene-*alt*-maleic anhydride) (DVB-MAn) microspheres and microgels at

the oil-water interface and fixing them in place via reaction of the surface anhydrides with amines, to form highly porous capsular structures. These capsular structures were named “tectocapsules”. The factors affecting self-assembly and fixation of the microspheres at the oil-water interface were investigated and a mechanism for tectocapsule formation and rupture has been proposed. This work generated a new family of microcapsules and laid the groundwork and understanding necessary for the development of the composite materials discussed later (Chapter 3).

2.5 Experimental

Reagents and Solvents

Divinylbenzene 55 (DVB-55), 4-methylstyrene, methylene chloride (HPLC grade), methyl ethyl ketone (MEK, 99%), polyethylenimine (Mn ca. 1200, 50% in water), polyethylenimine (Mn ca. 60 000, 50% in water), polyvinylalcohol (PVA, Mn ca. 9000), polyvinylpyrrolidone (Mn ca. 10 000), propyl acetate (99%), heptane (HPLC grade), *p*-xylene (HPLC grade), tetraethylenepentamine (TEPA, tech.), and Tween 80 (polyoxyethylene (20) sorbitan monooleate) were purchased from Aldrich and used without further purification. Maleic anhydride (99%) was purchased from Aldrich and was recrystallized from methylene chloride. IGEPAL CA 630 (polyoxyethylene (9) isooctylphenyl ether) was purchased from Sigma and used as received. Polyethylenimine (Mn ca. 9 000, 30% in water) was purchased from Polyscience, Inc. and was used without further purification.

Microgel Synthesis

The two types of microgel were prepared according to procedures reported earlier.³² Poly(DVB55-*alt*-MAn) microgels: Maleic anhydride (1.90 g) was dissolved in methylethylketone (56 mL) in a Nalgene bottle (125 mL). Heptane (24 mL) was added, followed by DVB-55 (1.6 g) and azo-bis-*iso*-butyronitrile (AIBN) (0.064 g). Poly(DVB6-*alt*-MAn) gels: Maleic anhydride (1.90 g) was dissolved in MEK (32 mL) in a Nalgene bottle (125 mL). Heptane (48 mL) was added, followed by DVB-55 (0.16 g), 4-methylstyrene (1.22 g) and AIBN (0.064 g).

In each case, the reaction mixtures were transferred to several 25 mL glass scintillation vials. The vials were closed tightly and placed in a polymerization reactor[†] at 70°C for 24 hours. At the end of the reaction the microspheres were collected by centrifugation, and washed with MEK. Following washing, MEK was exchanged for reagent grade propyl acetate, the preferred solvent for tectocapsule formation. Microgels were stored in water-saturated propyl acetate for about two weeks prior to use in tectocapsule formation, to allow for hydrolysis of some of the anhydride functionalities.

Microsphere Synthesis

The microspheres were prepared according to a procedure reported earlier.³² Maleic anhydride (0.80 g) was dissolved in MEK (8 mL) in a glass scintillation vial (20 mL). Heptane (12 mL) was added, followed by DVB-55 (0.73 g) and AIBN (0.016 g). The vial was closed tightly and placed in the polymerization reactor at 70°C for 24 hours. At

the end of the reaction the microspheres were collected by centrifugation, and washed with MEK. The microspheres were then dried at room temperature in a vacuum oven overnight.

Characterization of Microspheres and Microgels

The diameter of the microspheres and microgels was measured by environmental scanning electron microscopy (ESEM) as well as with a Beckman-Coulter LS 230 light scattering particle sizer.

The presence of succinic acid and succinic anhydride in the microspheres and microgels was monitored using several techniques and is discussed further in the Results and Discussion section below.

Fourier Transform Infrared (FT-IR) Spectroscopy. Samples were mixed with KBr powder and spectra were collected using a diffuse reflectance attachment on a ThermoNicolet Mattson IR 300.

Nuclear Magnetic Resonance (NMR) Spectroscopy. Samples were run at room temperature as neat solids. CP-MAS proton spectra were collected on a Bruker AV300 Spectrometer and solid state ^1H spectra were collected on a Bruker DRX 500 Spectrometer.

Scanning Transmission X-ray Microscopy (STXM). Succinic anhydride and succinic acid were dropped from solutions of acetone and distilled water, respectively, onto silicon nitride windows and allowed to dry in air at room temperature before imaging. Both

[‡]The polymerization reactor is a modified commercial hotdog roller, fitted with an insulating lid, a heating panel, a thermocouple and a circulating fan. The temperature in the reactor can be controlled to within 1 degree centigrade, and small vials roll horizontally at a rate of approximately 5 vial rotations per minute.

compounds crystallised upon loss of solvent. Spectra were collected at the ALS 5.3.2 STXM according to the procedures described in Chapter One.

Thermal Gravimetric Analysis (TGA). Experiments were carried out using a Bruker NETZSCH STA 409 instrument. Samples were contained in Pt pans and heated from 25 to 320°C in air at a rate of 30°C/min.

Typical Procedure for Interfacial Assembly and Cross-linking of Microgels

The organic phase (0.02g microgels suspended in 0.25 mL propyl acetate) was carefully layered onto the aqueous phase (1 mL of water containing 0.4% w/w PVA) placed in a 4 mL glass vial. Up to 10 such vials were attached to a laboratory wrist shaker modified with a multi-sample plate, and the mixtures emulsified by shaking at 384 rpm for 30 seconds. After emulsification the shaking rate was reduced to 215 rpm and 0.25 mL of a 1% w/w aqueous amine solution was added through one or more syringes to each vial over a period of 10 seconds, unless indicated otherwise. The mixture was shaken for 2 minutes, after which samples were withdrawn and observed by optical as well as both scanning and transmission electron microscopy.

2.6 Results and Discussion

2.6.1 Experimental Set-up and Design

In initial experiments, tectocapsules were prepared from an aqueous phase of 0.1 w/w% Igepal in water and an organic phase consisting of 2 g/mL poly(divinylbenzene-*alt*-maleic anhydride) microspheres suspended in a 50/50 (v/v) mixture of propyl acetate and *p*-xylene. The two phases were combined in a 4 mL glass vial and shaken by hand.

After shaking for two minutes dilute tetraethylenepentamine (TEPA) was added and the system was shaken for a further 30 seconds. The resulting capsular structures, shown in Figure 2.4 below, were stable when wet and emptied completely upon drying.

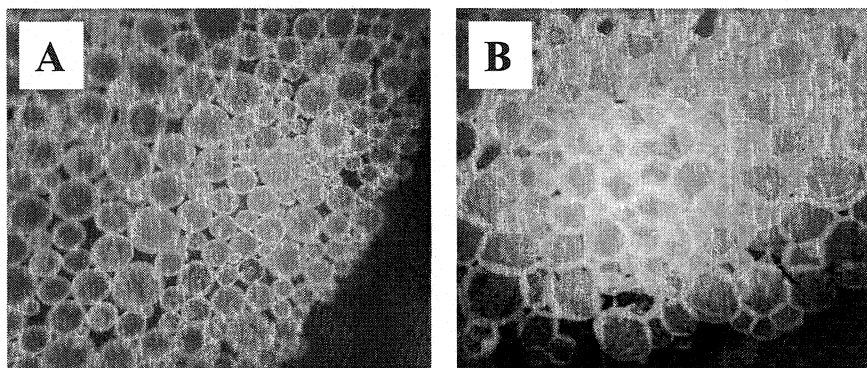


Figure 2. 4 Optical micrographs of wet (A) and dry (B) tectocapsules prepared by hand shaking.

Despite the success of this method, it was not feasible to continue to use hand shaking to form the oil-water emulsion since it may not be reproducible from one sample to the next. Tectocapsules were also successfully prepared using an overhead mixer. However, this set-up was limited to volumes of 50 mL and greater, which resulted in the use of large volumes of particles and produced increased amounts of waste. For these reasons a laboratory hand shaker was purchased and modified for use in tectocapsules preparation.

2.6.1.1 Shaker Design

A Labline, Multi Wrist Shaker was fitted with a 5" x 8" x 2" aluminium block drilled with 5, ½" diameter holes at each end to hold 4 mL glass vials (Figure 2.5). The vials were held in place using small aluminium clips, which were designed not to impede

reagent addition via syringe while shaking. The block was prepared from aluminium to facilitate heating and/or temperature control during reaction.

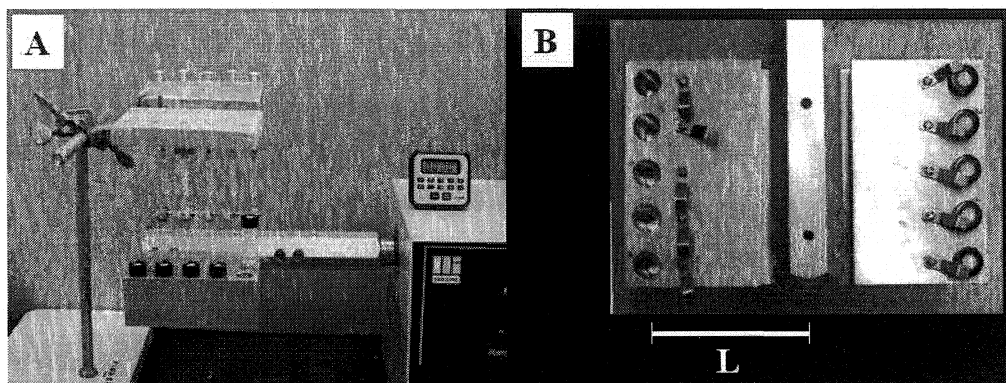


Figure 2.5 Modified wrist shaker used for tectocapsules preparation, shown from the front view (A) and from above the aluminium plate (B), where $L = 3.5''$ and is the distance from the centre of rotation to the centre of the vials.

2.6.1.2 Shaker Arm Length

One final variable that was investigated was the distance between the centre of the vial and the centre of rotation (L , Figure 2.5). This was investigated by replacing the aluminium sample block with a standard lab clamp, which could be fixed at various distances from the centre of rotation. It was found that the appearance of the resulting tectocapsules improved, in terms of smaller size and size distribution, when the distance of the vial from the centre of rotation increased.

Based on this observation, all reactions were carried out using lab clamps set to $8''$ from the centre of rotation.

2.6.1.3 Surfactants versus Stabilizers

When the formulation used for the initial hand shaken experiments was transferred to the wrist shaker stable tectocapsules were not formed. Instead, optical microscopy revealed capsule wall fragments, free particles and oil. As a result a number of surfactants and stabilizers were investigated to determine the optimum choice.

	<i>Percent in H₂O (w/w)</i>	<i>Capsules</i>	<i>Observations</i>
Surfactants			
Igepal CA 630*	0.01	No	Wall fragments and free particles
Tween 80*	0.01	No	Wall fragments and free particles
Stabilizers			
Polyvinyl alcohol (PVA)	0.04	Yes	Spherical capsules
Polyvinyl pyrrolidone (PVP)*	0.04	Yes	Large, oddly shaped capsules
Mixtures			
Tween 80/PVA	0.005/0.02	Yes	Spherical capsules
Igepal/PVA*	0.005/0.02	Yes	Spherical capsules

Table 2. 1 Table of surfactants and stabilisers evaluated for use with the modified wrist shaker. The core solvent was a 50/50 (v/v) mixture of *p*-xylene and PrOAc. Note: Systems marked with an asterisk (*) were prepared by Danielle Lewis, a co-op student in our group working under my supervision.

It was found that none of the surfactants tested resulted in stable capsules when the shaker was used to form emulsions. Instead, wall fragments and significant particle crossover into the aqueous phase was observed. In the case of both PVA and PVP, capsule wall formation was observed, however systems containing PVP resulted in many large (>500 µm) non-spherical capsules. It is believed that these observed differences between systems containing surfactants and stabilizers results from the differences in how surfactants and stabilizers behave at the oil-water interface.

Forming an emulsion is a balance between droplet formation, which is energetically unfavourable in an oil-water system, and droplet recombination or coalescence, which is energetically favourable since it reduces interfacial area. Therefore, emulsion formation can be facilitated by either reducing the energetic penalty associated with interface formation or by inhibiting droplet coalescence.

Surfactants reduce the droplet size in an emulsion by coating the oil-water interface, lowering surface tension in the system.^{4,33} This surfactant layer is considered to be “liquid” and surfactant molecules at the interface are in equilibrium with those remaining in solution. Stabilizers, on the other hand, tend to be polymeric in nature and form a “hard” coating on the oil-water interface³⁴ since it is more difficult for the large polymer molecules to escape the interface. This polymeric coating reduces droplet coalescence and therefore droplet size via steric repulsions of polymer chains at the interfaces of two approaching droplets.

Since capsule formation in the presence of surfactant did occur in systems shaken by hand but did not when the mechanical shaker was used, it can be concluded that high surface tension is not responsible for destabilisation of the system. Rather that the mechanical shaker acted to force coalescence of oil droplets, likely as a result of the abrupt stops encountered by the vials at the top and bottom of the axis of shaking/rotation.

In summary, it was found that the use of PVA improved tectocapsule formation. For this reason the remaining experiments in this thesis were carried out using PVA as the stabilizer and in the absence of any surfactant.

2.6.2 Tectocapsule Formation

The tectocapsules were prepared according to the procedure shown in Figure 2.6. First, the microspheres were dispersed in the organic core solvent using sonication (A). An excess of aqueous phase was added to the organic phase (B), and the mixture was shaken on a mechanical wrist action shaker for 30 seconds in order to emulsify the microsphere-containing oil phase (C). Finally, a polyamine dissolved in water was added by syringe to start the interfacial polyaddition reaction (D).

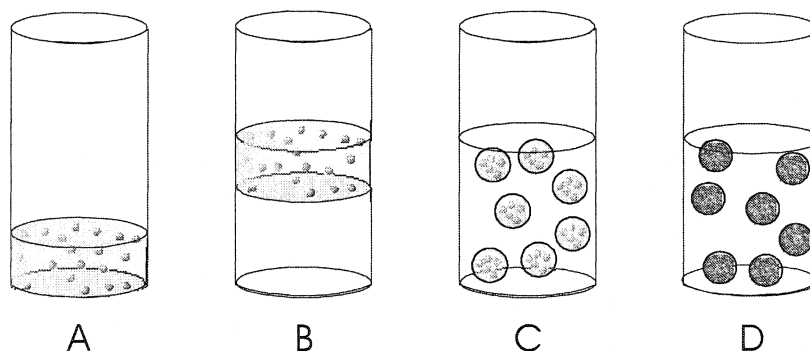


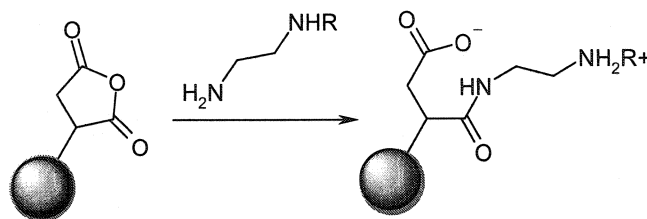
Figure 2. 6 Reactive microspheres are suspended in the organic phase in 4mL glass vials

(A). An aqueous phase containing a dispersant is then added to the vial (B). Agitation using a mechanical wrist shaker results in emulsification of the organic phase (C).

Addition of polyamine causes the interfacial reaction (D).

Initial experiments were carried out with poly(divinylbenzene-*alt*-maleic anhydride) (DVB-MAn) microspheres. Based on earlier work in our group with linear poly(styrene-*alt*-maleic anhydride) (SMA),³⁵ it was expected that reaction of these microspheres with amine would result in ring-opening of the anhydride moiety resulting in the formation of charged species on the microsphere surface (Scheme 2.1). These charged microspheres

were then expected to migrate to the oil-water interface, in analogy with what was observed in the linear polymer systems. Once at the interface, amine would react with unopened anhydride groups on neighbouring microspheres, cross-linking them together and forming a capsular wall at the oil-water interface. Several factors were expected to affect the assembly and cross-linking of the microspheres at the interface, these will be discussed below.



Scheme 2. 1 Predicted reaction of the succinic anhydride groups on the surface of the DVB-MAN particles with aliphatic amines.

2.6.2.1 Amine Molecular Weight Effects

Poly(ethylene imines) with molecular weights of ca. 189 g/mol (tetraethylene pentamine, TEPA), number average molecular weights (M_n) of ca. 1200, ca. 6500 (weight average molecular weights (M_w) of ca. 70 000) and ca. 60 000 (M_w ca. 750 000),[§] were compared, using a 50/50 mixture of propyl acetate/xylene as organic phase.

Using the shaker, no capsules were formed with TEPA, only oil-in-water emulsions with the microspheres largely transferred to the aqueous phase. A few wall fragments

[§] Molecular weight distributions are broad due to the branched nature of the PEI.

could be seen by optical microscopy, indicating that some reaction at the oil-water interface had occurred. The failure of TEPA to form tectocapsules can be attributed to two factors. First, connections between neighbouring microspheres would be weak due to the small size of the bridging TEPA molecules. Secondly, rapid in-diffusion of the small TEPA molecules into the organic phase may have resulted in particles with surfaces entirely functionalized with amine. Such particles would not be able to cross-link at the oil-water interface to form walls, and would most likely transfer to the aqueous phase.

Tectocapsules were successfully prepared with all other molecular weights of PEI. A noticeable increase in capsule stability was observed as the PEI molecular weight was increased from 1200 to 6500. Observation by optical microscopy indicated no further increase in stability and mechanical strength when the molecular weight was increased to 60 000. These results are illustrated in Figure 2.7.

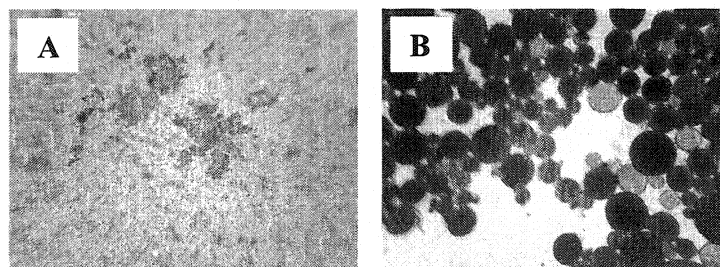


Figure 2. 7 Optical microscope images of (A) capsule fragments obtained from reaction with TEPA, and (B) capsules formed in reactions with PEI ($M_n \sim 1200$). The larger microcapsules shown in Figure B are approximately 100 micrometer in diameter.

2.6.2.2 Effects of Amine Addition Rate

Our previous studies involving interfacial addition reactions between linear styrene-maleic anhydride copolymers and TEPA, showed that the rate of amine addition can drastically affect the morphology of the resulting capsules, particularly in systems with effective partitioning of amine into the organic phase.³⁵ Slow rates of amine addition allowed for slow reaction of the anhydride groups of the SMA. The slow rate of reaction allowed the polymer to migrate to the oil-water interface resulting in capsular morphologies. On the other hand when amine was added rapidly it partitioned into the oil phase, reacting rapidly with the SMA. This rapid reaction caused precipitation of the SMA from the organic phase and the formation of matrix-like morphologies. As well, literature describing the assembly of charged latex particles at the oil-water interface indicates that better 2-D ordering was observed when the particles could be assembled prior to fixation.³⁶ Thus it was thought that the rate of amine addition to our system may affect the ordering of the spheres assembling at the interface, as well as the tectocapsule stability.

For these experiments, 0.25ml of a 1% w/w aqueous solution of PEI of Mn 1200 were added continuously to the agitated suspension of microspheres in a 50/50 wt% mixture of propyl acetate/*p*-xylene over periods of 10 seconds, 10 minutes and 1.5 hours, using a syringe pump. No noticeable difference in the formation or stability of the tectocapsules was observed by optical microscopy. ESEM imaging also did not indicate any difference in the ordering of particles on the capsular surface as a function of addition time. This suggests that at least some of the microspheres are already assembled at the interface prior to addition of amine.

2.6.2.3 Microsphere Chemistry

This assembly of microspheres at the oil-water interface prior to addition of the amine was surprising since it was the salt functionality formed by reaction of the anhydride groups with amine that caused migration of the SMA polymers to the interface. The possibility existed that the DVB-MAN microspheres contained carboxylic acid groups formed by the hydrolysis of succinic anhydride groups. This would explain the apparent ease of microsphere assembly at the oil-water interface.

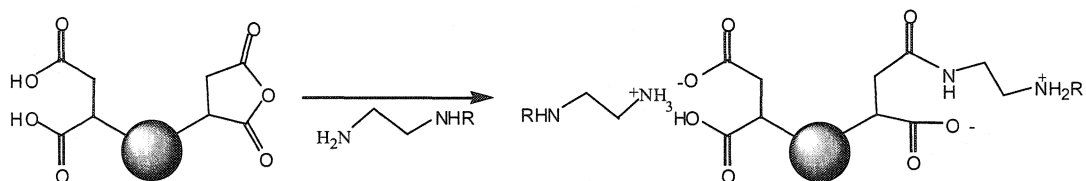
Analysis of the DVB-MAN microspheres by Fourier transfer infrared (FT-IR) spectroscopy revealed the presence of styrenic species (2880, 2935, 2968, 3028 cm^{-1}), succinic anhydride (1780, 1858 cm^{-1}) and succinic acid (1738 cm^{-1}). These acid groups are the product of anhydride hydrolysis. Anhydride hydrolysis may have occurred at four stages: prior to microsphere synthesis during monomer storage, during the microsphere forming reaction, during post reaction microsphere work up, or during microsphere storage.

It is believed that the majority of anhydride hydrolysis occurs during the microsphere forming reaction when it is carried out using reagent grade solvents. Subsequent reactions carried out in the presence of dry solvents showed a significant reduction in acid content. It is not possible to determine if the acid was completely removed from the system using FT-IR since there is significant overlap of the anhydride peak at $\sim 1780 \text{ cm}^{-1}$ and the acid peak found at $\sim 1740 \text{ cm}^{-1}$. In addition, some hydrolysis of the anhydride functionality of the microspheres could be seen during storage of the microspheres in air. The hydrolysis at room temperature was slow as it could only be detected in samples stored on the bench

top for at least a year. Despite this slow rate of reaction, all samples were stored in a dessicator to minimise the rate of anhydride hydrolysis.

The Effect of Acid Content. Suspensions of low-acid microspheres were used to repeat the standard experiments described above, however, tectocapsules were not formed. This suggests that the acid contributed to wall formation. Addition of acid groups to the microspheres surface significantly increases the polarity of the microspheres, accounting for the observation that it was more difficult to suspend them in organic solvents. It would also increase the driving force for microsphere migration to the oil-water interface. Microsphere self-assembly at the oil-water interface would also explain the systems' lack of response to changes in the rate at which amine was added. Based on these observations it is believed that it is the acid functionalities which are responsible for microsphere assembly at the oil-water interface, rather than the salts formed when anhydride reacts with amine, as was the case in SMA systems.³⁵

As a result, the picture of what occurs on the microsphere surface in the presence of amine must be modified to include the presence of acid groups (Scheme 2.2). Amine addition to these microspheres would result in the formation of two different salt groups. The first results as the acid groups are titrated by protonated amine, the other occurs as a consequence of the ring opening reaction with the anhydride.



Scheme 2. 2 Linkage reactions of amines with acid and anhydride groups present in the poly(divinylbenzene-*alt*-maleic anhydride/maleic acid) (DVB-*alt*-MAn/MA) microgels and microspheres.

Determining the Acid:Anhydride Ratio in DVB-MAn Microspheres. It has been determined that acid content of the microspheres was important for tectocapsule formation but it was not known how much acid was needed to facilitate microsphere self-assembly at the oil-water interface. It was therefore important to develop a method to monitor the acid to anhydride ratio in these microspheres. As discussed above it was not possible to use FT-IR due to the overlap of the acid and anhydride bands; thus a number of different techniques were investigated.

Nuclear Magnetic Resonance Spectroscopy (NMR). DVB-MAn microspheres are densely cross-linked and therefore standard solution NMR techniques can not be used. Attempts to use the solid state NMR technique of cross-polarised magic angle spinning (CP-MAS) was also not successful as a result of overlapping acid and anhydride proton peaks. Subsequent solid state ^1H NMR of the microspheres was also not able to resolve the necessary peaks.

NEXAFS Spectroscopy. The STXM technique described in chapter one was used to collect NEXAFS spectra of succinic acid and succinic anhydride. This was difficult because both species formed crystals and therefore their spectra were sensitive to the orientation of the crystals within the x-ray beam. Although spectra were collected, it has not yet been possible to differentiate acid from anhydride. Work in this area will continue and will be carried out with SMA and hydrolysed SMA in an attempt to alleviate the polarisation dependence of the spectra.

Thermal Gravimetric Analysis (TGA). As a result of the difficulties encountered using spectroscopic methods to characterise the acid content, TGA experiments were carried out. Here it was expected that the amount of water lost by regeneration of anhydride during heating of the microspheres could be quantified. Monitoring water loss from the microspheres was complicated by several factors. Water lost during heating of the microspheres may be water adsorbed onto the microsphere rather than that generated by anhydride regeneration. The system is further complicated by the fact that microspheres are three dimensional and can lose water slowly over time, first from the surface and then from progressively closer to the core. To simplify the system, initial experiments were carried out using a commercial SMA sample that showed both acid and anhydride peaks in its FT-IR spectrum. These experiments showed the loss of two species between 75 and 150°C, where water is expected to appear, for a total mass loss of ~5%. It was not possible to determine if both or either of these reflect loss of water or if other species were lost. Once again, these experiments were inconclusive.

It is not currently possible to fully characterise the acid content of the DVB-MAN microspheres. Currently we can only state that some level of acid is required for successful tectocapsule formation.

2.6.2.4 Core Solvent Effects

Based on our prior experience with linear poly(styrene-*alt*-maleic anhydrides), *n*-propyl, *n*-butyl and *n*-hexyl acetate were selected as core solvents.³⁵ Lower alkyl acetates such as ethyl and methyl acetate are too soluble in water, while acetates with alkyl chains higher than hexyl show little change in their solubility parameter. In addition to the three neat acetates, a 50/50 (vol/vol) mixture of propyl acetate and *p*-xylene, was used. Such binary solvent systems are attractive, as they may in future allow for small changes in solvent polarity by altering the ratio of the solvents in the mixture.

Solubility parameters are useful to interpret the role of solvents in polymer reactions. The Hildebrand solubility parameter is a measure of the cohesive energy density of a material, and is often used to predict solubilities or swellability of polymers in particular solvents. The Hansen solubility parameters are an attempt to divide the polymer solvent interactions into dispersive, polar and hydrogen bonding components. The Hansen parameters, especially the polar and hydrogen bonding parameters, are hence often found more suitable to describe systems containing polar or hydrogen-bonding interactions. For example, while the Hildebrand solubility parameters for *p*-xylene and propyl acetate are identical, their Hansen parameters show the higher dipolar and hydrogen bonding ability of the ester (Table 2.2).

Solvent	Hildebrand Solubility Parameter δ [Mpa ^{1/2}]	Hansen Dispersive Parameter δ_d [Mpa ^{1/2}]	Hansen Polar Parameter δ_p [Mpa ^{1/2}]	Hansen H-Bonding Parameter δ_h [Mpa ^{1/2}]	Boiling Point [°C]	Solubility in Water [g/100mL]
<i>p</i> -xylene	18.1	16.5	7.0	2.2	137-144	< 0.1
<i>p</i> -xylene / propyl acetate 50/50	18	15.3	7.5	5		
ethyl acetate	18.2	13.3	8.6	8.9	77	10
propyl acetate	18.0	14.1	8.1	7.8	102	1.6
butyl acetate	17.8	14.5	7.8	6.8	124-126	0.8
hexyl acetate	(~17)				168-170	<0.8

Table 2. 2 Table 1. Solvent Properties³⁷

Within the acetate series, propyl acetate (PrOAc) gave the best results. Microspheres were observed to assemble at the oil-water interface and form capsular walls upon addition of amine. However, these walls ruptured after about 30 seconds of observation under the optical microscope (Figure 2.8 A). Propyl acetate is quite water soluble, and the capsule rupture is in part due to rapid loss of the propyl acetate through the water layer into the air. Covering the aqueous capsule suspension with a layer of propyl acetate significantly improves the capsule stability as observed under the optical microscope. Capsule walls formed using butyl acetate, and especially using hexyl acetate, ruptured almost immediately, releasing their oil phase and leaving only small wall fragments behind. Adding a solvent overlay in these cases did not improve capsule stability.

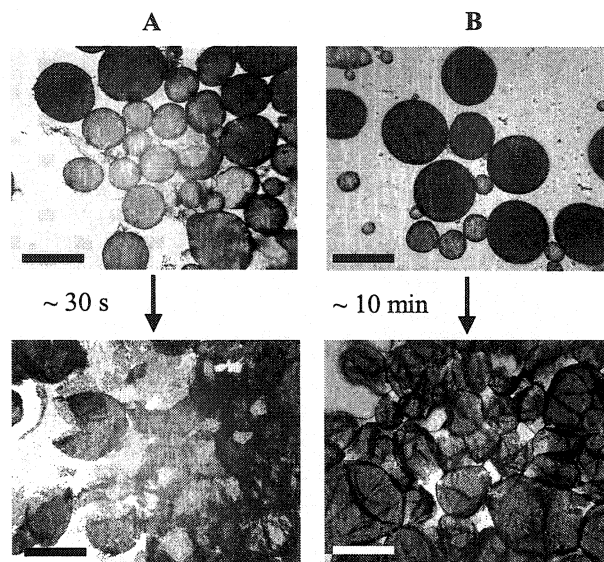


Figure 2. 8 Optical microscopy images taken immediately after the reaction, and after 30 s and 10 mins, respectively. A. Capsules formed with propyl acetate. B. Capsules formed with a 50/50 vol% mixture of propyl acetate and xylene. The larger capsules shown in these figures are approximately 200 μm in diameter. Scale bar is 250 μm .

Capsules prepared with *p*-xylene as well as with binary mixtures of PrOAc and *p*-xylene (Figure 2.8 B) were much more stable and did not rupture while wet.

Propyl acetate and *p*-xylene have identical Hildebrand solubility parameters of about 18 $\text{MPa}^{1/2}$. According to the Hansen parameters shown in Table 1, the high dispersive component for *p*-xylene compensates for its much lower hydrogen bonding and dipolar interactions. The higher apparent stability of the capsules prepared in mixed solvents and neat *p*-xylene suggests that dipolar or hydrogen bonding ability is not essential for

capsule formation. Conversely, it is plausible that the presence of *p*-xylene causes the microspheres to more efficiently assemble at the interface prior to amine addition, permitting cross-linking rather than simple functionalisation with amine. Finally, *p*-xylene has a lower water solubility and higher boiling point than PrOAc, which would also contribute to increase capsule stability.

2.6.2.5 Particle Loading Effects

Higher particle loading in the organic phase should result in thicker tectocapsule walls. Hence, tectocapsules were prepared with particle loadings of 0.04 g/mL oil and 0.16 g/mL oil, respectively, using PEI 1200 as the amine, and 50/50 wt% propyl acetate / *p*-xylene as organic phase.

The particle loading effects can be seen clearly in Figures 2.9 and 2.10. Optical micrographs 2.9A and 2.9B show an increase in opacity with higher particle loading. TEM images 2.9C and 2.9D of capsule cross-sections reveal that wall thickness increases with particle loading. They, as well as higher resolution ESEM images (not shown), reveal significant free volume between the microspheres that make up the tectocapsule walls, suggesting swelling of the capsule wall during assembly, likely due to absorption of water into the zwitter-ionic surface region. The resulting capsular membrane hence has interstitial pores that should scale with the microsphere diameter, and with the thickness of the swellable, cross-linked surface layers.

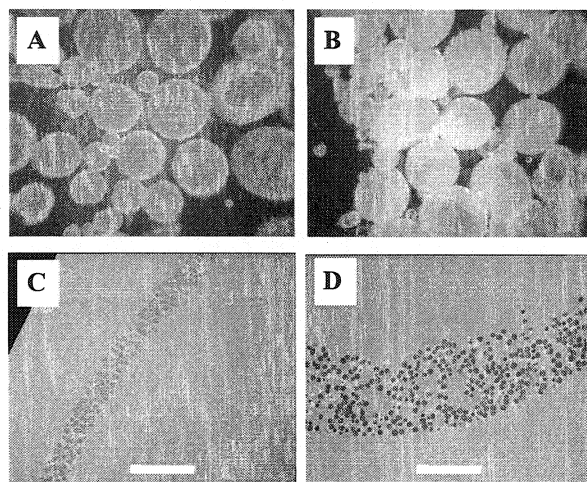


Figure 2. 9 Optical microscope (A, B) images of tectocapsules and TEM (C, D) images of cross-sections of tectocapsule walls formed with particle loadings in the organic phase of 0.04 (A,C) and 0.16g/mL (B,D), respectively. The larger microcapsules in Figures A and B are approximately 200 μm in diameter. The scale bars in Figures C and D are 10 μm .

ESEM images (Figure 2.10) confirm that tectocapsules with a higher particle loading are more structurally sound. Tectocapsules formed at 0.04g/mL particle loading collapse upon drying (Figure 2.10 A), while those formed with 0.16g/mL particle loading form self-supporting capsule walls (Figure 2.10 B and C).

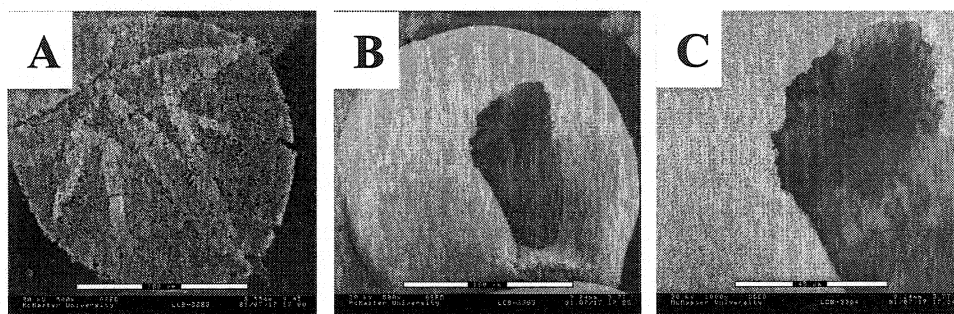


Figure 2. 10 ESEM images of tectocapsules formed with particle loadings of 0.04 g/mL (A) and 0.16g/mL (B and C) in the organic phase. The scale bars are 100 μm for Figures A and B, and 45 μm for Figure C.

The outer surface of the tectocapsules is smooth, consistent both with the presence of a distinct liquid-liquid interface, and with the assembly of the microspheres at this interface prior to addition of amine. The inner surface of the capsules is rougher, in agreement with a subsequent random deposition and anchoring of microspheres upon addition of amine.

The ultimate particle loading can be achieved using a water-miscible solvent such as MEK as the organic phase. This leads to the formation of smaller “tectoparticles” (Figure 2.11A) with densely packed cores (Figure 2.11B) since the solvent mixes with water, leaving the microspheres behind.

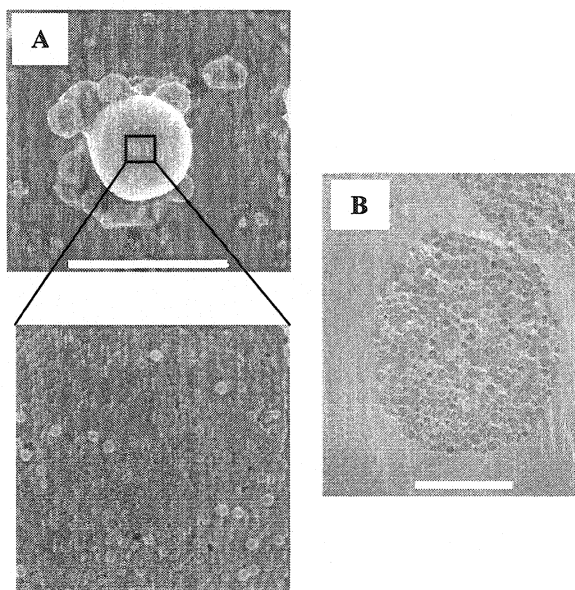


Figure 2. 11 ESEM (A) and TEM cross-section (B) images of tectoparticles prepared with the water miscible solvent MEK. The scale bars are 100 and 1 μm , respectively.

2.6.3 Gel-Tectocapsules

The above systems were prepared with highly cross-linked 600 nm diameter poly(divinylbenzene-*alt*-maleic anhydride) microspheres and lead to highly porous tectocapsules. The hard surface of these microspheres resulted in large interstitial pores, but also caused weak microsphere-microsphere interconnections. To improve the interconnection of neighbouring microspheres in the tectocapsule wall analogous interfacial membranes were prepared using two types of swellable, lightly cross-linked poly(divinylbenzene-*alt*-maleic anhydride) microgels in place of the hard microspheres.

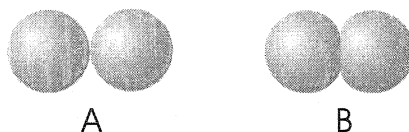


Figure 2. 12 Cartoon depicting the change in particle-particle contact area between two hard spheres (**A**) such as the poly(DVB55-*alt*-MAn) microspheres and two malleable spheres (**B**) such as poly(DVB6-*alt*-MAn) microgels.

Poly(DVB6-*alt*-MAn) microgels were formed by replacing some of the DVB55 with 4-methylstyrene, which resulted in large, 650 nm diameter, swellable microgels.** Poly(DVB55-*alt*-MAn) microgels were chemically identical to the poly(DVB55-*alt*-MAn) microspheres used previously, but were prepared in a better solvent and hence show a lower cross-link efficiency, and a smaller diameter of 150 nm.³² Both types of microgels were prepared by precipitation polymerisation and were therefore free of added steric or ionic colloidal stabilizer.

Earlier experiments with microspheres indicated the need for some succinic acid groups to facilitate self-assembly at the interface prior to covalent fixation. Thus, following polymerization, the microgels were transferred into reagent grade propyl acetate and stored for a minimum of two weeks to allow for hydrolysis of some of the anhydride functionalities to succinic acid.^{††}

** DVB-55 is a commercial mixture containing 55% *meta* and *para* divinylbenzene isomers and 45% ethylvinylbenzene isomers. DVB6 (6% DVB isomers) is prepared by diluting DVB55 with the appropriate amount of 4-methylstyrene, a monovinyl monomer with properties similar to those of ethylvinyl benzene.

†† An alternate approach for introducing succinic acid into the microgels would be to copolymerize a mixture of maleic anhydride and maleic acid with the divinylbenzene. Both maleic anhydride and maleic acid are known to copolymerize in a largely alternating fashion with styrenic monomers. In the present case, this approach was rejected in favour of slow, partial hydrolysis, as the use of maleic acid would have

The gel-tectocapsules were prepared according to the procedure discussed previously for the formation of tectocapsules from poly(DVB55-*alt*-MAn) microspheres. First, a suspension of microgels in propylacetate was added to an excess of aqueous phase containing polyvinylalcohol as a stabilizer. The mixture was shaken on a mechanical wrist action shaker for 30 seconds in order to emulsify the microgel-containing oil phase and permit self-assembly at the oil-water interface. Finally, a polyamine dissolved in water was added by syringe to covalently cross-link the microgels at the interface via nucleophilic attack at the anhydride moiety (Scheme 2.1). By analogy to the interfacial reaction between amines and both linear poly(styrene-*alt*-maleic anhydride),³⁸ and poly(DVB-*alt*-MAn) microspheres, the amine is expected to form mainly covalent amide links, in addition to some ionic linkages (Scheme 2.1, above). In contrast to purely ionic aggregates of poly(styrene-*alt*-maleic acid) and PEI, gel-tecto capsule walls subjected to concentrated sodium chloride solution, 0.1N hydrochloric acid or 0.1N sodium hydroxide showed no change in their morphology, confirming the presence of a significant amount of covalent linkages.

The core solvent in both microgel systems was limited to propyl acetate, which is a good solvent^{‡‡,39} for the microgels and yet has minimal solubility in water. If higher

required limiting the copolymerizations to low conversions to prevent drift of the anhydride/acid ratio, adjusting the cosolvent mixture to accommodate the much more polar maleic acid, and dealing with further complications due to Harwood Bootstrap differential partitioning of the comonomers into the forming oligomers and/or particles.

‡‡ A “good” solvent is one that swells the microgels, a “bad” solvent would result in collapse and coagulation of the microgels. The appropriateness of a solvent is often predicted using the Hildebrand solubility parameters³⁷ of the solvent and polymer. The closer the values of the solubility parameters of the two the more likely it is that the solvent will dissolve (or swell in the case of cross-linked materials) the polymer.

acetates, such as butyl and hexyl were used, the microgels would coagulate prior to emulsification. Figure 2.13 shows microgel tectocapsules prepared using both poly(DVB6-*alt*-MAn) (A, C) and poly(DVB55-*alt*-MAn) (B, D).

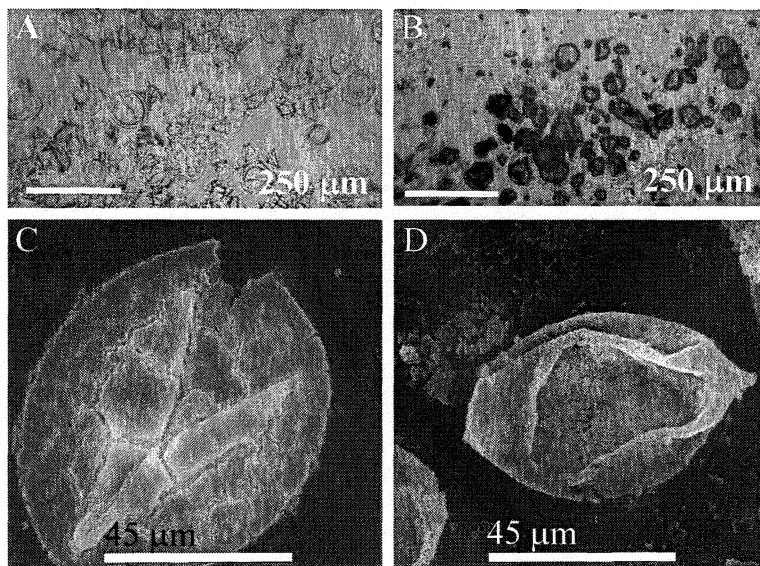


Figure 2. 13 Optical (A,B) and ESEM (C,D) micrographs of gel-tectocapsules prepared with poly(DVB55-*alt*-MAn) (A, C) and poly(DVB6-*alt*-MAn) (B, D) microgels. In both cases TEPA was used as the cross-linking agent.

In both gel-tectocapsule systems discussed above, core oil is lost rapidly, prior to complete evaporation of the aqueous phase. This rapid loss of core solvent is similar to that with microsphere tectocapsules discussed above. However, in that case the rapid release of core solvent resulted in rupture of the capsule wall rather than collapse, which was observed in gel-tectocapsule systems. The increase in apparent capsule wall stability for the gel-tectocapsules, is attributed both to the malleable nature of the microgels, and

improved linkages between the particles due to the increased penetration of the TEPA into the swellable microgels.

The rapid release of PrOAc from tectocapsules can be attributed to several factors: the high porosity of the capsule walls, and the low boiling point and high water solubility of propyl acetate.

As a result of the observed difference between linear polymer systems and the microspheres systems the effects of amine molecular weight and rate of amine addition, in the gel-tectocapsule systems were investigated and will be discussed below.

2.6.3.1 Amine Molecular Weight.

Similar to systems discussed above with hard microspheres, increased amine molecular weight was expected to result in increased wall stability as a result of better intermicrogel connections. Here, amine molecular weight was varied from tetraethylenepentamine (TEPA) to PEI with M_n of ca. 60 000 g/mol. All amines formed stable capsular walls with increasing strength at higher amine molecular weight (Figure 2.14). However, at the highest amine molecular weight, M_n of 60 000 g/mol, the capsules aggregated, especially in the case of poly(DVB55-*alt*-MAn) microgels. This loss of colloidal stability at higher amine molecular weights may result from ionic or covalent intercapsule bridging.

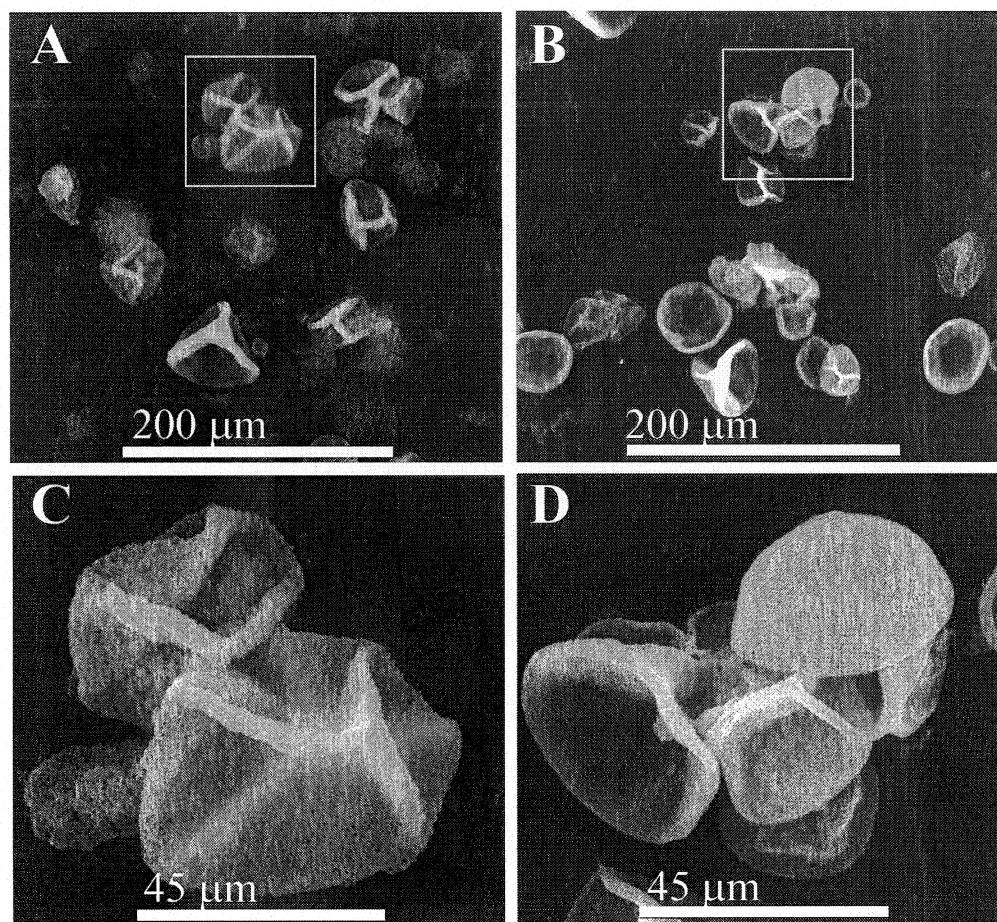


Figure 2. 14 ESEM micrographs of poly(DVB6-*alt*-MAn) gel-tectocapsules prepared with PEI with Mn of ca. 1200 g/mol (A) and PEI with Mn of ca. 60 000 g/mol (B). Inset box in A and B indicates the regions of higher magnification shown in C and D respectively.

The capsule membrane in the center of Figure 2.14 D shows significant crystalline ordering of the wall-forming microgels. In contrast, the microspheres of the capsules shown in Figure 2.14 C are largely random. However, when a number of capsules in both systems are observed, both ordered and non-ordered membranes can be found, suggesting

that particle ordering is not dependant on amine molecular weight or particle type. If in fact the microspheres are self-assembling at oil-water interface there should be some tendency towards ordering. It is believed that the high shear conditions present during tectocapsule formation, and perhaps the sample work up prior to imaging may disrupt particle ordering in the walls of the tectocapsules.

2.6.3.2 Amine Addition Rate.

In the case of tectocapsules formed from microspheres, amine addition rate did not affect wall morphology, indicating that the microspheres had pre-assembled at the interface prior to addition of amine. In order to confirm that microgels behave similarly, the effects of amine addition rate were once again evaluated.

In the present work, increasing the time used to add the same amount of TEPA from 10 seconds to 90 minutes did not affect the capsule structure in the case of poly(DVB55-*alt*-MAN) microgels. This lack of response to the rate of amine addition supports the fact that the partly hydrolyzed poly(DVB-*alt*-MAN) microgels self-assemble at the oil-water interface *prior* to amine addition contrary to what was observed for linear SMA polymers containing little or no succinic acid.³⁵ The amine then largely acts to covalently fix the microgels, but is not primarily responsible for migration or assembly of the microspheres at the interface.

The aggregation seen for molecular weights higher than that of TEPA, is attributed to intercapsule bridging. Slowing the rate of amine addition should increase aggregation by creating charge mosaic surfaces, consisting of cationic amine patches together with anionic domains.

2.6.4 Mechanism of Tectocapsule Formation and Bursting

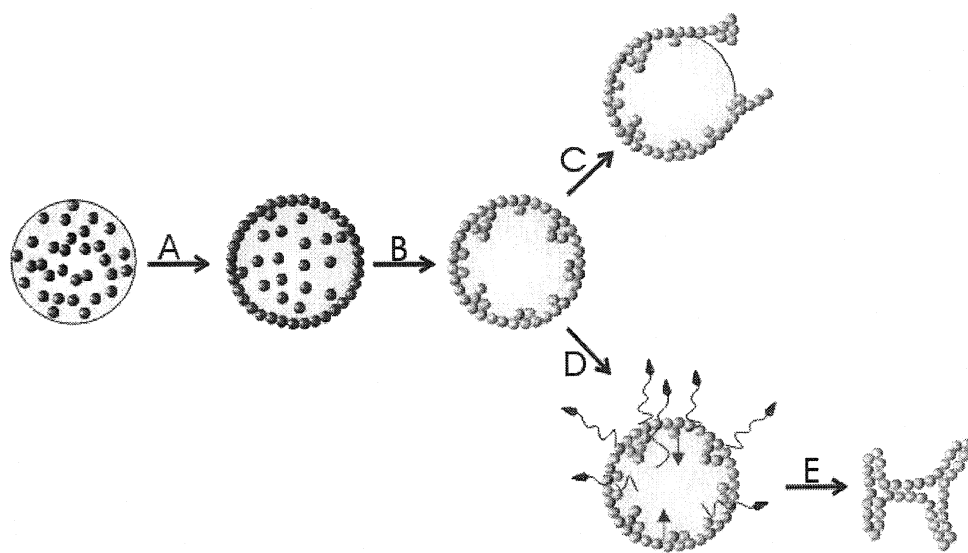


Figure 2. 15 Illustration of the mechanism of tectocapsule formation and collapse/rupture. A) self-assembly; B) covalent fixation; C) rupture due to the swelling of weakly cross-linked, charged walls formed from hard microspheres; and (D and E) release through more highly cross-linked gel walls, followed by collapse.

Based on observations of the tectocapsules formed with hard microspheres and the gel-tectocapsule, we propose the following mechanism for the formation and destruction of materials in the tectocapsule family.

For capsule walls to form, the change in Gibb's free energy of the system as a result of wall formation must be negative (Equation 1). For this condition to be met the oil-water interfacial tension (γ_{ow}) must be greater than the sum of the oil-polymer (γ_{op}) and polymer-water (γ_{pw}) interfacial tensions.¹⁹ In all tectocapsule systems, where the microgel or microspheres had some (~20%) succinic acid functionality, walls were seen to form, indicating that initially the interfacial conditions for wall formation were met (**A**). Since the rate of amine addition had no observable effect on wall structure or particle packing, it is believed that particle assembly at the oil-water interface occurs prior to amine addition.

$$\Delta G = (\gamma_{op} + \gamma_{pw}) - \gamma_{ow} \quad \text{Equation 2.1}$$

We attribute the subsequent instability of the tectocapsules to the increased polarity of the microspheres after reaction with amine (**B**), where zwitter-ionic salt groups are formed on the microsphere surface (Scheme 1). This increase in surface polarity increases the oil-polymer interfacial tension (γ_{op}) and decreases the polymer-water interfacial tension (γ_{pw}) to the extent that it may no longer be favourable to have a capsule wall. Instead the capsule walls break releasing the core oil (**C**), forming oil-water and polymer-water interfaces at the expense of the oil-polymer interface (Step C, Figure 2.16). If this were the case, the tectocapsules would be more likely to rupture as the core solvent polarity is decreased. This was observed in the case of tectocapsules prepared with hard microspheres. Parallel experiments with the microgel systems were not

possible since solvents of lower polarity than PrOAc, such as butyl acetate, cause coagulation of the microgels prior to emulsification of the oil phase.

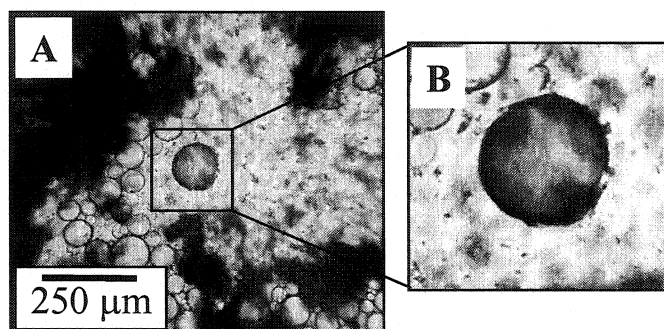


Figure 2. 16 Tectocapsules formed with highly cross-linked poly(DVB-alt-MAn) microspheres with hexylacetate as a core solvent (A). After only 10 seconds the formed tectocapsules walls can be seen “peeling” off the oil droplets (B). This phenomenon is believed to result from the increased polarity of the microspheres after reaction with amine.

Alternatively, evaporation of a low boiling core solvent through the capsule wall (D) will cause collapse (E) of the capsule wall. If microsphere-microsphere connections are weak, as in the case of tectocapsules prepared with hard microspheres, solvent evaporation (D) will cause rupture of the capsule wall rather than collapse. This mechanism of tectocapsule rupture/collapse is supported by the fact that rupture/release can be stopped when core solvent evaporation is eliminated by covering the aqueous suspension of capsules with a layer of free solvent (Figure 2.16). Rupture/release from these systems resumes when the layer of free solvent has itself evaporated.

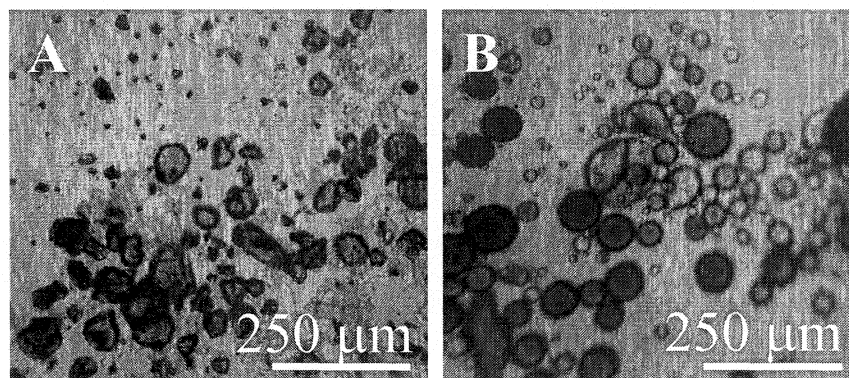


Figure 2. 17 Optical micrographs of aqueous gel-tectocapsules prepared with poly(DVB6-alt-MAN) microgels and TEPA as a linker rupturing when open to air (A) and surviving longer when their aqueous suspension is covered with a layer of PrOAc (B).

2.7 Conclusions

In conclusion, this work has demonstrated that DVB/MAN based microspheres and microgels can be assembled and covalently linked at the oil-water interface. Assembly of the particles at the oil-water interface required that some level of maleic acid is present. Several variables such as microsphere loading, amine molecular weight and addition rate were investigated in an effort to increase the strength of interparticle connections within the capsule wall and the overall mechanical strength of the capsule wall. In general, it was found that increased particle loading and amine molecular weight resulted in more stable capsule walls. As well, a mechanism for the formation and rupture of tectocapsules has been presented.

References

- ¹ Ramsden, W. *Proc. Royal. Soc. (London)*, **72**, 156, (1903).
- ² Pickering, S.U., *J. Chem. Soc.*, **91-92**, 2001, (1907).
- ³ Bancroft, W.D. *Applied Colloid Chemistry*, McGraw-Hill Book Co., New York, 1922.
- ⁴ Finkle, P.; Draper, H.D.; Hildebrand, J.H., *JACS*, **45**, 2780, (1923).
- ⁵ Daintith, J., Edit. *Oxford Dictionary of Chemistry*, Oxford University Press, Oxford, 1996.
- ⁶ Binks, B.P.; Clint, J.H. *Langmuir*, **18**, 1270, (2002).
- ⁷ Wiley, M.R. *J. Colloid Sci.*, **9**, 427, (1954).
- ⁸ Lai, R.W.M.; Fuerstenau, D.W. *AIME Transactions*, **241**, 549, (1968).
- ⁹ Gaudin, A.M. *Flotation*, 2nd Ed., McGraw-Hill Book Co., Inc., New York, 1957.
- ¹⁰ Pieranki, P. *Phys. Rev. Lett.*, **45**, 569, (1980).
- ¹¹ Onoda, G.Y. *Phys. Rev. Lett.*, **55**, 226, (1985).
- ¹² Caruso, F.; Lichtenfeld, H.; Giersig, M.; Möhwald, H. *J. Am. Chem. Soc.*, **120**, 8523, (1998).
- ¹³ Caruso, F.; Caruso, R.A.; Möhwald, H. *Chem. Mater.* **11**, 3309, (1999).
- ¹⁴ Velev, O.D.; Furusawa, K.; Nagayama, K. *Langmuir* **12**, 2374, (1996).

- ¹⁵ Velev, O.D.; Furusawa, K.; Nagayama, K. *Langmuir* **12**, 2385 (1996).
- ¹⁶ Velev, O.D.; Nagayama, K. *Langmuir* **13**, 1856 (1997).
- ¹⁷ Dinsmore, A.D.; Hsu, M.F.; Nikolaidis, M.G.; Marquez, M.; Bausch, A.R.; Weitz, D.A. *Science* **298**, 1006, (2002).
- ¹⁸ Torza, S., Mason, S.G., *J. Colloid Interface Sci.*, **33**, 67, (1970).
- ¹⁹ Sundburg, D.C.; Casassa, A.P.; Pantazopoulos, J.; Muscato, M.R.; Kronberg, B.; Berg, J. *J. Appl. Polym. Sci.*, **41**, 1425, (1990).
- ²⁰ Muscato, M.R.; Sundberg, D.C. *J. Polym. Sci., Part B*, **29**, 1021, (1991).
- ²¹ Durant, Y.G.; Sundberg, D.C, in *Technology for Waterborne Coatings*, 44, ACS, 1997.
- ²² Berg, J.; Sundberg, D.; Kronberg, B. *J. Microencapsulation*, **6**, 327, (1989).
- ²³ Loxley, A.; Vincent, B. *J. Colloid Interface Sci.*, **208**, 49, (1998).
- ²⁴ Moy, J. EP 0 539 142 B1, 1992.
- ²⁵ Lovell, P.A.; El-Aasser, M.S. *Emulsion Polymerization and Emulsion Polymers*, John Wiley and Sons, Chichester, 1997.
- ²⁶ Lin, Y.; Skaff, H.; Emrick, T.; Dinsmore, A.D.; Russell, T.P. *Science*, 299, (2003).
- ²⁷ Arshady, R. *Polymer Eng. and Sci.*, **29**, 1746, (1989).

-
- ²⁸ Odian, G *Principles of Polymerization, 3rd Ed.*, John Wiley and Sons, Inc., New York, 1991.
- ²⁹ El-Aasser, M.S. *Emulsion Polymerizations and Emulsion Polymers*, Wiley, New York, 1997.
- ³⁰ Ugelstad, J.; Kaggerud, K.H.; Hansen, F.K.; Berge A. *Makromol. Chem.* **180**, 737 (1979).
- ³¹ Cheng, C.M.; Micale, F.J.; Vanderhoff, J.W.; El-Aasser, M.S. *J. Polym. Sci., A*, **30**, 235 (1992).
- ³² Frank. R.S. "*Copolymerization of Divinylbenzene and Maleic Anhydride*", Ph.D. Thesis, McMaster University, 2000.
- ³³ Atkins, P. *Physical Chemistry, 5th Ed.*, W.H. Freeman and Co., New York, (1994).
- ³⁴ Dowding, P.J.; Goodwin, J.W.; Vincent, B. *Colloid Polym. Sci.* **278**, 346 (2000).
- ³⁵ Shulkin, A.; Stöver, Harald D.H. *J. Membr. Sci.*, **209**(2), 433-444 (2002).
- ³⁶ Tomalia, D.A.; Uppuluri, S.; Swanson, D.R.; Li, J. *Pure Appl. Chem.*, **72**, 2358, (2000).
- ³⁷ Barton, A. F. M., Ed.. *CRC Handbook of Solubility Parameters and Other Cohesion Parameters*, CRC Press, pp. 94-110, 1983.

³⁸ Shulkin, A. Preformed Polymers as Building Blocks in Microencapsulations, Ph.D. Thesis, McMaster University, 2002.

³⁹ Brandrup, J.; Immergut, E.H.; Grulke, E.A., Editors, "*Polymer Handbook, 4th Ed*". John-Wiley and Sons, New York, 1999.

CHAPTER 3 - COMPOSITE TECTOAPSULE WITH POROUS MICROSPHERE RELEASE GATES

3.0 Introduction

In current microcapsule diffusion release systems, control over the rate of diffusion of core material is limited to the parameters of the shell material that can be altered during wall formation, such as thickness, porosity, and chemical composition. However, these parameters are often dependent on the environment in which the polymer forms, and are therefore different for every core material used.¹ This dependence on core solvent, which is discussed in detail below, can be a problem since each new fill may require re-optimisation of the capsule wall.

One way would be to develop a model for solvency effects on release and then, using a mixture of active and solvent, design the core solvent such that the desired release could be achieved. Another way to gain complete control over release from a capsule is to independently prepare the channels through which release occurs. We approach this by introducing preformed polymer spheres into the capsular wall. By designing a system where release occurs only through the polymer spheres, release control may be achieved independently of the core solvent environment.

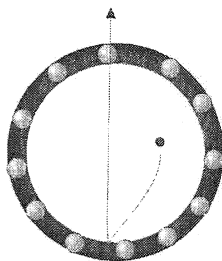


Figure 3. 1 Cartoon illustration of a composite capsule system where release occurs through the embedded spheres and not through the surrounding polymeric matrix.

Such a release system would have a composite wall made of two components: a) permeable polymer particles and b) a non-permeable capsule wall which would hold the particles in place and provide structural stability. Several factors must be considered when selecting microspheres for such a system: 1) It must be possible to assemble the microspheres at the oil-water interface. Therefore the polarity of the microspheres must be controllable. 2) The microspheres must function as release channels for the core oil; therefore they must have permanent, controlled porosity. 3) If these systems are to be easily prepared, the microspheres used must be easily prepared or readily available commercially.

As discussed previously in Chapter 2, existing literature in the area of polymer particle self-assembly has largely focused on the area of electrostatic assembly of latex particles. In these systems, latex particles are assembled at the oil water interface^{2,3,4,5,6} to form capsules, in the oil phase of an emulsion⁷ to form particles, or on the surface of a solid particle⁸ to form core shell particles. In all these systems the assembled particles

are charged and are fixed in place using a polymer of opposite charge⁸ or a salt² such as CaCl₂.

Such microcapsules prepared by the assembly of particles at the oil-water interface are generally characterized by large pore size, resulting in rapid release of core material, and limited mechanical stability as a result of poor particle-particle connections. Although they are very applicable for the containment of larger sized materials such as cells, they are less applicable for molecular size active materials such as pharmaceuticals and agricultural chemicals. The systems presented here are different in that they will be useful for the encapsulation and controlled delivery of smaller active materials.

In related work, inorganic particles have been incorporated into polymeric membranes as stabilizers,⁹ porogens,^{10,11} transport channels,¹² and structural agents.¹³ Polymeric particles have also been incorporated into polymers^{14,15} to increase the mechanical strength of the resulting material.

3.1 Microcapsule Release

The use of microencapsulation for controlled delivery dates back to the 1950's.^{16,17} Release of the core material from a microcapsule can occur by dissolution, degradation, or rupture of the microcapsule shell, or by diffusion of the core material through the polymeric wall. Release by rupture is used in applications such as contact adhesives and printing inks, whereas release of core material by diffusion is currently used for the delivery of many agricultural and pharmaceutical compounds. Release of liquid core material by diffusion through the capsular wall and evaporation into air will be the focus of the remainder of this chapter.

Small molecule diffusion from capsules with polymeric walls has been discussed in a number of different sources.^{18,19} In a system where release of the core material occurs by diffusion, (i.e. the capsule wall remains intact), the polymer of the wall may be porous or non-porous. In systems with porous walls, the core material diffuses through the pores or channels in the capsule wall. However, when the capsular wall is non-porous, the core material must diffuse through the bulk polymer. In such systems the rate of diffusion of a given core material depends on several factors: **1)** the thickness of the wall, **2)** the chain mobility of the wall polymer, **3)** swelling of the wall by core solvents and **4)** the composition of the wall material. Each of these factors will be discussed in more detail below.

There are two main classes of microcapsules, matrix and reservoir.¹⁹ A matrix capsule is one where the material to be released is dispersed throughout a polymer matrix. In a reservoir type of capsule, a droplet of the material to be released is surrounded by a polymer wall. This polymer wall controls the rate of release of the core material. The formation and function of such membranes is the focus of this thesis chapter.

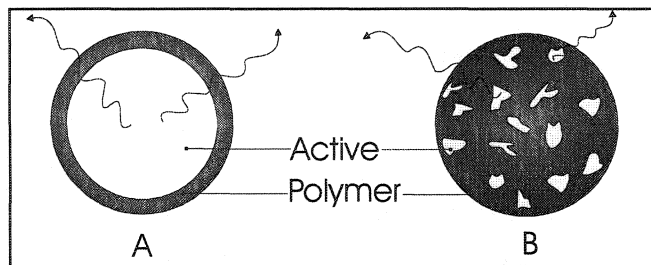


Figure 3. 2 Diffusion release into air from microcapsules, A) a reservoir capsule, having a liquid core and a polymeric wall and B) a matrix capsule where the material being released is dispersed throughout the polymer.

The thickness of the capsule membrane can be related to the rate of release of the core material as shown in Equation 3.1, where D = diffusion coefficient, K = distribution coefficient, ΔC = the concentration difference across the wall, r_i = the radius to the inner side of the membrane and r_o = the radius measured to the outer edge of the shell (i.e. $r_o - r_i$ = wall thickness).¹⁹ As the wall of the capsule becomes thicker the rate of release from the capsule decreases.

$$\text{ReleaseRate} = 4\pi DK\Delta C \frac{r_o r_i}{r_o - r_i} \quad \text{Equation 3. 1}$$

Although the above relation suggests a linear rate of release over time, the actual release curve for these systems is much more complex. In general, the release rate curve seen for encapsulated pesticides has three distinct regions (Figure 3.3).¹⁹ Initially a period

of rapid release is observed. This “burst” effect is common to many encapsulated systems, including polyurea systems, and is usually attributed to active* or solvent, which migrated into the polymeric wall during wall formation and during the post wall formation storage. The second stage is a region of constant release, which continues as long as the concentration or activity of active in the core remains constant. The third region shows a drop-off in release rate as a result of the declining active concentration in the core of the microcapsule.

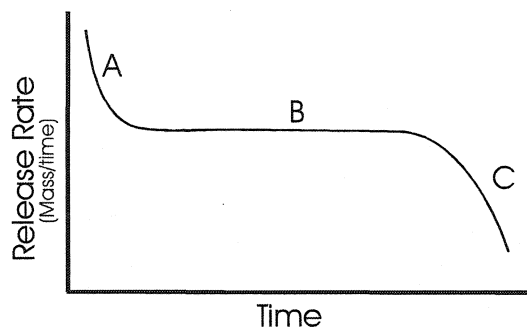


Figure 3. 3 A typical release rate versus time curve for an encapsulated pesticide system.

A) region of rapid release, believed to be a result of pesticide in the membrane, B) region of constant release, where pesticide content in the core remains constant, and C) region of rapid decline of the release rate attributed to the declining concentration of pesticide in

the core. Figure adapted H. Scher et al.(1977).¹⁹

A second factor affecting release through the bulk polymer of a microcapsule is the chain mobility and crystallinity of the wall polymer.^{19,20} Reduced chain mobility in the

* The “active” in a capsule is the material, which will serve some function in the end use, e.g. the pesticide, pheromone or drug.

polymeric wall has been found to decrease the rate of release from a capsule. Therefore, increased van der Waal's, dipolar and hydrogen bonding interactions all contribute to a decrease in release rate. Consequently, it has been observed that an increased crystallinity of the wall polymer results in decreased rates of release.²⁰ High levels of cross-linking also lead to reduced chain mobility and decreased release rates.

In a system where the polymeric wall is swollen or plasticized by a co-solvent, the rate of release is faster until the plasticizer itself is exhausted. This increased rate of release occurs as a result of the increased swelling and local mobility of polymer chains in the capsule wall.¹ This situation can be advantageous in systems where the active would have little or no solubility in the unplasticized polymer. However, it can also be detrimental, in that as the plasticizer is lost from the capsule the polymer in the wall collapses and the active can be trapped in the core. Alternatively, the active itself is able to slightly swell the polymer wall. In such systems, release of the active occurs at a constant rate until it begins to deplete, which causes the swollen polymer to collapse, thereby reducing the rate of release.¹⁹

3.2 An Example of Core Solvent Effects

Early work in solvency effects focused on a solvent of interest to our group, dodecyl acetate (C12 OAc) and clearly illustrates the change in morphology and release rate, which can occur as a result of changing the core solvent. This solvent is interesting because it serves as a model compound for sex pheromones of many species of moths. Dodecyl acetate was chosen as a model compound because it has an acetate head group attached to a long aliphatic tail, a structure common in moth pheromones, but is not a

recognized pheromone by itself. In this work, a series of polyurea capsules was prepared with mixed *p*-xylene/C12 OAc core solvents. The mixtures used contained 0, 10, 20 and 32.6 % C12 OAc in xylene. These samples were prepared from Mondur MRS and TEPA at room temperature with a Mondur MRS loading of 20% w/w of the oil phase. Conversion of Mondur MRS in all samples prepared at room temperature was <10%.

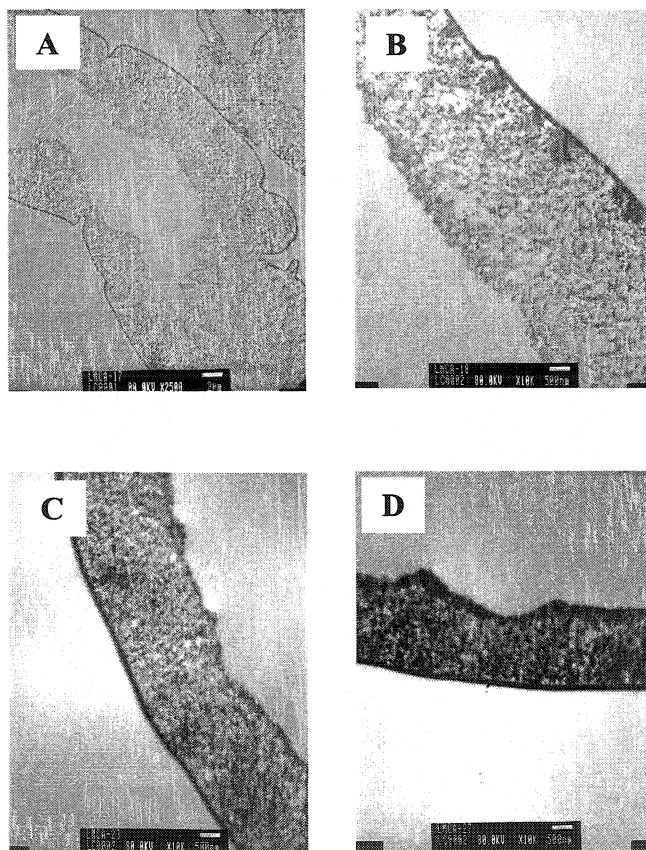


Figure 3. 4 Transmission electron images of cross-sections of polyurea capsule embedded in Spurr's resin. Samples were prepared at room temperature from Mondur MRS and TEPA, with mixed solvents of *p*-xylene and A) 0% C12 OAc, B) 10% C12 OAc, C) 20% C12 OAc, D) 32.6% C12 OAc. Scale bars are 2 μ m for A and 500 nm for B-D. All samples were stored in water for five months prior to TEM imaging

The TEM images in Figure 3.4 show that there are two distinct morphological regions in all samples. The first is a dense outer skin that is approximately the same thickness in all samples. The second is a loose porous region on the inside (oil side) of the membrane. This asymmetric morphology of membranes formed by interfacial polymerization is common and has often been commented on in the literature.²¹

Release of core material from the series of C12 OAc containing capsules was monitored gravimetrically. The results of release testing are shown in Figure 3.5 below.

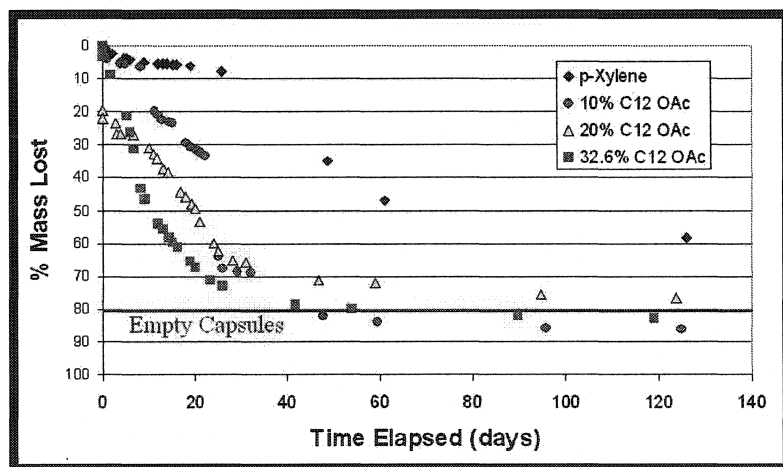


Figure 3. 5 Release of core material over time for the series of capsules containing 0 to 32.6% C12 OAc in *p*-xylene.

As C12 OAc content increases so does the rate of release of core material. The hydrogen bonding affinity of the two core solvents can be used to explain these observations. Polyureas are, generally, rigid, insoluble polymers as a result of the extensive hydrogen bonding that occurs between urea moieties in neighbouring polymer

chains. As discussed above, such hydrogen bonding reduces the mobility of the polymer chains, and therefore reduces the rate of release of core material. The carbonyl group of dodecyl acetate is a hydrogen bond accepting group, and can plasticize the forming capsule wall by disrupting the hydrogen bonding. In so doing, the mobility of the polymer chains and the capsule release rate are increased.

3.3 Objective and Scope of Research

The goal of this research was to use precipitation microspheres and gels in conjunction with polyurea to make composite microcapsule called composite tectocapsules. This work parallels work described in chapter 2 where tectocapsules were prepared by self-assembly of microspheres^{4,22} or microgels⁵ in the absence of a second polymer. Here it is shown that porous microspheres of the correct polarity can be incorporated into a polyurea matrix and that their presence in the microcapsule wall greatly affects the release properties.

3.4 Experimental

Materials

Diethylenetriamine (DETA, 99%), divinylbenzene-55 (DVB-55, a commercial mixture of 55% *meta* and *para*-divinylbenzene, with 45% *meta* and *para*-ethylvinylbenzene), heptane (HPLC grade) methylene chloride (HPLC grade), methyl ethyl ketone (MEK, 2-butanone, HPLC grade) 4-methylstyrene (4-MeSt, 96%), polyethylenimine (Mn ca. 1200, 50% in water), polyethylenimine (Mn ca. 60 000, 50% in

water), polyvinylalcohol (PVA, 80% hydrolyzed, Mn ca 9000), propyl acetate (99%), tetraethylenepentamine (TEPA, tech.), *p*-xylene (HPLC grade) were purchased from Aldrich and used without further purification. Maleic anhydride (99%) was purchased from Aldrich and was recrystallized from methylene chloride. Mondur ML (a mixture of 2,4- and 4,4-diphenylmethane-diisocyanate) was donated by Bayer and used as received. 2,2'-Azobisisobutyronitrile (AIBN) was donated by DuPont Canada and was recrystallized from methylene chloride prior to use. Polyethylenimine (Mn ca. 9 000, 30% in water) was purchased from Polysciences, Inc. and was used without purification.

Poly(Divinylbenzene-55-*alt*-Maleic Anhydride) Microsphere Synthesis.

The microspheres were prepared according to a procedure reported earlier.²³ Maleic anhydride (0.80 g) was dissolved in MEK (8 mL) in a glass scintillation vial (20 mL). Heptane (12 mL) was added, followed by DVB-55 (0.73 g) and AIBN (0.016 g). The vial was closed tightly and placed in the polymerization reactor[†] at 70°C for 24 hours. At the end of the reaction the microspheres were collected by centrifugation, and washed with MEK. The microspheres were then dried at room temperature in a vacuum oven overnight and stored in a dessicator. Typical yields were 95%.

Poly(Divinylbenzene-*alt*-Maleic Anhydride) Microgel Synthesis.

The two types of microgel were prepared according to procedure reported earlier.²³
Poly(DVB55-*alt*-MAn) gels: Maleic anhydride (1.90 g) was dissolved in MEK (56 mL)

in a Nalgene bottle (125 mL). Heptane (24 mL) was added, followed by DVB-55 (1.6 g) and AIBN (0.064 g). Poly(DVB5-*alt*-MAn) gels: Maleic anhydride (1.90 g) was dissolved in MEK (32 mL) in a Nalgene bottle (125 mL). Heptane (48 mL) was added, followed by DVB-55 (0.16 g), 4-methylstyrene (1.22 g) and AIBN (0.064 g).

In each case, 18 mL of the reaction mixture was transferred to a glass scintillation vial. The vials were closed tightly and placed in the polymerization reactor at 70°C for 24 hours. At the end of the reaction the microspheres were collected by centrifugation, and resuspended repeatedly in MEK. Subsequently MEK was exchanged for reagent grade PrOAc or other fill solvents. Typical yields are 40-60%. Microgels were stored in wet PrOAc for a minimum of two weeks prior to use in tectocapsule formation to allow for hydrolysis of approximately 20% of the anhydride functionalities.

Microsphere and microgel diameters were measured using a Phillips ElectroScan 2020 environmental scanning electron microscopy (ESEM) and a Coulter LS 230 particle sizer. Infrared spectra were recorded using a Thermo Nicolet FTIR.

Poly(Divinylbenzene-55) Microsphere Synthesis.

The microspheres were prepared according to a procedure reported earlier.²⁴ DVB-55 (18.23 g) and AIBN (0.365 g) were added to acetonitrile (950 mL) in a 1L Nalgene bottle. The bottle was shaken, closed tightly and placed in the polymerization reactor at room temperature. The temperature was then ramped according to the following profile: 25 °C

[†] The polymerization reactor is a modified commercial hotdog roller. The temperature in the reactor can be controlled ($\pm 1^\circ\text{C}$) and vials roll at a rate of approximately 5 vial rotations per minute.

to 60 °C over one hour, 60 °C to 70°C over one hour and 40 minutes. Subsequently the reaction temperature was held at 70 °C for 24 hours. At the end of the reaction the microspheres were collected by vacuum-filtration over a 0.2 µm Teflon membrane, and washed three times with THF, and once each with acetone and methanol. The microspheres were then dried at 40°C in a vacuum oven for 3 days and stored in a desiccator. Typical yields are 40%.

Porous Poly(Divinylbenzene-55) Microsphere Synthesis.²⁵

DVB-55 (18.23 g) and AIBN (0.365 g) were added to a mixture of acetonitrile (710 mL) and toluene (250 mL) in a 1L Nalgene bottle, and the reaction carried out as described above.

Typical procedure for Maleic Acid functionalization of porous and non-porous Poly(Divinylbenzene-55) Microspheres.

Porous poly(DVB55) microspheres (2.5 g) were suspended in MEK (40 mL) in a two neck, jacketed round bottom flask, using a magnetic stir bar. The temperature of the system was increased to 65°C and an excess of maleic acid (MA, 1.2 g) was added. After the system was allowed to mix for 5 minutes to ensure complete dissolution of the MA, AIBN (0.85 g) was added, and the reaction continued for 24 hours. Following the reaction, microspheres were collected by filtration, re-suspended in MEK and left to soak overnight. This collection and re-suspension procedure was repeated three times, and the washed microspheres were dried in a vacuum oven at 45°C and stored in a desiccator

(yield: 2.78g). Diffuse reflectance FT-IR analysis shows the presence of both acid (s, 1731 cm^{-1}) and anhydride functionalities (s, 1786 cm^{-1}). The anhydride groups may be due to anhydride present in the maleic acid monomer, or may have been generated during the drying of the particles.

Characterisation.

Microparticle diameters were measured by environmental scanning electron microscopy (ESEM) as well as by static light scattering using a Coulter LS 230 particle sizer. Chemical composition was monitored using a ThermoNicolet FTIR. ESEM samples were prepared by washing a sample of the capsules several times with distilled water to remove PVA and excess amine, depositing a drop of capsule suspension on a sample stub and gold-coating to 5nm prior to imaging. Transmission electron microscopy was carried out on microtomed sections of capsules prepared according to the following method. The capsule slurries were first filtered to remove water, and dried in air. The dried capsules were then crushed under liquid nitrogen and extracted with *p*-xylene to remove any residual isocyanate. The resulting wall fragments were collected by filtration and dried overnight at room temperature. The capsule fragments were then embedded in Spurr's epoxy resin, microtomed to 100 nm thickness, and mounted on 3 mm TEM grids.

Typical Encapsulation Procedures.

A) poly(DVB-*alt*-MAN) based microsphere systems. A solution of Mondur ML (0.24 g) dissolved in 2 mL PrOAc was prepared in a 20 mL scintillation vial. 0.125 mL of this stock solution was combined with 0.125 mL of microsphere or microgel suspension in a 4 mL glass vial and shaken not stirred until well mixed. The aqueous phase consisting of 0.4 w/w% PVA in 1 mL distilled water was added, and the resulting two-phase system emulsified by shaking on a modified laboratory wrist shaker at 384 excursions per minute (epm) for 2.5 minutes. Subsequently, the rate of shaking was reduced to 215 epm and TEPA (0.25 mL, 0.95 M in distilled water) was added by syringe over 30 seconds. After the amine addition the reaction was allowed to continue overnight.

B) Poly(DVB55) based microsphere systems. A jacketed glass reactor (500 mL) fitted with 4-prong stainless steel baffles (length 6 cm, width 1.1 cm) was charged with distilled water (150 g) and PVA (0.15 g). A six-bladed, 2" stainless steel stirrer was then inserted into the aqueous phase and the reactor was closed with a three-neck glass lid. The mixture was stirred at 300 rpm for 15 minutes to ensure complete dissolution of the PVA. The temperature of the reaction was controlled at 70°C using a circulating bath. Next, a suspension of microspheres (2.20 g) in a mixture of isocyanate (5.00 g) and *p*-xylene (43.20 g), was added the reactor. The resulting two-phase system was allowed to emulsify for 10 minutes at 400 rpm. Following emulsification, the mixing speed was reduced to 250 rpm and DETA (5.00 g dissolved in a mixture of 0.05 g PVA in 50 g of distilled water) was added drop-wise to the oil-in-water emulsion over about 10 minutes.

After the amine addition the reaction was allowed to continue for four hours. The mixture was then transferred to a separatory funnel (1 L) and washed three times with distilled water. Samples of the washed capsules were taken and stored in glass scintillation vials. Conversion to polyurea was typically 25-30%.

Fill Release Measurements.

Fill release was measured gravimetrically from samples in aluminum weigh dishes stored at room temperature or at 50°C. Aluminum weigh dishes were prepared for release samples by soaking in Na₂CO₃ solution (~ 2% w/w) for several hours. After treatment, the aluminum dishes were rinsed three times with distilled water and left to dry for several days. This procedure etches the surface of the aluminum and allows better wetting by the aqueous sample. About 0.5mL of representative aqueous dispersions of capsules were transferred to a treated dish. Weight loss measurements were carried out in triplicate.

Weight losses were recorded initially every half-hour, and later on a daily or weekly basis as appropriate. Room temperature samples were stored uncovered in a fumehood for the duration of the release test. 50°C samples were stored in an oven set to 50°C ± 1°.

STXM Analysis

Composite tectocapsules were prepared for STXM by first crushing the capsules under liquid nitrogen. The resulting capsule fragments were washed with *p*-xylene on a filter, dried, embedded in an epoxy resin designed to contain no aromatic or carbonyl

groups, and microtomed to a thickness of 100 nm. The Polymer STXM Beamline 5.3.2 at the ALS in Berkeley was used for these analyses.

3.5 Results and Discussion

This work was designed to explore using porous microspheres embedded across otherwise impermeable polyurea capsule walls as fill release control devices. First, we used easily available poly(divinylbenzene-*alt*-maleic anhydride) microspheres and microgels to study the interfacial assembly and fixation of such polar particles in presence of isocyanates. Second, we prepared porous and non-porous poly(divinylbenzene-55) microspheres, and functionalized their surfaces with maleic acid to enable similar interfacial assembly of these release control microspheres. Here, we studied morphology and fill release profiles, looking for evidence of through-microsphere fill release.

Third, we use Scanning Transmission X-ray Spectromicroscopy (STXM) to study the chemical composition of some of these tectocapsules at high spatial and chemical resolution.

3.5.1 Composite capsules containing Poly(divinylbenzene-55-*alt*-maleic anhydride) Microspheres and Microgels.

Monodisperse poly(DVB55-*alt*-MAN) microspheres and two types of poly(DVB-*alt*-MAN) microgels were incorporated into interfacial polyurea capsule walls. The microspheres were prepared by precipitation copolymerization of stoichiometric amounts

of DVB55 and maleic anhydride in 40% MEK/Heptane mixtures at 2% monomer loading, to give poly(DVB55-*alt*-MAn) microspheres of 550 nm diameter.²³ The analogous swellable poly(DVB55-*alt*-MAn) microgels, with 150 nm diameter, were formed under similar conditions but in 80% MEK/Heptane. Finally, the larger poly(DVB5-*alt*-MAn) microgels, with 650 nm diameter, were prepared in 40% MEK/Heptane by replacing 91% of the DVB55 with 4-methylstyrene.

Composite tectocapsules containing these poly(DVB-*alt*-MAn) particles were prepared by shaking glass vials containing isocyanates and microparticles in the organic phase, as well as a four-fold excess of aqueous phase containing polyvinylalcohol (PVA). During this emulsification process, many of the microparticles self-assembled at the oil-water interface. While shaking, an aqueous polyamine solution was added by syringe, to both covalently cross-link the microspheres and commence polyurea wall formation. Some ionic interactions are also expected to occur between the acid groups of the microspheres/microgels and the amine groups.

Propyl acetate (PrOAc) was used as core solvent for the model encapsulations of all three poly(DVB-*alt*-MAn) microspheres and microgels. In addition, a 50/50 (v/v) PrOAc/*p*-xylene mixture, while unable to disperse either of the microgels, was used as core solvent for the encapsulation of the poly(DVB55-*alt*-MAn) microspheres.

Propylacetate/*p*-Xylene Mixed Core Solvent. Stable composite capsules were formed from poly(DVB55-*alt*-MAn) microspheres using the PrOAc/*p*-xylene mixed core solvent. Transmission (TEM, not shown) and environmental scanning electron microscope images (ESEM, Figure 3.6) of the resulting composite tectocapsules showed the microspheres just piercing the outer polyurea membrane, suggesting that the particles assembled at the interface prior to the bulk of polyurea wall formation, which occurs mainly after amine is added to the system. This is consistent with the self-assembly of microspheres and microgels prior to amine addition, as observed earlier in the absence of polyurea.

These composite capsules retained their fill for several days, an order of magnitude longer than those prepared with 100% PrOAc as the core solvent described below. This is attributed to a denser, less permeable polyurea membrane formed in the presence of 50% xylene. Still, the presence of 50% PrOAc ensures some permeability of the wall, and thus should enable slow fill release by diffusion through the polyurea wall.

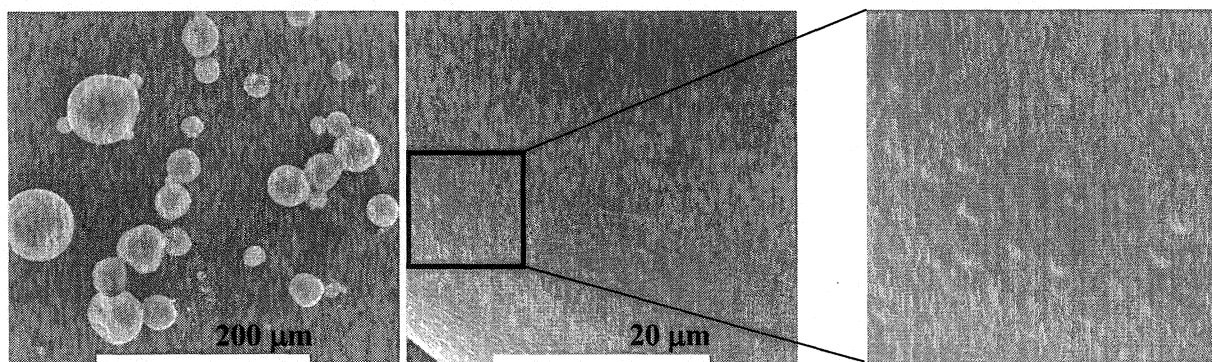


Figure 3. 6 Scanning transmission electron micrographs of composite tectocapsules prepared with 50/50 (v/v) PrOAc/*p*-xylene as mixed core solvent. The tops of poly(DVB55-*alt*-MAN) microspheres can be seen protruding from the polyurea wall.

Propyl Acetate (PrAc) as Single Core Solvent. Composite tectocapsules involving all three poly(DVB-*alt*-MAN) microspheres and microgels were prepared using PrOAc as the core solvent. All three composite tectocapsule systems released their fill within hours of removal from the aqueous phase. Fill release may happen by diffusion through the highly permeable polyurea walls formed in a polar core solvent,¹ as well as by diffusion through the microgels located at the interface. The resulting capsule systems were studied by optical microscopy (Figure 3.7) as well as by both ESEM (Figure 3.8) and TEM (Figure 3.9).

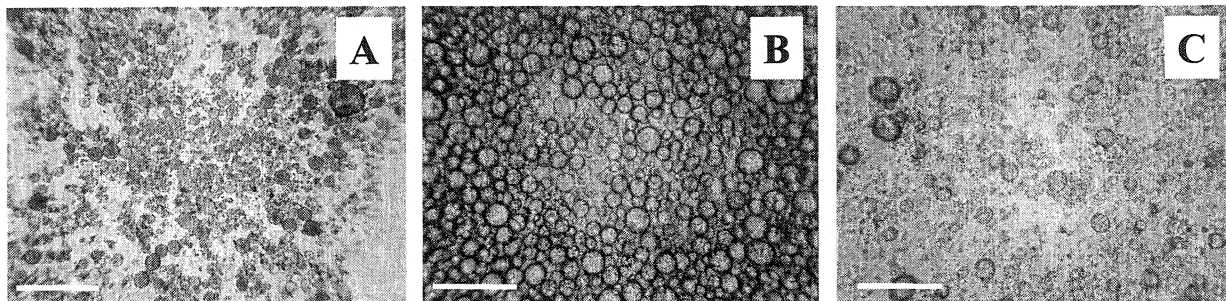


Figure 3. 7 Optical micrographs of wet composite propylacetate-filled tectocapsules made with poly(DVB55-*alt*-MAn) microspheres (A) or microgels (B), and with poly(DVB5-*alt*-MAn) microgels (C). The scale bar is approximately 250 μm .

The optical microscope images (Figure 3.7) show spherical capsules. The microspheres and microgels were too small to be resolved by this technique.

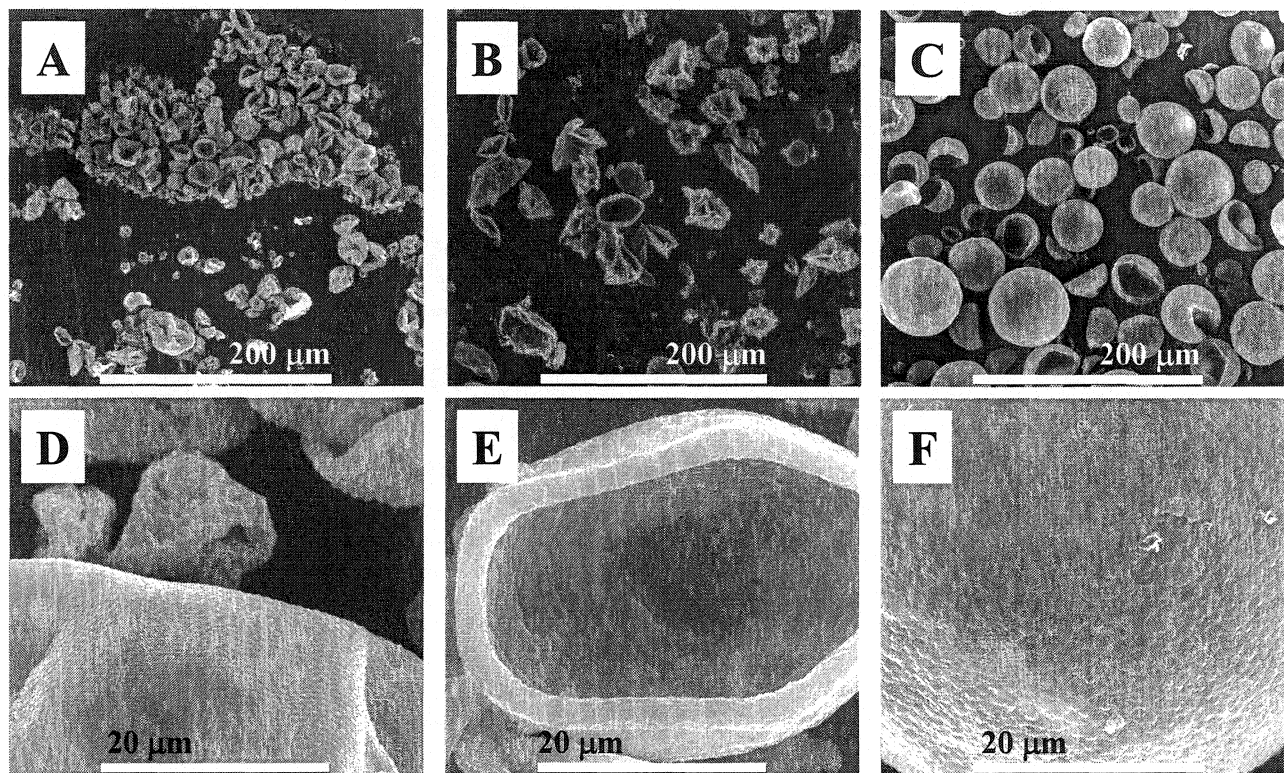


Figure 3. 8 Environmental scanning electron micrographs (ESEM) of dry tectocapsules prepared with poly(DVB55-*alt*-MAN) microspheres (A, D) and microgels (B, E), and poly(DVB5-*alt*-MAN) microgels (C, F).

The ESEM images clearly show the poly(DVB55-*alt*-MAN) microspheres and the large poly(DVB5-*alt*-MAN) microgels protruding through the polyurea wall (Figures 3.8 D and F). Although the small poly(DVB55-*alt*-MAN) microgels are not clearly visible in the ESEM image (Figure 3.8 E), the hexagonal close packing of the other particles strongly suggests that they assemble at the interface prior to amine addition. Amine addition then leads to rapid interfacial polyurea formation, with fixation of the microparticle arrays at the interface.

TEM images of the composite capsules embedded in Spurr's[†] epoxy resin and sectioned, confirm that the microspheres and microgels are predominantly located at or near the oil-water interface (Figure 3.9).

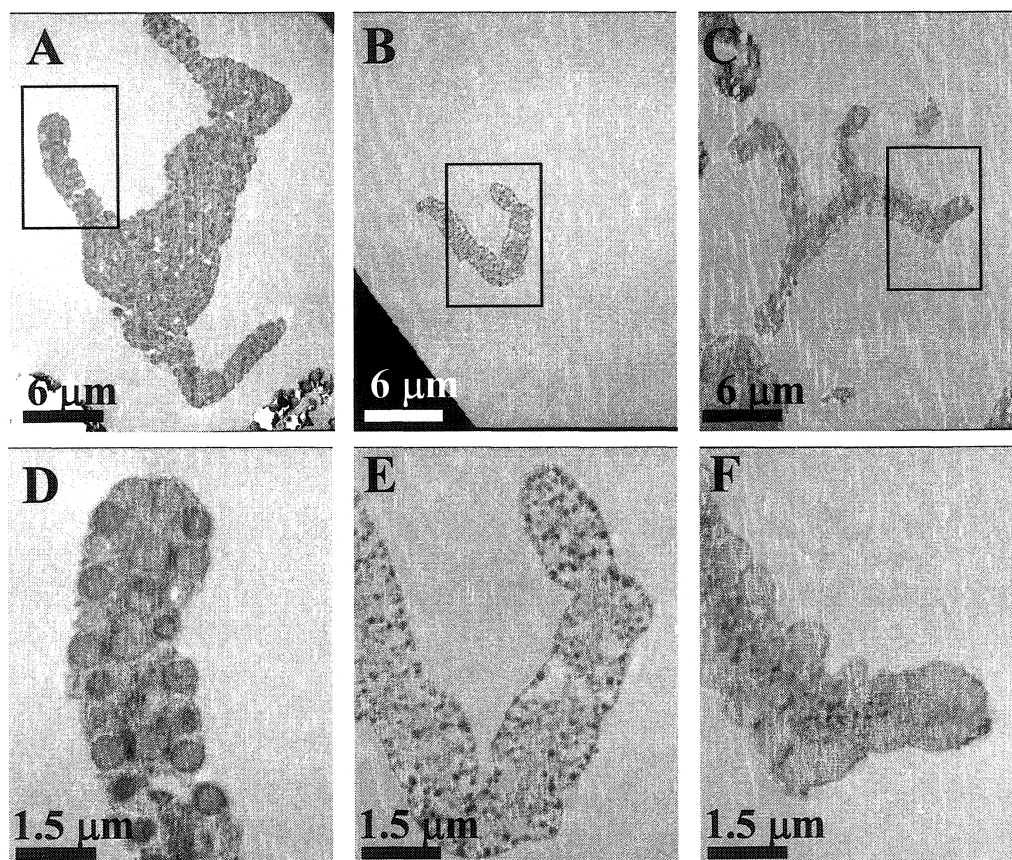


Figure 3. 9 Transmission electron micrographs (TEM) of composite tectocapsules prepared with (DVB55-*alt*-MAN) microspheres (A, D) and microgels (B, E), and poly(DVB5-*alt*-MAN) microgels (C, F). embedded in Spurr's resin and sectioned. The box shown on the upper images indicates the field of view for the lower images.

[†] Spurr's Resin is a common embedding medium, comprised of: nonenyl succinic anhydride (NSA), the diglycidyl ether of poly(propylene glycol) (DER 736), vinylcyclohexene dioxide (ERL 4206), and 2-dimethylaminoethanol (DMAE).

3.5.2 Composite Tectocapsules with Porous Poly(Divinylbenzene-55) Precipitation Microspheres.

The poly(DVB-*alt*-MAn) microspheres and microgels described above are good model particles for developing composite tectocapsules. However, they are not porous, and are too polar to be dispersed in core solvents containing 50% xylene or more. As described above, the proposed separation of wall formation from release control requires a combination of porous amphiphilic microspheres, with nonpolar core solvents such as xylene that form impermeable polyurea walls.¹ To address these issues we prepared non-porous and porous poly(DVB55) microspheres by precipitation polymerization of divinylbenzene-55 in acetonitrile, and in a mixture of acetonitrile and toluene, respectively.²⁵ These microspheres were subsequently surface-functionalized by radical grafting of maleic acid onto the residual double bonds in presence of AIBN, in order to ensure their assembly at the oil-water interface.

Optical microscopy of polyurea capsules prepared with both functionalized and non-functionalized porous poly(DVB55) microspheres revealed very different interfacial properties (Figure 3.10). Capsules prepared with non-functionalized microspheres featured distinct opaque patches (Figure 3.10 A), while the capsules formed with maleic acid functionalized microspheres showed less internal contrast, suggesting a more even distribution of microspheres within the capsule wall (Figure 3.10 B). The inset in Figure 3.10 B is an expanded view of the microcapsule contained in the box on the main image and clearly shows microspheres in the capsular wall.

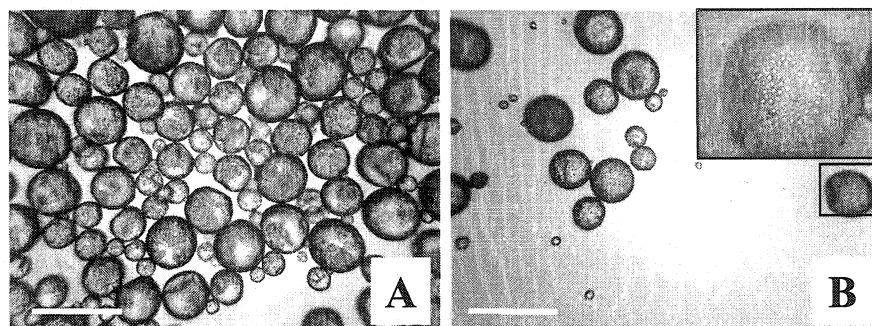


Figure 3. 10 Optical micrographs of wet composite tectocapsules containing non-functionalized (A) and maleic acid functionalized (B) porous poly(DVB55) microspheres. The inset in image B is an expanded view of the capsule in the box on the main image.

ESEM images of the tectocapsules prepared with non-functionalized porous microspheres showed smooth outer surfaces, suggesting that these microspheres remained in the core of the microcapsules (Figure 3.11, A and C). In contrast, the maleic acid functionalized microspheres clearly breach the polyurea capsule wall (Figure 3.11, B and D), suggesting that they self-assembled at the oil-water interface prior to polyurea formation. Representative TEM images of wall fragments similarly show the maleic acid functionalized microspheres breaching the polyurea capsule wall (Figure 3.12 B), while the non-functionalized microspheres stay in the interior of the polyurea capsules (Figure 3.12 A). The non-functionalized microspheres also appear fuzzy, suggesting they are coated with polyurea.

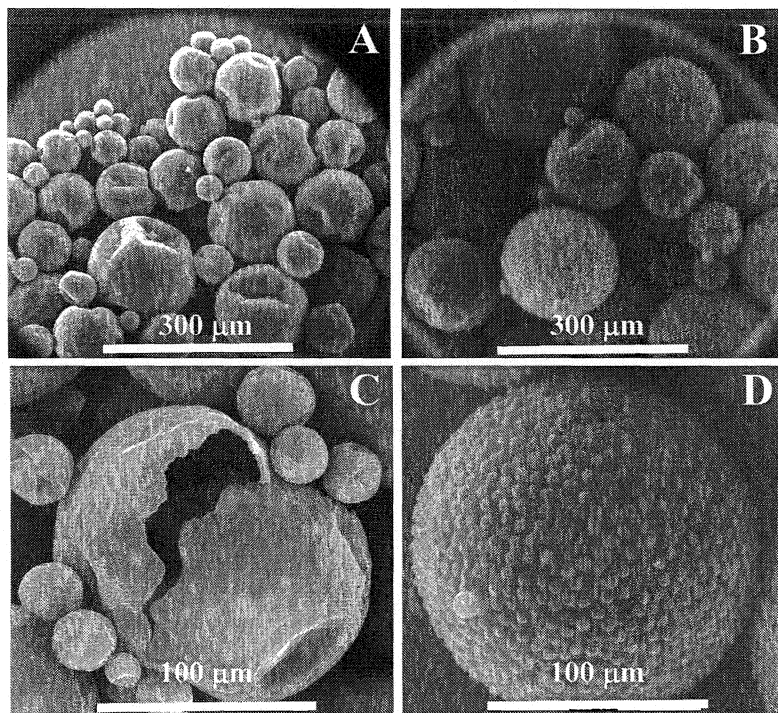


Figure 3. 11 Environmental scanning electron micrographs (ESEM) of composite tectocapsules made with non-functionalized (A, C) and maleic acid functionalized (B, D) porous poly(DVB55) microspheres.

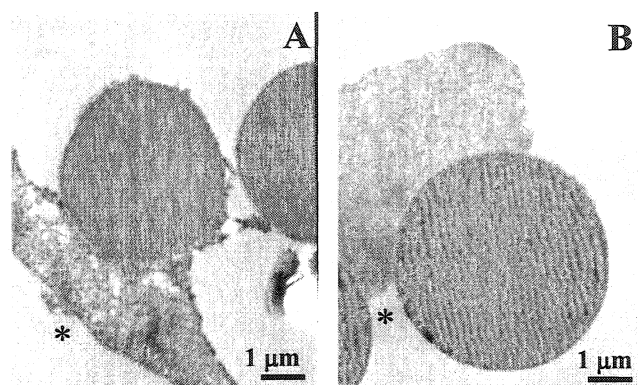


Figure 3. 12 Transmission electron micrographs of sections of composite tectocapsules made with non-functionalized (A) and maleic acid functionalized (B) porous poly(DVB55) microspheres, embedded in Spurr's resin. The asterix indicates the outer, aqueous side of the capsule wall.

3.5.2.1 Fill Release from Composite Tectocapsules

Release of xylenes from three different types of composite tectocapsules was monitored gravimetrically, both at room temperature and at 50°C. Release data shown (Figure 3.13) represent the average of three different release samples, and are normalized to the initial weight of the samples.

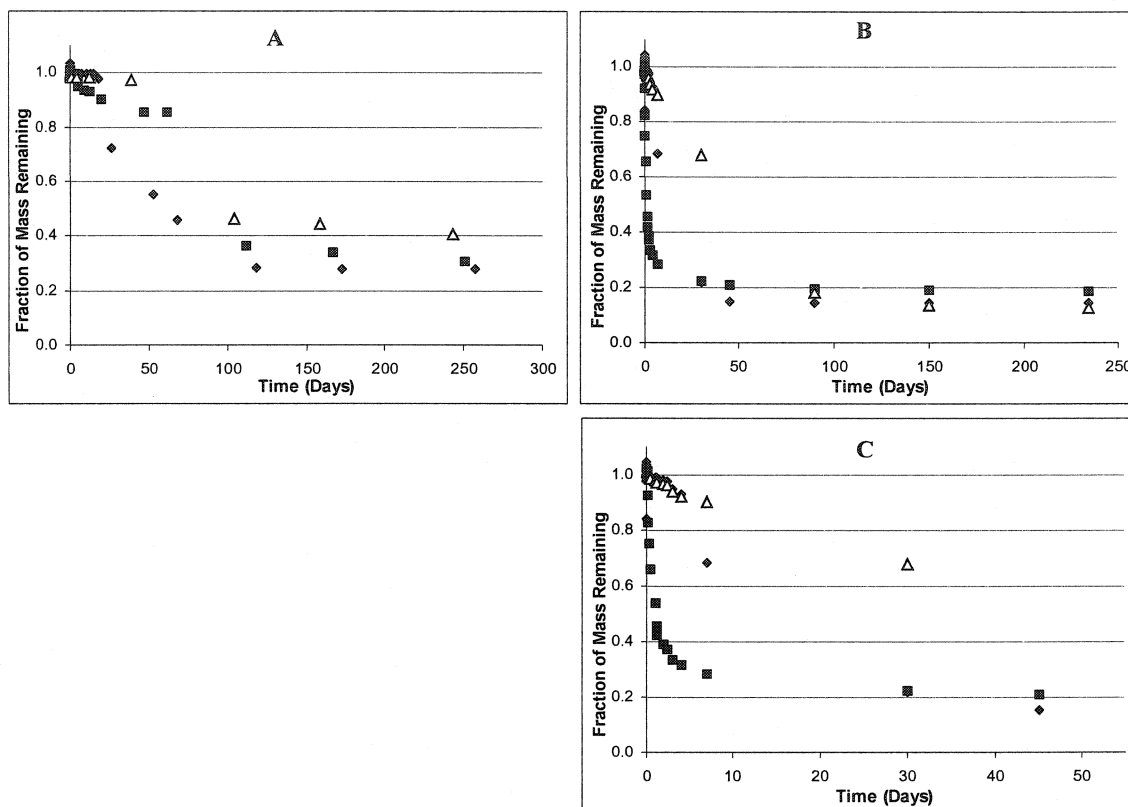


Figure 3.13 Release curves at room temperature (A) and 50 °C (B) for tectocapsules prepared with non-functionalised (◆) and functionalised (■ 2.2g particles, Δ 0.2g particles) porous poly(DVB) precipitation microspheres. Plot C expands the region of rapid weight loss observed between 0 and ~60 day in plot B.

At room temperature, the tectocapsules containing the non-functionalized poly(DVB55) microspheres show little mass loss until 20 days at which point mass decreases rapidly. This discontinuous release profile is similar to those seen previously for polyurea capsules containing xylenes as fill.¹ It is attributed to the superposition of two release mechanisms: very slow, diffusion-controlled release through intact capsule

walls, and a much faster wall strain-induced release from capsules that adhere to each other.¹ A similar step-wise release profile is observed at 50°C. In these capsules, the non-functionalized microspheres do not play a role in wall formation, and hence do not influence the release process.

Tectocapsules prepared with porous poly(DVB55) microspheres functionalized with maleic anhydride showed different release profiles depending upon microsphere loading. Capsules prepared with 0.2 and 2.2g microspheres, respectively, both show evidence for significant diffusion release during the first 40 – 60 days. These initial release rates are much faster than those seen in polyurea capsules not containing interfacial microspheres, and appear to scale with microsphere loading. Following this initial, diffusion release period, both capsule samples show rapid weight loss reminiscent of wall strain-induced release. At 50°C, these two capsules show rapid, near-linear release over approximately 100 and 10 days, again in agreement with their different microsphere loading. At this higher temperature there is no evidence of discontinuous release attributable to wall strain-induced release.

After approximately 120 days at room temperature, release from all three types of capsules slows dramatically. This could be due to the end of wall strain-induced release and a return to diffusion-controlled release. Alternatively, it may be due to slow release from capsules containing few microspheres, or having stronger polyurea walls.

These results show that interfacially active, porous microspheres can strongly enhance the release of xylene from polyurea capsules. At the same time, they raise several new questions:

1. Is the enhanced release due to a mechanical weakening of the capsule walls, leading to more pronounced strain-induced release?
2. Is the enhanced release from tectocapsules due to diffusion through the microsphere pores, or due to diffusion through the microsphere-polyurea interface?
3. What is the nature of the microsphere-polyurea interface, and does polyurea form within the porous microspheres?

No cracks associated with the polyurea-microsphere interfaces were seen in ESEM images, leading us to discount a mechanical weakening by the embedded microspheres. The following two sections will address the remaining two questions presented above.

3.5.3 Composite Tectocapsules with Non-porous Poly(Divinylbenzene-55) Precipitation Microspheres.

The microsphere-polyurea interface is likely composed of a finite hydrophilic gel layer. The poly(divinylbenzene-55) microspheres are known to have a ~50nm thick surface layer of lightly cross-linked poly(divinylbenzene).^{26,27} Functionalization with maleic acid would convert this organo-gel layer into a polar layer containing a mixture of succinic acid as well as some succinic anhydride groups formed by dehydration during microsphere work-up. Reaction with polyamine during the capsule formation would lead to a combination of electrostatic and covalent bonding, and form an amphiphilic interfacial film. During release, xylenes could diffuse through this lightly cross-linked,

amphiphilic interfacial layer between microspheres and impermeable polyurea. Therefore, while the release rates appear to scale with microsphere loading, it is difficult to distinguish between through-pore and interfacial layer release of xylenes. One method of doing so was to prepare composite tectocapsule with non-porous maleic acid functionalized poly(DVB55) microspheres, thereby eliminating the potential for through pore release.

Once again release from the composite capsules was measured gravimetrically and the resulting release curve is shown in Figure 3.14 along with those for the composites containing functionalized and non-functionalized porous microspheres previously shown in Figure 3.13. Surprisingly, release from the composite capsules prepared with non-porous microspheres is very rapid and the capsules empty completely within a few hours.

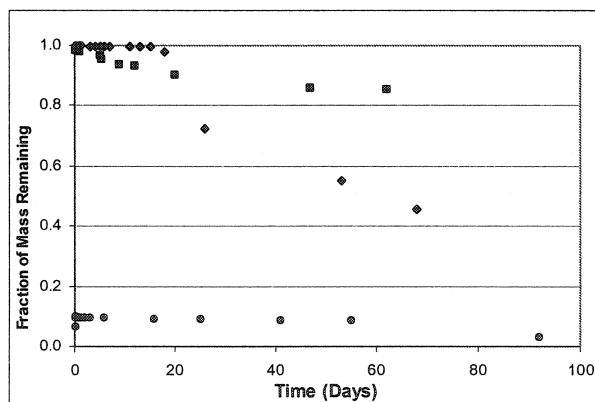


Figure 3. 14 Release curves at room temperature for tectocapsules prepared with non-functionalised (◆), functionalised porous (■) and non-porous (●) poly(DVB) precipitation microspheres.

This rapid release suggests that a strong interface between the microspheres and polyurea is required for controlled release from the composite tectocapsules. Since the rate of release from the composites containing non-porous microspheres is much more rapid than from the composites having porous microspheres it can be inferred that the non-porous microspheres are less well anchored than the porous microspheres.

3.5.4 STXM Analysis of Composite Tectocapsules

In the final section below we map the chemical distribution in the composite tectocapsules using STXM,²⁸ (refer to Chapter 1 for description) to determine if polyurea growth does occur within the microsphere pores.

Using standard spectra for the polyurea, poly(divinylbenzene-55), and the succinic acid present in the sample, it is possible to generate maps showing the distribution of these species within a sample (Figure 10).

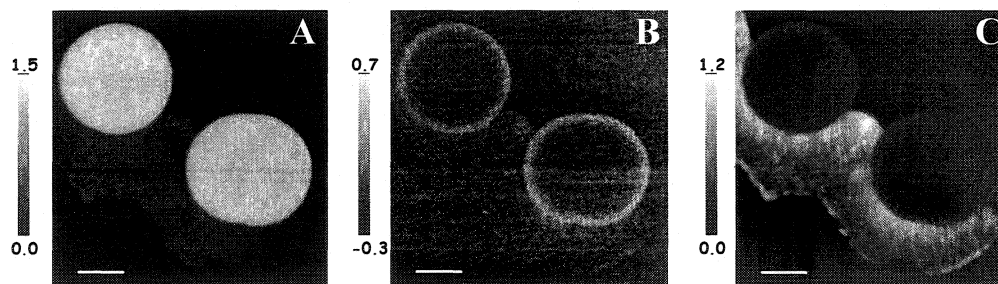


Figure 3. 15 STXM individual component maps of a wall fragment of a composite tectocapsule having porous maleic acid functionalised microspheres embedded in the polyurea capsule wall. A) poly(divinylbenzene55), B) succinic acid; C) polyurea matrix. The intensity in the images is proportional to the amount of each component present in the sample.

Overlaying these individual component maps leads to a composite component map that depicts the distribution of all three species within the sample imaged (Figure 11).

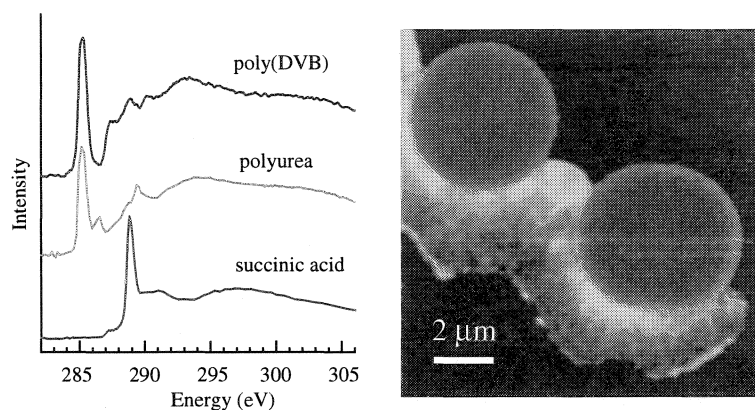


Figure 3. 16 STXM composite component map and the corresponding x-ray spectra.

These STXM results indicate that polyurea is excluded from the microspheres pores, within the detection limit of about 10%. Since both the isocyanates and amines used are smaller than the pore exclusion molecular weight of 500Da, the absence of polyurea from the pores is attributed to slow diffusion of the wall former, especially amine, through the pores. Any oligomers formed would be too large to enter the pores. Secondly, no polyurea could be seen on the outer surface of the microspheres, once again suggesting that microsphere self-assembly occurs prior to polyurea wall formation.

3.6 Conclusions

Described here are a new type of composite microcapsule, called composite tectocapsules. The tectocapsules presented here, fit into two categories, those that have microspheres or microgels polar enough to self-assemble at the oil-water interface and become embedded in the polyurea matrix (Figure 17 A) and those in which the microspheres are non-polar and become contained in the capsular core (Figure 17 B).

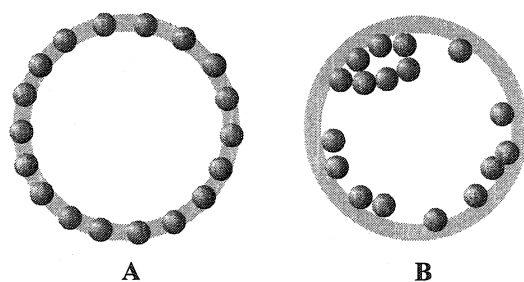


Figure 3. 17 Cartoon of two types of composite capsules that result when polar precipitation (A) or non-polar (B) precipitation microspheres are used during encapsulation

We have shown that those systems where the porous microspheres penetrate across the dense outer polyurea membrane exhibit accelerated release of the core solvent at 50°C and slower more controlled release of core solvent at room temperature versus systems where the microspheres are simply encapsulated within the core. Release in from the tectocapsule having microspheres in the capsule membrane is proposed to occur via two routes: the microcapsule pores and the microsphere-polyurea interface.

Finally, scanning transmission spectromicroscopic (STXM) analysis of the composite tectocapsules containing maleic acid functionalized porous microspheres showed that polyurea growth was largely excluded from the microsphere pores.

References

-
- ¹ Li, W.H.; Stöver, H.D.H *J. Membrane. Sci.* Accepted.
- ² Velev, O.D., Furusawa, K., Nagayama, K., *Langmuir*, **12**, 2374, (1996).
- ³ Velev, O.D., Nagayama, K., *Langmuir*, **13**, 1856, (1997).
- ⁴ Croll, L.M.; Stöver, H.D.H.; *Langmuir*, **19**, 5918, (2003).
- ⁵ Croll, L.M.; Stöver, H.D.H.; *Langmuir*, in press, 2003.
- ⁶ Dinsmore, D.A.; Hsu, M.F.; Nikolaidis, M.G.; Marquez, M.; Bausch, A.R.; Weitz, D.A. *Science*, **298**, 1006, (2002).
- ⁷ Velev, O.D., Furusawa, K., Nagayama, K., *Langmuir*, **12**, 2385, (1996).
- ⁸ Caruso, F., Lichtenfeld, H., Giersig, M., Möhwald, H., *J. Am. Chem. Soc.*, **120**, 8523, (1998).
- ⁹ Moy, J. *EU 0 539 142 B1*, (1992).
- ¹⁰ Bottino, A.; Capannelli, G.; D'Asti, V.; Piaggio, P. *Sep. and Purif. Tech*, **22-23**, 269, (2001).
- ¹¹ Parvulescu, V.; Buhoci, L.; Roman, G.; Albu, B.; Popescu, G. *Sep. and Purif. Tech*, **25**, 25, (2001).
- ¹² Freeland, W.E.W.; Tomkinson, D.L. *US 4 756 844*, (1988).

-
- ¹³ Nakahara, T.; Kurimoto, J.; Goseki, Y.; Koshio, T.; Ochi, H.; Ushiyama, H.; Matsumoto, T.; Ohsaki, I.; Wakamiya, K.; Yamazaki, M. *US 4 740 443*, (1988).
- ¹⁴ Hourston, D.J.; Schafer, F.U.; Bates, J.S., *J. Appl. Polym. Sci*, **60**, 2409, (1996).
- ¹⁵ Hiosington, M.A.; Seferis, J.C. in *Toughened Plastics*, ACS 233, Washington, DC, 1993.
- ¹⁶ Green, B.K. and Schleicher, L., US Patent 2 730 456 (1956).
- ¹⁷ Green, B.K. and Schleicher, L., US Patent 2 730 457 (1956).
- ¹⁸ Polishchuk, A. Y., and Zaikov, G.E., *Multicomponent Transport in Polymer Systems for Controlled Release*, Gordon and Breach Science Publishers, Australia, (1997).
- ¹⁹ Scher, H.B., *Controlled Release Pesticides*, Am. Chem. Soc., (1977).
- ²⁰ Yadav, S.K., Khilar, K.C., and Suresh, A.K., *AIChE J.*, **42**, 2616, (1996).
- ²¹ Mathiowitz, E.; Cohen, M.D. *J. Membr. Sci.* **40**, 1, (1989).
- ²² Croll, L.M.; Stöver, H.D.H US Pat Application, file May 2003.
- ²³ Frank R.S.; Downey, J.S.; Yu, K.; Stöver, H.D.H, *Macromolecules*, **35**, 2728, (2002).
- ²⁴ Downey, Jeffrey S.; McIsaac, Geoff; Frank, Randy S.; Stöver, Harald D. H. *Macromolecules*, **34**, 4534, (2001).
- ²⁵ Li, W.-H.; Stöver, H.D.H. *J. Polym. Sci, Polym. Chem.*, **36**, 1543, (1998).

²⁶ Zheng, G.; Stöver, H.D.H., *Macromolecules*, **35**, 6828, (2002).

²⁷ Downey, J.S.; Frank, R.S.; Li, W.-L.; Stöver, H.D.H., *Macromolecules*, **32**, 2838, (1999).

²⁸ Koprinarov, I.; Hitchcock, A.P. *X-ray Spectromicroscopy of Polymers*, (<http://unicorn.chemistry.mcmaster.ca/research/stxm-intro/polySTXMintro-all.html>), (2000).

CHAPTER 4 –RELATED ONGOING RESEARCH AND PROPOSED FUTURE DIRECTION

4.0 Introduction

This chapter outlines some present and future work related to material presented in this thesis.

4.1 Related Ongoing Research

4.1.1 Industrially Relevant Composite Tectocapsules

The composite tectocapsules described above were designed as an “ideal” system where the surface chemistry of the microspheres could be controlled since they were prepared by precipitation polymerisation in the absence of surfactant and stabilizer. The use of such model microspheres facilitated an understanding of the factors that affected particle self-assembly and allowed for proof of concept. Despite the great success of these systems they may not be attractive for industrial applications because precipitation polymerisation can be difficult to control, gives a product with low solids content (2-4% w/w) and a high volume of solvent waste. In addition the systems described above were prepared with xylenes as the core solvent in the absence of any active material. For these reasons, we wished to develop additional systems that would be more easily transferable to an industrial product.

4.1.1.1 Introduction of Suspension Microspheres

Suspension microspheres were chosen as the preferred replacement for the precipitation microspheres used in the composites presented above since they could be prepared as cross-linked beads with pores of various sizes. When prepared from DVB they were expected to retain some unreacted vinyl groups, which could be used to add

desired chemistry in a post-polymerisation reaction. Drawbacks associated with the use of suspension microspheres include larger microspheres size, generally several microns in diameter, broad size distribution and the presence of stabiliser. The work presented here was carried out by Danielle Lewis under the supervision of Dr. Harald Stöver, Mrs. WenHui Li and myself.

Initial attempts to prepare composite tectocapsules using traditional DVB suspension particles were not successful. It was found that the microspheres did not assemble at the oil-water interface. The microspheres were found to be coated in polyurea and were either contained within the capsule core or anchored to the interior of the capsule wall. It is also believed that the large particle size, 5-10 μm , caused weakening and therefore rupture and much faster release of core solvent versus traditional polyurea capsules.

More recently several batches of smaller (1-5 μm) suspension microspheres with varying porosity have been prepared and functionalised with maleic acid to facilitate assembly at the oil-water interface. In the future, these microspheres will be incorporated into polyurea microcapsules. It is expected that self-assembly of the microspheres will occur and that these novel tectocapsules will have pore-size dependent release properties.

4.1.1.2 Release of Mixed Fills

Two series of composite capsules will be prepared with the above microspheres. One will be prepared with xylenes as the core solvent and will parallel the work done with porous precipitation microspheres. The second series will contain core solvent mixtures. These mixtures will be comprised of several solvents of different polarity and boiling

points. The release rate of each of the components will be determined and related to the volatility and polarity.

The undifferentiated release of mixed fills is an important issue in the perfume industry. Perfumes are mixtures of compounds that must reach the nose in the appropriate ratio to produce the desired scent. This is difficult in a traditional microcapsule based controlled release system where release may not be determined only by volatility but also by a component's solubility in the capsule wall polymer. Microencapsulated scents hence often smell different than the neat fill or perfume, and this has to be corrected by manipulating the fill composition.

We believe that release through porous microspheres in composite tectocapsule systems should not differentiate between components based on their solubility in the capsule wall, and therefore, should show more representative release of mixed fills. This work is on going.

4.1.2 Confirmation of the Mechanism of Release from Composite Tectocapsules

Composite tectocapsules were designed to control release through the number and the porosity of the microspheres used in their construction. This implies that release must occur through the pores of the microspheres. However, we currently can not exclude release occurring via the channels between the microspheres and the polyurea matrix.

To distinguish between pore and channel release a series of composite tectocapsules will be prepared using a series of microspheres having increasing pore size. If release is occurring via the microsphere pores, increased pore size should result in a corresponding

increase in release rate. This is a generic experiment that could be carried out with a number of different fills if needed, since all fills may not follow the same release path.

Current work with suspension microspheres, started by Danielle Lewis, is expected to provide some information regarding the path of release from composite microspheres.

4.2 Proposed Future Work

4.2.1 Polyurea Membrane Analysis by STXM

The analysis of polyurea membranes by STXM, described in Chapter 1 above, proved challenging for three reasons. A) the spectroscopic similarities of the symmetric and asymmetric polyureas being studied; B) studying features close to the spatial resolution limit of STXM 5.3.2 (50 nm); and C) difficulties in ascertaining the orientation of the capsule wall fragments within the microtomed sections.

- A) Careful selection of the materials used to generate model spectra for the two polyureas allowed for resolution of the two urea species. This was discussed above in Chapter 1 and will not be considered further here.
- B) Current spatial resolution limits in STXM are the result of restrictions to the line spacing of the zone plates used to focus the x-rays, as well as the level of environmental vibration at a given facility. In the future, the spatial resolution will be improved as new zone plates with smaller ring spacing become available.
- C) One further limiting factor that will be encountered in studies with thin membranes such as ours is controlling the orientation of samples during

embedding and microtoming. Some suggestions regarding these difficulties will be discussed below.

4.2.1.1 Microspheres as Wall Markers

The composite tectocapsules presented in Chapter 3 show that it is possible to form polyurea membranes in the presence of polymer microspheres. Therefore such polymer microspheres can serve as a marker of the exterior of a capsule wall or other interfacially formed membrane. Such “internal” markers would alleviate the need for the gold coating used in Chapter 1.

4.2.1.2 Model Membranes

The polyurea membranes studied above were prepared as microcapsules. These capsules were then crushed under liquid nitrogen, washed, dried and embedded in resin such that they could be microtomed to ~100-200 nm thick slices. During this process the membranes become twisted and it is believed that this twisting results in blurring of the chemical gradient present in the membrane. It is proposed to prepare analogous flat polyurea membranes at a flat oil-water interface. These flat interfacial membranes can be captured using a copper TEM grid and rinsed with acetone. After embedding, the copper grid would act as a marker for membrane orientation during microscopy.

4.2.2 Chemistry of Microspheres used for Capsule Construction

DVB-MAn microspheres were initially used in the tectocapsule and composite tectocapsule work because the polar anhydride facilitated microsphere assembly at the oil-water interface, and provides a mechanism for cross-linking the microspheres to each other, or to a second polymer, via the use of nucleophilic linkers. However the facile

hydrolysis of the anhydride makes it difficult to control the polarity of the materials made, and therefore their assembly behaviour. Future work in this area should consider the use of other functionalities, that may be added post-particle formation and are less sensitive to hydrolysis but still allow for the use of nucleophilic linkers. Such groups might include epoxies such as glycidyl methacrylate (GMA, Figure 4.1 A) potentially together with tri(ethylene glycol) methyl vinyl ether (Figure 4.1 B) or poly(ethylene glycol) methyl ether methacrylate (Figure 4.1 C) to impart sufficient polarity for self-assembly.

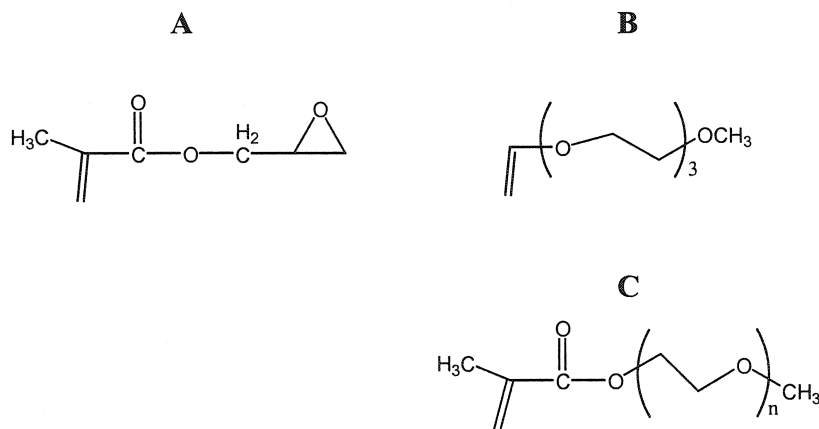


Figure 4. 1 Possible monomers for microsphere functionalisation, **A**) glycidyl methacrylate (GMA), **B**) tri(ethylene glycol) methyl vinyl ether and **C**) poly(ethylene glycol) methyl ether methacrylate.

4.2.2.1 Location of Functionalisation Reaction

Porous DVB particles functionalised with maleic acid were characterised using FT-IR and STXM. IR analysis showed the presence of both anhydride and acid groups, but

could not reveal the location of the new functional groups within the microspheres. STXM indicated that the functionalisation reaction was limited to the particle surface, perhaps due to the small pore size.

The question of the location of the functionalisation reaction is interesting both for scientific and practical reasons. For example, pores coated with polar groups may inhibit the release of non-polar fills that cannot properly wet a hydrophilic surface. In addition, if the functionalisation was limited to the microsphere surface because the reaction solvent did not wet the microsphere pores, it may be difficult to get release of capsule fill through the same pores.

For these reasons it is important to continue studying the location of the microsphere functionalisation reaction as part of any composite tectocapsule work. Variables to be considered are microsphere pore size, reaction solvent, reaction temperature, sonication of the microspheres in: solvent prior to reaction, solvent and reagents prior to reaction, and during the entire reaction.

4.2.3 Tectocapsules as Vehicles for the Encapsulation of Highly Viscous Liquids and Waxy Solids

While the tectocapsule systems presented above in Chapter 2 are currently not applicable for the controlled delivery of most small molecule fills due to their large pores, they may be useful for the encapsulation of other fills, such as viscous liquids or waxy solids, such as dodecyl acetate.

To form such capsules, the core materials would be heated to reduce the viscosity or melt the wax such that an oil-in-water emulsion could be formed. Following emulsification, particle self-assembly and the wall forming cross-linking reaction would

be performed at the same elevated temperature. Such systems would then be cooled to room temperature where core material would thicken and therefore be retained within the macroporous capsule wall.

Such capsules prepared with viscous oil may be useful for release applications where an applied force would cause the liquid to flow through the interstitial pores or rupture the shell. They may also be applicable for the slow release of viscous oil, which may show extremely low or negligible release rates through the less porous traditional capsule walls.

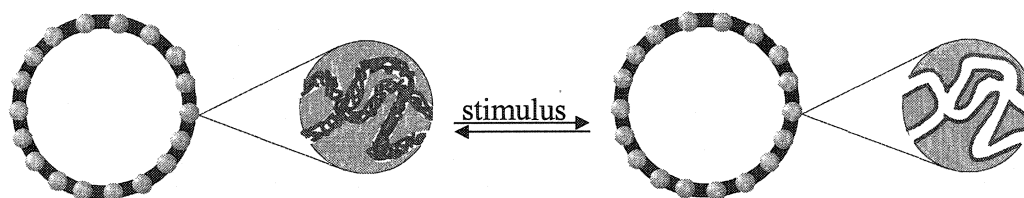
An additional advantage of tectocapsules prepared with waxy solids, such as 8,10-E-E dodecadienol, as the core material may simply be the ability to prepare such capsules. Alcohols are traditionally very difficult materials to encapsulate as a result of their reactivity towards electrophiles, like isocyanates, as well as their surface activity in oil-water emulsions, which tends to disrupt wall formation in traditional capsule systems. Polyurea systems for successful encapsulation of alcohols can be prepared using acetates or phthalates as polar cosolvents.¹ The disadvantage of this method is that the active, the alcohol, only constitutes about 20% of the core oil.

All of the systems discussed above involve colloids contained in the organic phase. It is also possible to prepare tectocapsules using colloids assembling from the aqueous phase. Such systems may attract greater industrial interest since it would allow for the use of many commonly available latex particles and would eliminate the need for suspension of the particles in the organic phase prior to the encapsulation procedure. In

addition, with such systems it may be possible to overcome some of the problems associated with the encapsulation of functional fills, such as alcohols.

4.2.4 Functional Release Gates

On-Off Release Gates. Pore filled membranes consist of an “inert” porous scaffold filled with a polymeric gel which can be temperature and/or pH responsive. They have been developed for use in water purification² and controlled delivery³. Based on this technology it is not difficult to imagine a parallel composite tectocapsule system where



the release channels of the microspheres are coated with such a pH or temperature responsive polymer. In doing so, one would introduce the potential for temperature and or pH regulated release gates. Alternatively, the pH or temperature sensitive microgels could be used directly.

Figure 4. 2 Illustration of composite tectocapsules with pore filled microspheres functioning as pH or thermal on-off gates.

Catalytic Release Gates. In composite microcapsules where release of core material occurs via the pores of embedded microspheres it is not difficult to imagine systems where "chemistry" can be carried out as material passes through such pores.

Such systems would facilitate the encapsulation of compounds that are currently too reactive or have interfacial activity, such as amines and alcohols.

The use of protecting groups is common in the synthesis of complex molecules. Deprotection reactions tend to be facile and carried out under mild conditions.^{4,5} It would therefore be possible to incorporate acid functionalities into the pores of the microspheres such that deprotection of the encapsulated compound would occur upon release.

An example where an alcohol is protected by chlorotrimethylsilane (CITMS) is shown below. It is noted that the deprotection of the TMS may also occur via hydrolysis during the encapsulation. If this were the case a more stable triethylsilane group may be better.⁵

1. $\text{R-OH} \xrightarrow[\text{pyridine}]{\text{Me}_3\text{SiCl}} \text{R-OSiMe}_3$
2. Encapsulation of the protected alcohol
3. Release and deprotection of the alcohol via the microsphere pore

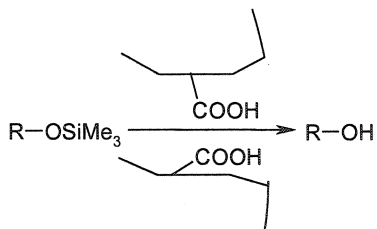


Figure 4. 3 Proposed scheme for protection and deprotection of alcohols.

References

¹ Li, E.H.; Stöver, H.D.H. *J. Membr. Sci.*, accepted.

² Mika, M.A.; Childs, R.F.; Dickson, J.M. *Desalination*, **121**,149, (1999)

³ Chu, L.Y.; Park, S.H.; Yamaguchi, T.; Nakao, S. *J. Membrane. Sci.* **192**, 27, (2001).

⁴ Smith, M.B. *Organic Synthesis*, McGraw-Hill, New York, (1994).

⁵ Greene, T.W. and Wuts, P.G.M. *Protective Groups in Organic Synthesis, 3rd Ed.*, John Wiley and Sons, New York, 1999.

Epilogue – Thesis Summary

The preface to this thesis described the objectives of this research. This section will summarize the outcomes of that work and the resulting contributions to polymer science. The objectives are reprinted for clarity.

Chapter 1: Compositional Mapping of the Internal Structure of Polyurea Microcapsule Walls by Soft X-ray Spectromicroscopy.

Research Objective:

The goal of this research was to develop a scanning transmission x-ray spectromicroscopy (STXM) method that could be used for the chemical speciation of polyurea microcapsules, allowing the level of isocyanate hydrolysis during microcapsule formation to be assessed with a spatial resolution of ~50 nm.

Outcome of Research:

It was found that the two polyureas formed by reaction of isocyanate with amine and water, respectively, could be distinguished spectroscopically using STXM. It was further found that the polyurea capsule walls are chemically asymmetric. This result confirmed that wall growth occurs on the organic side of the capsule wall and that the isocyanate reaction with amine is dominant.

In addition, an understanding of the STXM technique and the steps required for improved sample preparation and analysis were developed, laying the basis for future

quantitative compositional mapping of similar capsule walls. As a result of this work, STXM is being utilized for the analysis of many other materials within our group.

Chapter 2: Formation of Tectocapsules: Assembly of Poly(divinylbenzene-*alt*-maleic anhydride) Microspheres and Microgels at the Oil-Water Interface

Research Objective:

The goal of this research was to develop a method for assembling poly(divinylbenzene-*alt*-maleic anhydride) (DVB-MAn) microspheres at the oil-water interface and covalently fixing them in place to form highly porous capsular structures. The factors that affect the self-assembly and fixation of the microspheres at the oil-water interface were also investigated.

Outcome of Research:

Poly(divinylbenzene-*alt*-maleic anhydride) microspheres were successfully assembled at oil-water interfaces and fixed in place using polyethylenimenes (PEI) to form a new type of highly porous microcapsule called tectocapsules. A mechanism for the formation and rupture/release of tectocapsules was presented. It was found that a percentage of the succinic anhydride groups on the microspheres must be hydrolyzed to succinic acid in order to facilitate microsphere self-assembly. Rupture upon loss of water in some systems was shown to result from the rapid evaporation of low boiling core solvents.

Chapter 3: Composite Tectocapsules with Porous Microsphere Release Gates.

Research Objective:

The goal of this research was to prepare composite microcapsules with porous microsphere release gates and to compare the release of xylenes from these capsules with traditional microcapsules.

Outcome of Research:

Several different types of colloids were successfully incorporated into a polyurea matrix to produce composite tectocapsules. Initially, DVB-MAn microspheres and microgels were self-assembled at the oil-water interface and subsequently embedded in a polyurea membrane. These systems were prepared to establish that the presence of assembled microspheres did not disrupt polyurea wall formation. Following preparation of those systems, a second type of composite tectocapsule was prepared using porous poly(divinylbenzene) (DVB) microspheres functionalized with maleic acid. These microspheres were successfully incorporated into a polyurea matrix. Release of xylene from these composite microcapsules was monitored gravimetrically and showed that membranes containing porous microspheres release differently than standard polyurea microcapsules.

Chapter 4: Proposed Future Direction and Related Ongoing Research

This chapter presents ideas for future work and summarizes ongoing work related to and inspired by the work presented in this thesis.

The largest body of ongoing work is that where the microsphere used for the above work, prepared by precipitation polymerization, are being replaced by microspheres prepared by suspension polymerization. This work transfers the fundamental work of this thesis into a system that can be directly applied in industry.